Vietnamese-German University

COPYRIGHT WARNING

This paper is protected by copyright. You are advised to print or download **ONE COPY** of this paper for your own private reference, study and research purposes. You are prohibited having acts infringing upon copyright as stipulated in Laws and Regulations of Intellectual Property, including, but not limited to, appropriating, impersonating, publishing, distributing, modifying, altering, mutilating, distorting, reproducing, duplicating, displaying, communicating, disseminating, making derivative work, commercializing and converting to other forms the paper and/or any part of the paper. The acts could be done in actual life and/or via communication networks and by digital means without permission of copyright holders.

The users shall acknowledge and strictly respect to the copyright. The recitation must be reasonable and properly. If the users do not agree to all of these terms, do not use this paper. The users shall be responsible for legal issues if they make any copyright infringements. Failure to comply with this warning may expose you to:

VGU Vietnamese-German University

- Disciplinary action by the Vietnamese-German University.
- Legal action for copyright infringement.
- Heavy legal penalties and consequences shall be applied by the competent authorities.

The Vietnamese-German University and the authors reserve all their intellectual property rights.

Vietnamese-German University

Faculty of Engineering

Cracking in Reinforced Concrete Structures

Vietnamese-German University

Thesis

Submitted for the Degree of

Bachelor in Civil Engineering and Construction Management

Author

Nguyen Ngoc Anh Thu

Matriculation No.: 18775 (VGU), 547880 (HBC)

Supervisors

Dr.-Ing. habil. Ngoc Linh Tran (VGU)

Prof. Dr.-Ing. Christian Kulas (HBC)

March 27, 2026

Nguyen Ngoc Anh Thu

Cracking in Reinforced Concrete Structures

Civil Engineering and Construction Management Program

Thesis No.: BCE-2026-02

This thesis is available for public access at the library of Vietnamese-German University (VGU). A digital version of the thesis may also be archived in the institutional repository of VGU, subject to the university's publication and copyright policies. For further information regarding access or citation, readers are encouraged to contact the university library.

VGU
Vietnamese-German University

Abstract

Cracking in concrete structures poses a significant challenge in civil engineering as it directly affects structural stability, durability, serviceability and long-term performance. The recent update from EN 1992-1-1:2004 to EN 1992-1-1:2021 introduces refinements to the crack control model, which requires a clear evaluation of these changes into the practical implications for design engineers. This bachelor's thesis conducts a fundamental comparative analysis of the crack control methodologies in these two provisions of Eurocode 2.

The research integrates a theoretical parametric study with experimental validation. A series of 15 beams with varying depths and reinforcement diameters is analyzed using theoretical calculations to identify trends in predicted crack spacing and width. For experimental verification, crack patterns from three reinforced concrete beams tested at the Vietnamese-German University (VGU) laboratory are measured and compared with code-based predictions.

The findings present a change in the underlying mechanics between the two standards. The updated EN 1992-1-1:2021 provides a more refined and conservative approach. The key improvements include a refined definition of effective concrete area in tension, which links directly to reinforcement geometry (e.g. $h_{c,eff} = d_1 + 5\phi$) and the introduction of new coefficients (k_{fl}, $k_{1/r}$, k_w) that better capture local stress distribution and crack geometry. While EN 1992-1-1:2004 demonstrated high accuracy in predicting crack spacing for the tested specimens, the 2021 version offers more uniform, consistently conservative results. The study concludes that the new standard represents a significant improvement in reliability, although it increases the cost of conservatism. The thesis basically provides critical insights and practical recommendations for designers during the transition between these two codes.

VGU
Vietnamese-German University

Keywords: EN 1992-1-1, Crack Control, Reinforced Concrete Structures, Eurocode 2, Comparative Analysis, Serviceability Limit State

Notation

The units of parameters used in this study

kN	for loads
kNm	for moment
N/mm^2	for stress, elastic modulus, material strength
mm	for geometry dimensions, diameter
mm^2	for area

Abbreviation

AAR	alkali-aggregate reaction
CoV	coefficient of variation
ERC	exposure resistance class
ITZ	interfacial transition zone
MCD	maximum crack depth
SAP	superabsorbent polymer
SCM	supplementary cementitious material
SLS	serviceability limit state
SRA	shrinkage-reducing admixture
TCL	total crack length
ULS	ultimate limit state

Vietnamese-German University

Terms with Latin letters

a_g	maximum size of aggregates
A_{ct}	area of concrete in tension zone
$A_{ct,eff}$	effective tension area of concrete
A_s	the cross-sectional area of reinforcement
$A_{s,min}$	the minimum cross-sectional area of reinforcement

$A_{s,min,w1}$	the minimum cross-sectional area of reinforcement at the most tensioned face
$A_{s,min,w2}$	the minimum cross-sectional area of reinforcement at the least tensioned face
b	width of cross section
c	concrete cover thickness
c_{act}	actual concrete cover
c_d	nominal value of the concrete cover for designing the anchorage length
$c_{d,conf}$	nominal value of c_d in presence of confinement
$c_{min,dur}$	minimum concrete cover due to bond requirement
$c_{min,b}$	minimum concrete cover due to durability requirement
c_{nom}	nominal value of the concrete cover
c_s	clear distance between parallel reinforcement bars
d	effective depth of a cross section
E_{cm}	secant modulus of elasticity of concrete
E_s	modulus of elasticity of reinforcing steel
f_{ck}	characteristic compressive cylinder strength of concrete
f_{cd}	design value of concrete cylinder compressive strength
f_{cm}	mean value of concrete cylinder compressive strength
f_{ct}	the tensile strength of concrete
$f_{ct,eff}$	the effective tensile strength of concrete
f_{yk}	characteristic yield strength of reinforcement
f_{yd}	design yield strength of reinforcement
h	overall depth of a cross section
$h_{c,eff}$	effective height of the effective concrete area around reinforcement
k_b	bond strength factor
k_h	coefficient allowing for the effect of non-uniform self-equilibrating stresses
k_t	coefficient considering duration of the load on tension stiffening effects for cracking
k_x	relative depth of the compression zone

VGU Vietnamese-German University

k_{surf}	factor considering the difference between an increased crack width at the surface and the required mean crack width
$k_{1/r}$	a curvature coefficient for the increased of the crack width
k_{fl}	factor accounting for the stress distribution within the effective concrete in tension area
L	length of the span
L_{eff}	effective length of the span
M	bending moment
M_{Ed}	design value of internal bending moment
n_e	modulus ratio of steel and concrete
N_{Ed}	design value of normal force
q	distributed load
r	the edge distance of centroid of the first bar layer
s_1	center to center spacing of longitudinal bars
s_r	crack spacing
$s_{r,m,cal}$	mean value of crack spacing
$s_{r,max}$	maximum value of crack spacing
$s_{r,min}$	minimum value of crack spacing
V	shear force
w_k	characteristic crack width
$w_{lim,cal}$	limiting crack width
x	the depth of compression zone
z	lever arm of internal forces

VGU Vietnamese-German University

Terms with Greek letters

ε_{cm}	average concrete strain between cracks at the reinforcement layer
ε_{sm}	average strain of longitudinal reinforcing steel between cracks
γ_c	safety factor for concrete strength
ρ_s	reinforcement ratio of longitudinal reinforcement
ρ_{eff}	effective reinforcement ratio of longitudinal reinforcement
φ	reinforcement diameter

φ_{mand}	mandrel diameter for bent reinforcement bars
σ_c	compressive stress in the concrete
σ_s	reinforcement stress
$\sigma_{s,lim}$	limiting value of the serviceability steel stress

VGU
Vietnamese-German University

Contents

Foreword ii

Notation iv

1 Introduction 1
- 1.1 Motivation . . . 1
- 1.2 Purpose . . . 2
- 1.3 Structure of the bachelor thesis . . . 2

2 Literature Review 3
- 2.1 Types and causes of cracks in concrete . . . 3
  - 2.1.1 Load-induced cracks . . . 3
  - 2.1.2 Shrinkage cracks . . . 6
  - 2.1.3 Thermal cracks . . . 10
  - 2.1.4 Chemical-related cracks . . . 11
- 2.2 Crack propagation and its effects on structural durability . . . 14
  - 2.2.1 Mechanism of crack initiation and propagation . . . 14
  - 2.2.2 Crack control techniques in reinforced concrete structures . . . 17
- 2.3 Summary . . . 21

3 Code Provisions for Crack Control 22
- 3.1 New Eurocode 2 . . . 22
  - 3.1.1 General considerations . . . 22
  - 3.1.2 Minimum reinforcement areas . . . 25
  - 3.1.3 Simplified control of cracking . . . 28
  - 3.1.4 Refined control of cracking . . . 29
- 3.2 Existing Eurocode 2 . . . 33
  - 3.2.1 General considerations . . . 33
  - 3.2.2 Minimum reinforcement areas . . . 34
  - 3.2.3 Crack control without direct calculation . . . 36
  - 3.2.4 Crack control with direct calculation . . . 38
- 3.3 Summary . . . 41

4 Application 43
- 4.1 Example for crack control calculation . . . 43
  - 4.1.1 Objective of the example . . . 43

VGU Vietnamese-German University

4.1.2 Calculation procedure 43
4.1.3 Results of extended beam series 59
4.1.4 Comparative analysis 61
4.2 Experiment setup 66
4.3 Experimental results 67
4.3.1 Experiment calculation 67
4.3.2 Experiment results 67

5 Discussion **75**
5.1 Comparison between EN 1992-1-1:2004 and EN 1992-1-1:2021 75
5.2 Influence of key mechanical factors 76
5.3 Practical implications for designers 77
5.4 Limitation and future research 77

6 Conclusion and Recommendations **79**

Appendix **80**

References **85**

VGU
Vietnamese-German University

List of Figures

2.1 Flexural cracks [2] . . . 4
2.2 Shear cracks [2] . . . 5
2.3 Torsional cracks [2] . . . 5
2.4 Plastic shrinkage cracks [10] . . . 7
2.5 Autogenous shrinkage cracks [2] . . . 8
2.6 Drying shrinkage cracks [10] . . . 9
2.7 Thermal cracks [15] . . . 11
2.8 Chemical-related cracks [9] . . . 13
2.9 Carbonation progresses [25] . . . 16
2.10 Chloride ions penetration from surface concrete [25] . . . 17

3.1 Isolated bars . . . 31
3.2 Group of bars . . . 31

4.1 Simple reinforced slab and cross-section . . . 44
4.2 Maximum crack spacing for bar diameters D12, D14, and D16 according to (a) DIN EN 1992-1-1/NA, (b) EN 1992-1-1:2004, and (c) EN 1992-1-1:2021 . . . 62
4.3 Mean crack spacing for bar diameters D12, D14, and D16 according to (a) DIN EN 1992-1-1/NA, (b) EN 1992-1-1:2004, and (c) EN 1992-1-1:2021 . . . 63
4.4 Crack width for bar diameters D12, D14, and D16 according to (a) DIN EN 1992-1-1/NA, (b) EN 1992-1-1:2004, and (c) EN 1992-1-1:2021 . . . 65
4.5 Excel Based Results . . . 70
4.6 Excel Based Results . . . 71
4.7 Comparison of measured maximum crack spacing and calculated maximum crack spacing according to different methods . . . 72
4.8 Comparison of measured mean crack spacing and calculated mean crack spacing according to different methods . . . 73

A.1 Beam B01 . . . 80
A.2 Beam B02 . . . 81
A.3 Beam B03 . . . 82
A.4 Crack Spacing Record of Beam B02 . . . 83
A.5 Crack Spacing Record of Beam B03 . . . 83
A.6 Sample Testing Beam at VGU Lab . . . 84

List of Tables

3.1 Verifications, stress, and crack width limits for appearance (EN 1992-1-1:2021, Table 9.1 (NDP)) . . . 23
3.2 Verifications, stress, and crack width limits for durability (EN 1992-1-1:2021, Table 9.2 (NDP)) . . . 24
3.3 Minimum concrete cover $c_{min,dur}$ for carbon steel - Carbonation (EN 1992-1-1:2021, Table 6.3 (NDP)) . . . 25
3.4 Minimum concrete cover $c_{min,dur}$ for carbon steel - Chlorides (EN 1992-1-1:2021, Table 6.4 (NDP)) . . . 26
3.5 Recommended values of w_{max} (mm) (EN 1992-1-1:2004, Table 7.1N) . . . 33
3.6 Maximum bar diameter for crack control . . . 37
3.7 Maximum bar spacing for crack control . . . 37
3.8 Comparison of crack-control provisions in EN 1992-1-1:2004 and EN 1992-1-1:2021 . . . 42

4.1 Omega table without compression reinforcement. . . . 47
4.2 Crack control results according to EN 1992-1-1:2004 and EN 1992-1-1:2021 . . . 58
4.3 Parameters of beams . . . 59
4.4 Calculated crack spacing results . . . 60
4.5 Specimen specifications . . . 66
4.6 Measured and calculated crack spacings . . . 72
4.7 Measured and calculated crack spacing ratios . . . 73

Vietnamese-German University

1. Introduction

1.1 Motivation

Reinforced concrete is the cornerstone of modern civil infrastructure, forming the skeleton of buildings, bridges and other structures worldwide. Its widespread use is attributed to its versatility, durability, and cost efficiency. However, concrete has low tensile strength as its fundamental characteristic, which makes it susceptible to cracking [4][20].

The significance of cracking has far more meaning than just being aesthetically pleasing. Cracks act as direct pathways for aggressive agents such as moisture, chloride and carbon dioxide to penetrate the concrete and reach the reinforcement, leading to steel corrosion and eventual structural deterioration [24]. Therefore, accurately understanding, predicting and controlling crack widths is a fundamental aspect of the design process, ensuring both serviceability and long-term structural integrity.

Eurocode 2 (EN 1992-1-1:2004) is one of the most popular and critical standards for the design of concrete structures in Europe and many other countries. Recently, the revision of the original standard started since 2012 and the objectives of the revision were to modernize the code, trying to improve the accessibility of usage and decreasing reliance on nationally specified parameters [23]. Hence, EN 1992-1-1:2021 introduces refinements to various design methodologies, including the models for crack control. With this update outcome, it is crucial to comprehensively understand the practical implications of the changes, especially for designers and engineers, who require clarity on how the new provisions differ from the original ones and what impact these differences have on the predicted crack widths.

VGU
Vietnamese-German University

To address this evolution from EN 1992-1-1:2004 to EN 1992-1-1:2021, there are some essential questions raised in the following:

- What are the key theoretical differences in the crack control methods between EN 1992-1-1:2004 and EN 1992-1-1:2021?
- Does the refined model in the 2021 edition yield more accurate, consistently conservative and efficient for practical design?

These questions are vital for validating the theoretical improvements of the new code for engineers applying it in practical design, ensuring both economic and structural durability.

1.2 Purpose

The primary purpose of this bachelor's thesis is to perform a fundamental comparative analysis of the crack control methodologies in the existing EN 1992-1-1:2004 and the updated version EN 1992-1-1:2021. The study aims to identify the key differences in their underlying principles, formulas and parameters used for crack width calculation. This is achieved through a parametric study that generally analyzes a range of beam geometries to visualize trends in predicted crack spacing and width. To validate the theoretical findings, experimental data from reinforced concrete beams tested at the Vietnamese-German University (VGU) laboratory are used to compare calculated crack patterns from both standards with the measured ones. By integrating theoretical and experimental results, this study evaluates conservatism, accuracy, and suitability across different structural elements. The thesis concludes with a critical assessment of the refined model and provides some recommendations for designers and future research.

1.3 Structure of the bachelor thesis

The bachelor's thesis consists of five main chapters to show a logical investigation. Besides the chapter 1 "Introduction", which provides an overview of the motivation, the purpose, and the general structure of the thesis. The other chapters are structured as follows:

VGU Vietnamese-German University

Chapter 2 "Literature review" provides a fundamental background on cracking in reinforced concrete. It classifies the types and causes of cracks, explains the mechanisms of crack initiation and propagation, and describes the effects of cracking on structural durability. It also reviews crack control techniques, including design, materials and construction strategies.

Following Chapter 3 "Code provisions for crack control", this chapter presents a detailed description of the crack control provisions separately in EN 1992-1-1:2004 and EN 1992-1-1:2021. It systematically introduces the methods for calculating minimum reinforcement, crack spacing and crack width in both standards and highlights the key differences between the two codes.

In chapter 4 "Application", the theoretical framework from Chapter 3 is applied. It begins with a parametric study, then calculates crack widths for a series of beams using both standards. Afterwards, the experiment setup for the beams was tested at VGU, and the results are shown, followed by a comparative analysis between the code-based predictions and experimental measurements.

Chapter 5 "Conclusion and recommendations" summarizes the key findings of the research, giving final conclusions regarding the comparison between the two Eurocode versions and then provides recommendations for practical design and the proposals for further research directions.

2. Literature Review

2.1 Types and causes of cracks in concrete

A crack in reinforced concrete can be explained as a discontinuity in the material structure that results from microstructural failure or separation triggered by stress. The performance, durability and serviceability of the structure are all significantly impacted by these cracks. Thus, efficient monitoring, fracture identification and knowledge of various crack classifications are vital for reducing damage development and preventing potential structural failure [14].

The main types of cracks that are frequently observed in reinforced concrete are described in the following section. These include load-induced cracks, shrinkage cracks, thermal cracks, and chemical-related cracks. Each category includes a variety of distinct crack types, classified by their fundamental mechanics and features.

2.1.1 Load-induced cracks

When reinforced concrete components are subjected to external loads, load-induced cracks form. These cracks can form as torsional, shear or flexural types, depending on the forces in action. Each form offers additional information about member behavior, strength and serviceability while reflecting a distinct stress condition within the structure.

VGU
Vietnamese-German University

Flexural cracks

Flexural cracking is one of the most common forms of structural failure in reinforced concrete. The area where cracks frequently occur and where concrete has the lowest tensile strength is known as the tension zone. Concrete is prone to breaking when the tensile force reaches its maximum because of its significantly lower capacity, despite its great compressive strength [13][17][18].

Flexural cracks are normally divided into two kinds: primary and secondary. The bending moment creates primary cracks when the resulting tensile stresses are greater than the tensile capacity of the material, while secondary fractures usually result from the minor cracks that spread from main cracks for a variety of reasons, which include excessive stress, thermal expansions or shrinkage [14][17].

Material qualities, structural design, and environmental factors significantly impact the development and progression of flexural cracks. Appropriate selection of the quantity, size, and distribution of reinforcing bars is crucial for reducing and preventing of cracking. Through improved bond performance between steel and concrete, reinforcement detailing such as clear

cover, bar distribution and surface geometry further affects the formation of cracks [1].

Since the tension zone is where the concrete experiences the highest tensile stress, flexural cracks normally form as vertical cracks, as shown in Figure 2.1. These cracks appear in different locations, depending on the different types of members. For example, due to the bond interaction between the concrete and steel, cracks in reinforced concrete parts often originate near the reinforcement, resulting in localized stress concentrations. Like beams and slabs, where the largest tensile loads, cracks usually form in the lower part of the member [1][2][14][17].

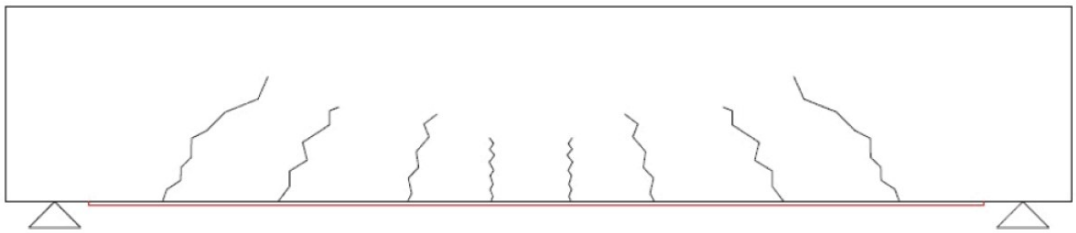


Figure 2.1: Flexural cracks [2]

Shear cracks

In reinforced concrete members, shear fractures occur when shear forces exceed the tensile strength of concrete, especially when shear force (V) and bending moment (M) combine, when shear cracks develop. Shear behavior is a crucial component in structural design as inclined cracks can reduce the capacity of load bearing and serviceability. Pure shear cracks and flexural-shear cracks are the two primary forms of shear cracking. Normally starting in the tension zone, flexural shear cracks move diagonally upward toward the compression zone. In contrast, pure shear cracks typically appear close to the support where shear stress predominates.

Shear cracks are often observed in areas of significant shear stress, particularly near supports or at certain locations along the span. These cracks arise from diagonal tensile strains induced by transverse loading in Figure 2.2. In some cases, shear cracks may also develop existing flexural cracks and expand along the longitudinal reinforcement or toward the compression zone. Further cracking may also arise from bond-related issues. Cracking may occur around reinforcement bars due to bond failure or inadequate anchorage [2][12][14].

Torsional cracks

Torsional cracking is more common in a structural element like a beam that experiences twisting forces that exceed its capacity. Although less frequent than flexural or shear cracking, torsional cracks are critical in certain structures, including balcony slab ring beams, edge floor joints, spatial frames, spiral staircases, and reinforced concrete arches. Under torsional loading, shear stresses develop along the cross-section, leading to crack formation.

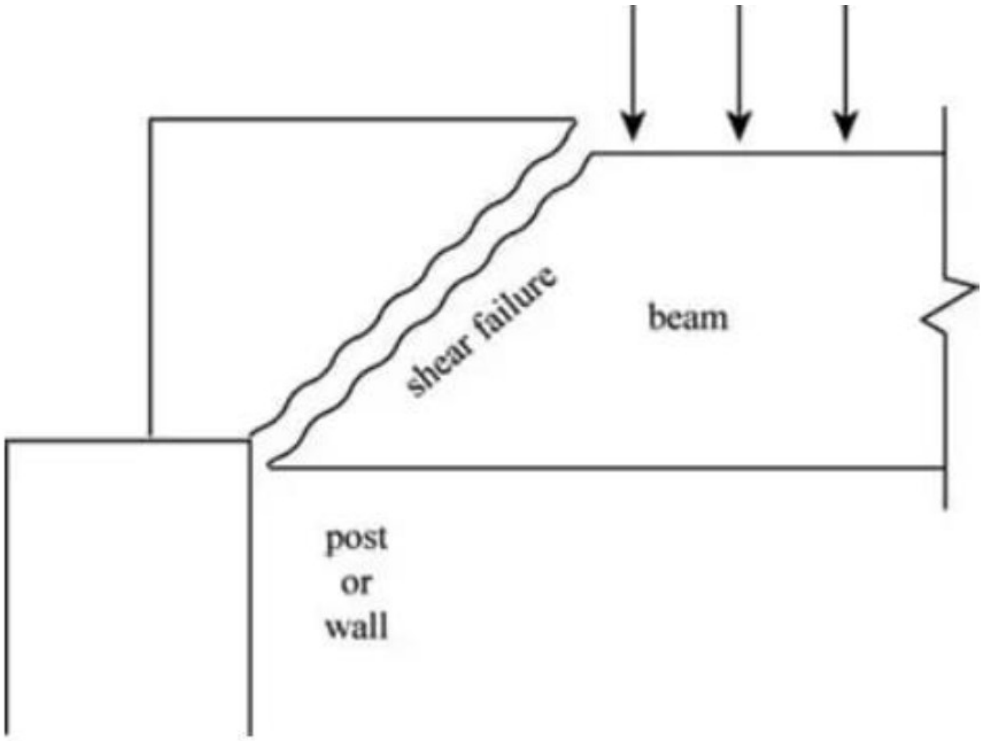


Figure 2.2: Shear cracks [2]

The appearance of cracks varies, depending on the severity of the applied stresses. They may prefer as fine microcracks and progress into wider macrocracks as the torsional demand increases. A distinguishing feature of torsional cracking is characterized by a helical pattern on all surfaces, while shear cracks appear only on the lateral faces, as shown in Figure 2.3.

Torsional cracks generally form at an approximately 45-degree angle to the longitudinal axis of the element. The crack progression in torsion follows a sequence of longer edges from the initial phase, then spreads to the short edge and the full surface grids before failure of the final phase [2][14].

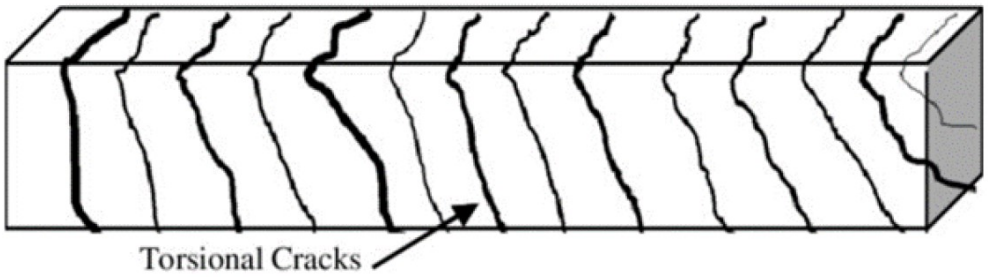


Figure 2.3: Torsional cracks [2]

Summary

In conclusion, load-induced cracks are caused by the stress condition inside a structural part. Shear cracks spread diagonally as a result of high shear stress, torsional fractures create a

distinctive helical pattern and flexural cracks begin in the tension zone. All of them are affected by the specifics of the reinforcement, but their fundamental distinction lies in the applied force. To improve strategies and safety implications for each type, this distinction is crucial.

2.1.2 Shrinkage cracks

External variables, including applied loads, temperature changes, and moisture content variations cause changes in concrete volume. Plastic shrinkage, which happens while the concrete is still fresh, and drying shrinkage, which happens after the concrete has cured, are the two primary stages of shrinkage behavior. Drying shrinkage can be further divided into two specific cases that happen at early ages: autogenous shrinkage and early drying shrinkage. These early-age shrinkage phenomena occur before the concrete reaches its full maturity. The following section is intended to provide a comprehensive overview of the subject.

Plastic shrinkage

Plastic shrinkage is known as the quick evaporation of water from the concrete surface or formwork before it has set and hardened, resulting in a decrease in the volume of fresh concrete. When the amount of water lost per unit area is greater than the amount of water brought to the surface by bleeding, surface cracks develop. Surface cracks are the most experienced in large horizontal exposed surfaces such as slabs and pavements, as illustrated in Figure 2.4. Typical cracks caused by plastic shrinkage are usually deep, parallel to one another, spaced 0,3 to 1 meter apart. They can even reach the free edges of the concrete.

They are strongly influenced by environmental conditions, particularly high wind velocity, low relative humidity, and elevated air and concrete temperatures, all of which accelerate water evaporation. These conditions are more prevalent in the summertime, although they can occur at any time and lead to rapid decreases in surface moisture and the development of capillary pressure. Furthermore, the mixed proportions are also crucial to the concrete's design. Higher cement content and a lower water-to-cement (w/c) ratio, and retardation can influence both bleeding and shrinkage. For instance, retardation setting time allows more bleeding, which can increase the risk of plastic shrinkage [21][19].

Early-age shrinkage

a) Autogenous shrinkage cracks

Autogenous shrinkage, also referred to as autogenous volume change, is a type of internal volume contraction that occurs in hardened concrete due to internal moisture consumption during continued cement hydration. This process, known as self-desiccation, takes place without any exchange of moisture with the external environment. It arises when the remaining unhydrated cement continues to react by consuming water retained inside tiny pores of the hardened concrete. Internal relative humidity decreases when the water is consumed and



Figure 2.4: Plastic shrinkage cracks [10]

VGU Vietnamese-German University

then generates negative capillary pressure, causing a slight amount of internal shrinkage. The surrounding hydrated cement matrix and aggregate particles largely limit this shrinkage in concrete, resulting in much lesser magnitude of autogenous shrinkage than in pure cement paste [21].

Although the magnitude is smaller than in pure cement paste, aggregates provide internal restraint that can generate tensile stresses within the cement paste. These stresses can lead to the development of microcracks (Figure 2.5), especially in the interfacial transition zone (ITZ) where the aggregate meets the paste or adjacent to the reinforcing steel. These microcracks may facilitate the propagation of separation cracks act as the damage threshold for further cracking. While fly ash and slag have more varied effects based on their replacement levels and fineness, some studies have shown both decreases and increases in shrinkage under different conditions, using supplementary cementitious materials (SCMs) such as silica fumes can significantly enhance autogenous shrinkage. This variability highlights that the effect of SCMs on shrinkage is not inherent but rather highly reliant on mix design and material properties, making generalized guidelines challenging for engineers [7][25].



Figure 2.5: Autogenous shrinkage cracks [2]

b) Early drying shrinkage cracks

Early drying shrinkage occurs when immature concrete is exposed to unsaturated air before sufficient curing. Unlike autogenous shrinkage, it is primarily driven by external environmental conditions. Although the fundamental mechanism is the same as long-term drying shrinkage, namely, the loss of moisture from the cement paste matrix, the early age occurrence poses a higher risk due to the low tensile strength of the immature concrete. In the initial hours after placement, evaporation of surface moisture may initiate shrinkage, especially if proper curing is delayed or insufficient.

VGU Vietnamese-German University

The concrete member experiences nonuniform shrinkage throughout its thickness, with the exposed surface experiencing the most shrinkage. As seen in Figure 2.6, this shrinkage causes the surface to experience peak tensile stress, which may result in axial motions, warping or micro-cracking. Thin elements with high area-to-volume ratios, such as slabs, are most affected by this phenomenon. Environmental factors, including low humidity, high temperature and strong wind, can greatly increase the rate of moisture evaporation while timely curing remains the primary defense [7][21].

Long-term shrinkage (drying shrinkage cracks)

Long-term drying shrinkage is the gradual reduction in concrete volume that occurs over weeks or months as water evaporates from its pores. This inevitable process occurs as the moisture balances with the surrounding humidity. Drying shrinkage is a time-dependent volume reduction that results from the loss of moisture from the pores to the surrounding environment. Initially, the evaporation of free water from the large capillary pores happens with

minimal contraction. However, as the drying process progresses and more strongly adhered water is removed from the surface of the cement gel particles, capillary tension and surface tension effects begin to take effect. These internal forces cause a contraction in the overall size of the concrete [21][25].

The cement paste of a microstructure has a significant impact on both the rate and magnitude. Concrete tends to shrink more when it has a larger surface area and finer pores, such as those made with silica fume. Conversely, concrete contains coarser particles or is cured with high-pressure steam that exhibits less shrinkage. Another important factor is aggregate properties, which are larger or stiffer in size, and can minimize shrinkage. Compared to normal-weight concrete, lightweight aggregate materials result in lower modules of elasticity, which commonly causes considerable shrinkage. Inadequate restraints in the component due to improper mixture design might also cause microcracks and excessive shrinkage [21][19].


VGU
Vietnamese-German University

Figure 2.6: Drying shrinkage cracks [10]

Summary

In conclusion, shrinkage cracking is a time-dependent risk that evolves over different phases. Initially, the mechanism changes from external evaporation to internal moisture consumption and long-term drying through. The concrete transitions from rapid moisture loss during the plastic stage to internal self-desiccation, followed by the drying stage with a longer timeframe. Immediate curing, controlling the paste content, and incorporating SCMs are essential

strategies for mitigating each phase.

2.1.3 Thermal cracks

Excessive temperature differences within or around a concrete structure form thermal cracking, causing uneven contraction. Tensile stress develops when the cooler areas are restrained by warmer ones. This stress results in cracking after exceeding the tensile strength of concrete, even in concrete members that are not classified as mass concrete [22]. In this paper, two common types of thermal cracking have been identified, including early-age thermal cracks due to heat of hydration cracking and external temperature cracking from environmental fluctuations.

Early-age thermal cracks (due to heat of hydration)

Heat-of-hydration cracking occurs mainly in mass concrete structures, such as foundations, dams, and thick walls. During the first few days after placement, hydration reactions release significant heat in the element's core. Because this heat generated cannot dissipate quickly, the surface cools rapidly when exposed to ambient conditions. This causes a temperature difference between the hot inside and the cooler on the surface, producing tensile stresses that may exceed the early-age tensile strength of the concrete. The resulting crack patterns often appear randomly, referring to checkerboard or patchwork patterns.

Several factors affect cracks caused by high cement content, section thickness, formwork restraint, adjoining elements, and the curing process. Mitigation strategies focus on controlling temperature rise and gradients. For example, using low-heat cements, incorporating supplementary cementitious materials such as fly ash, slag, or Portland cement, placing concrete in lifts, and monitoring time-temperature to keep the temperature difference balanced. A commonly recommended limit for temperature differences is approximately 20 degrees Celsius [15][22].

External temperature cracks

External temperature cracking arises from ambient temperature fluctuations over a longer time frame when hardened concrete structures are exposed. As concrete is exposed to seasonal cycles, it undergoes expansion during heating and contraction during cooling. When volume changes are restrained by inadequate joint spacing, tensile stress develops and eventually causes cracking. Pavements and slabs both commonly appear with cracks because the surface is more directly affected by temperature variations than the more protected bottom faces. Cracks are also typically positioned perpendicular to the longest dimension of the element, clearly illustrated in Figure 2.7.

The severity of external temperature cracking depends on the magnitude of the ambient temperature change, the concrete's thermal expansion coefficient, the absence of joints, and

exposure to weather conditions. In cold weather, the proper design of expansion joints and curing blankets, which can reduce heat loss from the surface, is an essential component of effective mitigation. In addition, limiting solar radiation heat at moderate temperatures can be achieved by placing concrete, providing shade, or misting. Therefore, effective mitigation involves well-designed expansion joints and curing blankets, which can limit heat loss from surfaces in cold weather. In addition, providing shade, misting, or concrete placement during moderate temperature conditions helps to reduce solar radiation heat [15][22].

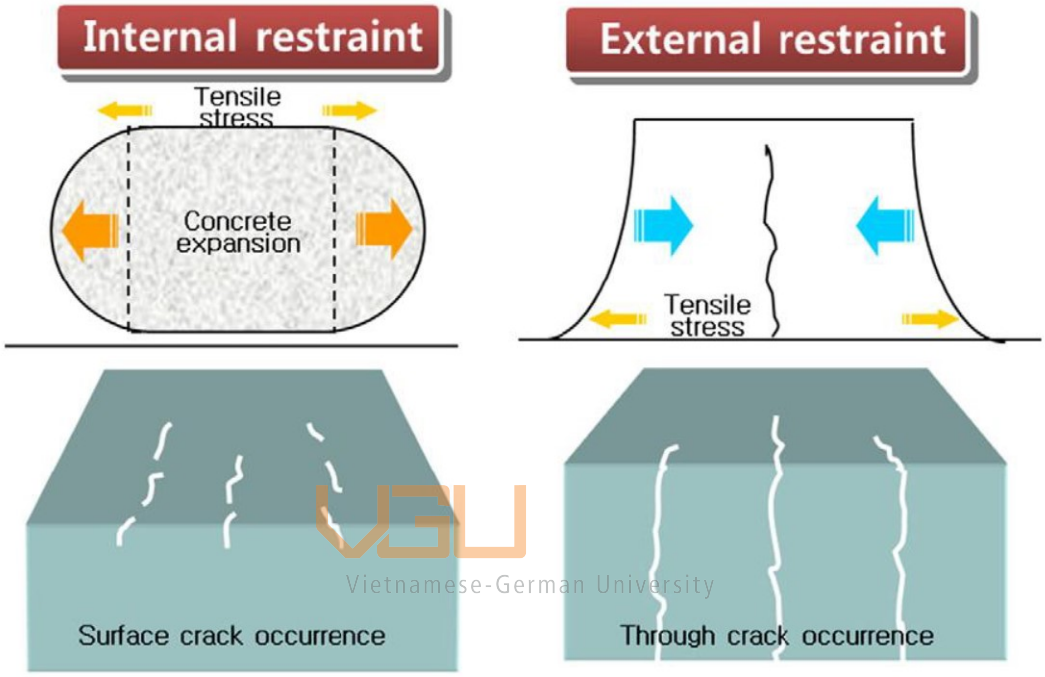


Figure 2.7: Thermal cracks [15]

Summary

Overall, thermal cracking occurs due to conflicting changes in restrained volume within an element and temperature differentials. The source of heat is the main fundamental difference: internal hydration versus external environmental cycles. To reduce the rise in core temperature, it is crucial to implement well-designed joints and control surface temperature.

2.1.4 Chemical-related cracks

Chemical-related cracks in concrete result from adverse reactions between material constituents and environmental exposure. These reactions can compromise structural integrity over time due to chemical-induced damage. There are two common types of chemical-related cracking: alkali-aggregate reaction (AAR) and carbonation-induced cracking. It is crucial to understand their mechanisms for better prevention and design.

Alkali-aggregate reaction cracks

The alkali-aggregate reaction (AAR) is a reaction between the alkali hydroxides in cement (mainly sodium and potassium) and certain reactive minerals, activated by the presence of amorphous silica in the aggregates. This internal reaction produces expansive gels or crystalline products, which absorb water, swell, and induce internal tensile stresses. Consequently, the concrete may deteriorate over time due to a rise in volumetric and fractures. When alkali-silica gel deposits accumulate along cracks, the crack patterns of AAR are normally irregular, linked spiderweb or map, frequently accompanied by white efflorescence in Figure 2.8. These cracks are easily found in damp structures such as bridges and foundations, especially in humid regions. Specifically, when the relative humidity is above 85%, high alkali content in cement, and large reactive aggregates can accelerate.

Because AAR is irreversible, preventive measures via material selection are critical. Strategies include using non-reactive aggregates, low-alkali cement, and pozzolanic materials such as fly ash, metakaolin or silica fume that consist of very fine materials and highly active silica, helping to bind free alkalis. For existing structures, techniques for monitoring and confinement may be able to control expansion stresses and minimize the progression of deterioration [6][9].

Carbonation-induced cracks

VGU
Vietnamese-German University

Carbonation in concrete is a phenomenon of a chemical reaction between carbon dioxide (CO2) in the atmosphere and calcium hydroxide (Ca(OH)2) in concrete, producing calcium carbonate (CaCO3). This reaction lowers the pH from approximately 13 to less than 9, negatively destroying the protective layer on rebars. As a result, reinforcement corrosion initiates, leading to microcracks from internal stress, progressing to spalling and reducing the durability of structural elements, such as columns and beams. The surface of cracks often appears as map cracking or longitudinal reinforcement. The width of cracks is greater than 0,15 mm, significantly increasing the depth of carbonation due to CO2 diffusion. Such cracks accelerate the degradation process, especially under dry-wet conditions.

Several factors influence the level of carbonation, including environmental factors such as humidity, temperature, and CO2 concentration. Optimal conditions for CO2 penetration range from 50% to 70%, with an optimal humidity level around 65%. With higher temperatures, CO2 diffusivity increases, which is common during exposure of building facades to weather conditions. In addition, the control of carbonation rate can be achieved through a combination of material selection, design methods, and monitoring techniques. An important strategy is to reduce the amount of CO2 by using concrete with a w/c ratio below 0,4 and ensuring proper curing and well-graded aggregates, including fine and coarse materials. Moreover, a concrete cover that is at least 40 mm thick will delay the entry of CO2 to the rebar level. Examples of surface treatments that can restrict further penetration include sealants, coatings

and waterproofing additives. To routinely track carbonation depth and conduct crack inspections, engineers can assess ongoing fractures and quality control measures more effectively [**alameeri˙2018**][11].



Figure 2.8: Chemical-related cracks [9]

Summary

In conclusion, chemical-related cracking is a progressive deterioration mechanism driven by expanding internal and chemical reactions. AAR results in the formation of a swollen gel that directly cracks the concrete and damages the interior. On the other hand, by allowing the chemical to enter the concrete and cause corrosive expansion, carbonation indirectly destroys the element. This suggests that AAR is a process that cannot be reversed, but carbonation-induced damage can be controlled through better design techniques, such as reducing permeability and providing adequate concrete cover to slow corrosion.

2.2 Crack propagation and its effects on structural durability

Although the various fracture types were categorized, this part examines the mechanisms underlying their formation and performance consequences. Fundamentally, assessing stiffness deterioration, corrosion start, and the overall longevity of the reinforced concrete structure requires an understanding of how cracks spread from micro to macro levels.

2.2.1 Mechanism of crack initiation and propagation

Concrete cracks arise over time, beginning as microscopic flaws caused by internal tensions and progressing to visible macrocracks due to environmental or mechanical factors. Understanding the onset and spread of fractures, as well as how they interact with durability and structural integrity elements, is crucial. Design requires this knowledge throughout its service life.

Microcracks formation (in cement paste, ITZ)

When concrete changes in volume, especially due to shrinkage, internal stresses can develop, leading to the formation of microcracks. This is particularly critical at an early age, when concrete is still young and its tensile strength is developing. The mechanism involves a complex interaction of material properties. As concrete matures, its elastic modulus increases, making it stiffer. At the same time, its creep capacity decreases, so it becomes less able to relieve stress through deformation. As a result, the shrinkage process can generate increasing tensile stresses over time, which may eventually exceed the local tensile strength of concrete and cause cracking [21].

Initiation of these microcracks most frequently occurs in the area surrounding aggregate particles, known as the Interfacial Transition Zone (ITZ). The ITZ is generally regarded as the ”weak link” in the concrete composite because it has a weaker microstructure, wider holes and higher porosity than the bulk cement paste. Since this zone makes up to 20 to 40% of the cement paste volume, it plays an important role in crack initiation and propagation. Therefore, cracks tend to form and spread preferentially in this region, which strongly influences the overall strength and longevity of the concrete [19].

These early microcracks are often due to plastic shrinkage, which is promoted by the generation of high capillary pressure during evaporation from the concrete surface. As menisci form in the pores during evaporation, they pull particles together and cause shrinkage. The resulting tensile strains can lead to visible cracking if this deformation is restrained by the substrate, formwork or internal temperature and moisture gradients. These cracks are also strongly influenced by environmental and material conditions and often appear as network-

like or parallel patterns. Factors such as clay in the aggregate, which can enhance shrinkage and reduce strength, high cement content, high placing temperatures and a high water-cement ratio can further increase the risk. Consequently, early-age cracking is rarely due to a single factor, but rather to a combination of interacting mechanisms [21][25].

Transition from microcracks to macrocracks

In real-world structures, the situation becomes more complex. The effective tensile strength is often lower than values obtained from laboratory tests due to numerous factors such as concreting direction, compaction quality, early-age microcracking caused by thermal and shrinkage stresses, and the long-term effects of sustained restraint from shrinkage and creep, all of which reduce the effective in-situ tensile resistance of concrete [25].

The further development of these cracks depends on the tensile strain capacity of the concrete, also known as tensile fracture elongation, which describes its ability to deform in tension up to maximum load. This strain capacity typically ranges from 0,08 to 0,15 mm/m and is influenced by parameters such as the water-cement ratio, admixtures, loading conditions, and aggregate stiffness. The brittleness during the early phases of curing arises from the low tensile strength and the rapidly rising modulus of elasticity, making even minor applied forces susceptible to fracture. Although long-term creep may improve the deformation capacity, it may also reduce the effective tensile strength, thereby increasing the likelihood of cracking [21][25].

Vietnamese-German University

As tensile stresses continue to act under restraint, the initially isolated microcracks propagate through the cement paste and along the aggregate–paste interface. The development of these microcracks at weak spots such as ITZ is, in most cases, initiated by early-age shrinkage processes as outlined in the previous section. Over time, these neighboring microcracks grow, connect and coalesce into visible macrocracks once effective tensile restraint is exceeded. This transition from distributed microcracking to discrete macrocracking governs the onset of structural cracking in reinforced concrete members and therefore directly influences the reinforcement required to control crack widths in service (DIN EN 1992-1-1).

In addition, the influence of the stress field on cracking is also reflected in tensile test methods used for concrete. The flexural test, which gives the modulus of rupture, measures an apparent tensile strength rather than the true direct tensile strength of concrete. Under third-point loading, a relatively large portion of the beam is subjected to high tensile stress, increasing the likelihood of activating a weak point, such as microcracks in the ITZ. At the same time, the less highly stressed concrete near the neutral axis partly restrains crack growth, so more energy is needed for complete failure. This is why flexural tests usually give higher tensile strength values than direct tension tests. In contrast, the splitting tensile test produces a more uniform tensile stress field and therefore gives results that are generally closer to the true tensile strength. This comparison shows that concrete failure initiates at the weakest point within the stressed volume and that the measured tensile strength depends on the stress

field and crack-propagation conditions, rather than being a fixed material property [21].

Link between crack propagation and reduction of stiffness and durability

Durability in reinforced concrete structures depends not only on material quality and design but also on the preservation of reinforcement and concrete functionality throughout the service life. Cracks are unavoidable under tensile stress and represent structural discontinuities that critically affect both stiffness and durability. Cracks allow the ingress of air and moisture into the structure, reaching the reinforcing steel. Oxygen and water initiate corrosion of steel, leading to a loss of functionality and long-term structural deterioration. Historical evidence demonstrates that without maintenance and exposed to weather conditions, cracked concrete suffers from water penetration, limescale, structural damage, and rusted reinforcement, confirming the link between crack development and loss of durability [21][25].

Carbonation- and chloride-induced corrosion processes in reinforced concrete are both strongly accelerated by cracks, which serve as direct transport pathways for aggressive agents. As illustrated in Figure 2.9 and Figure 2.10, calcium carbonate is generated by the reaction between CO2 and calcium hydroxide, reducing the pH to about 8 – 9, which may destroy the passive layer of the reinforcing steel. Similarly, when chloride ions are transported through cracks by moisture, they locally de-passivate the reinforcement if their concentration exceeds a critical threshold, initiating corrosion at exposed steel surfaces and compromising the surrounding concrete. According to ACI Committee 224 (2007), cracks provide easy access for oxygen, moisture, and chlorides, accelerating corrosion when they run parallel to reinforcement or are accompanied by inadequate concrete cover, while well-compacted, low-permeability concrete can limit such effects.

VGU Vietnamese-German University

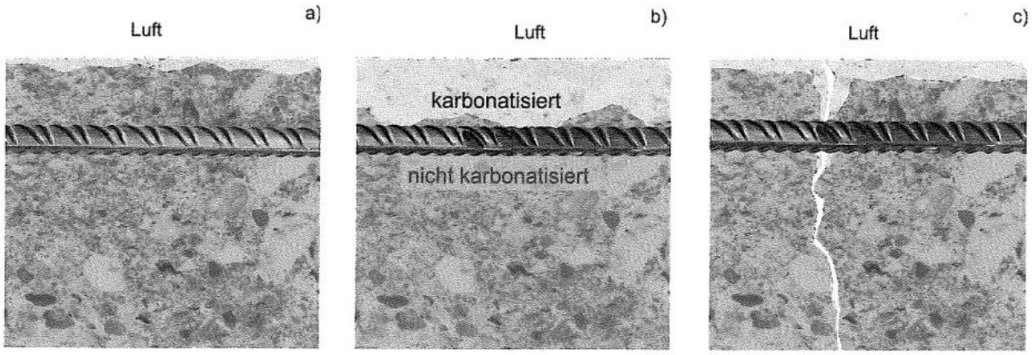


Figure 2.9: Carbonation progresses [25]

Although corrosion occurs in a small area within a crack, the chemical attack progresses rapidly and spreads into the surrounding concrete. Many factors contribute to the process, including crack width, pore structure, and the quality of the concrete cover, which are affected by the water-cement ratio, compaction, and curing quality. ACI Committee 224 (2007) notes that crack widths up to about 0,5 mm do not directly increase corrosion intensity, but they

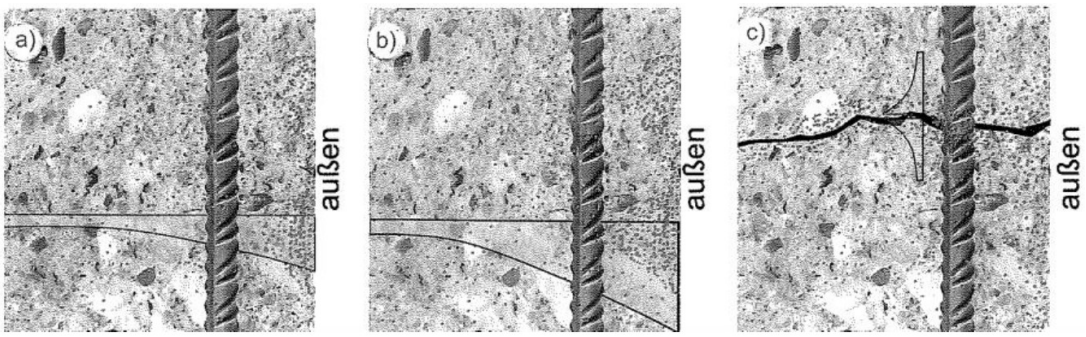


Figure 10: Chloride Ions Penetration from surface concrete (Röhling & Meichsner, 2017)

Figure 2.10: Chloride ions penetration from surface concrete [25]

accelerate the initiation phase by allowing faster transport of air and moisture. In this sense, cracks serve as accelerators of chemical deterioration, and when corrosion begins, the expansion of rust products induces secondary cracking and spalling. Hence, while cracks can start for mechanical reasons, chemical processes take over and progressively weaken the structure and reduce its durability over time [25].

Summary

In summary, crack propagation in concrete originates from the interaction between material properties and restraining stresses. Microcracks first form in weak zones, such as the ITZ, due to internal stresses from shrinkage and thermal effects. These can grow into larger macrocracks under increased tensile stress, weakening the structure and allowing harmful agents, such as carbonation- and chloride-induced corrosion, to cause deterioration. Understanding this process is vital for predicting service life and improving durability.

2.2.2 Crack control techniques in reinforced concrete structures

Understanding the mechanics of crack initiation and propagation is required to predict service life and to develop and implement efficient crack management techniques. In reinforced concrete structures, following the crack management methods specified by codes and design guidelines is considered important for reducing the width of cracks.

Design and detailing strategies for crack control

Although material properties define the inherent tendency of concrete to crack, design and detailing methods are paramount for controlling where and how cracks occur. The primary objective is to distribute reinforcement effectively to control crack widths within an acceptable limit, while the incorporation of joints may relieve tensile stresses before uncontrolled cracking occurs.

Providing sufficient reinforcement is the first step in controlling cracking. A minimum area of reinforcement must be provided to ensure that steel can carry the tensile force released when cracking occurs, thereby preventing sudden brittle failure. This principle appears consistently in Eurocode 2 and has also been emphasized in practical studies such as Röhling & Meichsner (2017).

Furthermore, for a given steel area, using a larger number of smaller-diameter bars at a closer spacing is more effective than using fewer, larger bars. In tests by Gilbert and Nejadi (2004), beams with closely spaced bars of smaller diameters exhibited finer and more closely spaced cracks, while fewer beams with fewer bars and larger spacing developed wider and more widely distributed cracks. This is because bond stress is transferred more efficiently between concrete and steel when the bars are placed closer together, resulting in a greater number of cracks with smaller individual crack widths.

In larger slabs, walls or other members subject to significant restraint, it is often more effective to guide cracking than to resist it. To prevent concrete from cracking in random, unsightly patterns, planned contraction joints can be used to relieve the internal stresses caused by shrinkage and temperature changes. This ensures that any cracks that form will follow straight, predictable lines, thus improving the appearance and durability of the structures [5].

Material-based measures

VGU Vietnamese-German University

Material composition plays a decisive role in controlling crack formation because it governs shrinkage, tensile capacity and internal restraint of the concrete. The fundamental strategy involves optimizing the constituent materials to mitigate the driving forces behind cracking and to enhance the resistance of concrete.

The most critical parameter is the water-cement ratio (w/c). A low w/c ratio (typically below 0,45) is crucial for achieving a high-strength paste matrix and low permeability, which helps limit the ingress of harmful agents such as chlorides and carbon dioxide. It is important to note, however, that while a low w/c ratio reduces drying shrinkage, it can increase the potential for autogenous shrinkage due to self-desiccation in finer capillary pores [21].

Bisschop [3] demonstrated that the aggregate skeleton provides internal restraint against shrinkage of the cement paste. Increasing aggregate volume is one of the most effective and fundamental strategies for reducing the total shrinkage of the cement paste matrix and increasing internal restraint. A higher aggregate volume can significantly reduce both the total crack length (TCL) and the maximum crack depth (MCD). To achieve greater restraint, an aggregate with a higher modulus of elasticity may be used to better resist matrix shrinkage. Similarly, composites containing glass, ceramic, or steel spheres have been shown to exhibit significantly less microcracking than those containing soft polymers. In addition, it is preferable to use more angular aggregates, which are associated with a moderate reduction in TCL and less extensive crack patterns compared with smooth spherical aggregates.

Modern research confirms that shrinkage-reducing admixtures (SRA) use surfactants to

lower capillary tension, effectively reducing both autogenous and drying shrinkage. Furthermore, internal curing using superabsorbent polymers (SAPs) helps maintain internal humidity during hydration, thereby mitigating early-age shrinkage in large-scale reinforced concrete members. In addition, SAPs enhance resistance to carbonation and chloride penetration, providing a practical strategy to improve the long-term durability of concrete structures [16][26].

Construction and curing practices

Even when the concrete mix and reinforcement are well-designed, poor construction and curing practices can still lead to problems. Therefore, proper placement, compaction, temperature control and curing are crucial for minimizing cracking at early stages. According to the report ACI Committee 224.1 published in 2007, many construction-related problems, including inadequate vibration, insufficient consolidation, and poor formwork support during placement, are among the principal causes of settlement and early cracking before the concrete reaches its mature strength.

Among all site measures, proper curing is the most effective and economical way to prevent plastic and drying shrinkage cracking. Thus, it is essential to maintain sufficient moisture and appropriate temperature conditions immediately after concrete finishing in order to support ongoing cement hydration. For example, applying a plastic covering or liquid-applied curing membrane can help keep the surface saturated and reduce tensile stresses. Effective curing also improves the concrete microstructure, thereby reducing permeability and the long-term risk of reinforcement corrosion [8].

VGU Vietnamese-German University

Code-based crack width prediction and limits

As crack formation in reinforced concrete is inevitable, design codes normally focus on controlling rather than preventing cracks. The main objective of code-based crack control is to ensure that cracks remain sufficiently narrow to avoid impairing the durability, stiffness and appearance of concrete throughout its service life. Hence, crack control is considered a serviceability limit state (SLS) rather than a strength requirement.

Normally, the conceptual design among standards is largely similar, although the analytical procedures may differ. Crack control is achieved by limiting steel stress and tensile strain through an adequate distribution of reinforcement. In particular, the Eurocode 2 design philosophy adopts a strain-based approach, derived from the mean strain difference between steel and concrete, ensuring that the concrete envelope protects the reinforcement and that crack widths remain compatible with durability requirements. Other international codes, such as ACI 318 and the fib Model Code 2010, follow the same principle but apply alternative empirical methods.

Regarding the numerical limits on crack widths, the codes are primarily concerned with environmental exposure rather than structural strength. In EN 1992-1-1:2004, characteristic

crack width limits range from 0,4 mm to 0,2 mm. The draft EN 1992-1-1:2021 maintains quite a similarity but introduces more explicit guidance for highly aggressive exposure classes. These limits reflect durability and aesthetic considerations that corrosion initiation and moisture ingress occur slowly enough to be negligible within the structural design provisions.

Summary

Efficient crack management in reinforced concrete requires a balance among design, materials, construction techniques, and codified compliance. It begins at the design stage: well-positioned joints and sufficiently spaced reinforcement help balance structural reaction and tensile demand, leading to small, innocuous cracks. Material optimization includes a low water-to-cement ratio, sufficient aggregate content and sophisticated admixtures such as SRA or SAP in pursuit of improved internal restraint and reduced shrinkage. Hydration and continuity are maintained by appropriate compaction, temperature control and curing in order to avoid early-age cracking. Finally, code-based standards such as Eurocode 2, which distill the physical mechanics of cracking into useful and service design guidance, formalize and validate those practical solutions. These code provisions limit the allowable crack width based on environmental exposure, ensuring long-term structural performance and providing the framework for the comparative code evaluation in the following chapter.

VGU
Vietnamese-German University

2.3 Summary

The reviewed literature shows that cracking in concrete is not a single isolated phenomenon; rather, it results from the interaction of mechanical, shrinkage, and chemical processes. Although these explanations for cracks are useful, their mechanisms often overlap in real structures. In practice, cracking is usually governed not only by the presence of tensile stress, but also by restraint conditions, bond behavior, reinforcement detailing, member geometry, curing quality and environmental exposure.

A key outcome of the literature review is that not all crack types are equally relevant to code-based crack-width prediction. Load-induced cracking is most directly related to the crack control methods used in reinforced concrete design, which are linked to reinforcement strain, crack spacing, and the effective zone. In contrast, shrinkage and thermal cracks are more strongly influenced by restraints, moisture loss, and hydration effects, which are more difficult to capture with a simplified design method alone. This suggests that code provisions are effective for normal flexural crack control, but they cannot fully replace good detailing, curing, and construction practice when early-age or restraint-induced cracking governs.

The literature also makes clear that propagation from microcracks to macrocracks is the critical link between serviceability and durability. Microcracks first develop in weak zones such as the interfacial transition zone, then spread larger and connect under continued tensile stress. Once visible cracks form, they create pathways for moisture, carbon dioxide, and chlorides, accelerating corrosion and causing long-term deterioration. As a result, crack control should not be understood only as an aesthetic requirement, but also as a fundamental durability strategy.

From the perspective of this thesis, the most important implication is that crack control models must be evaluated not only by their mathematical formulation, but also by how well they reflect the physical mechanisms of cracking in reinforced concrete members. For this reason, the following chapter compares the provisions of EN 1992-1-1:2004 and EN 1992-1-1:2021 not merely as different calculation procedures, but as two different approaches to representing crack spacing, strain development and crack width in structural design.

3. Code Provisions for Crack Control

Reinforced concrete structures are prone to cracking. It cannot be completely avoided; therefore, it must be managed to guarantee the structure's serviceability, longevity, and aesthetic performance. This chapter describes the crack control procedures outlined in Eurocode 2 (EN 1992-1-1), focusing on the notable improvements introduced in the 2021 version.

The primary objective of this section is to outline the code provisions governing crack width calculations and control. The crack width w_k is calculated based on three principal factors, including the average strain in the reinforcement and concrete, the average crack spacing and the stress level in the reinforcement. Whether simplified or refined approaches are used, these models are built upon the fundamental relationship expressed in Equation (3.22). This chapter will explore the application of this principle in both the 2004 and 2021 versions of Eurocode 2, citing the relevant clauses throughout.

3.1 New Eurocode 2

VGU
Vietnamese-German University

Significant improvements over the 2004 version are included in the most recent iteration of Eurocode 2 (EN 1992-1-1:2021), which aims to enhance material optimization, design efficiency and usability. Improved crack width calculations and reinforcement detailing guidelines are two important updates that guarantee structures fulfill strict serviceability and durability standards over time.

3.1.1 General considerations

Cracking in reinforced concrete structures is a normal occurrence due to direct loading or restrained imposed deformations. Other factors, such as plastic shrinkage or expansive chemical reactions, can also cause cracking. Where crack control is required, minimum reinforcement in accordance with Clause 3.2.2 should be provided in all sections where tensile stresses are expected. This applies where the reinforcement has not already been determined by ultimate limit state (ULS) design in accordance with sections 3.2.3 and 3.2.4. For lapping bar diameters exceeding 32 mm, transverse reinforcement should be provided, along with additional skin reinforcement along the lap length.

In cases where crack widths exceed 0,4 mm, several risks can occur in member locations after suddenly changing the stress, including changes of section, near concentrated loads, positions where bars are curtailed, and areas of high bond stress. Therefore, to limit the crack width, the following measures may be applied:

- Choosing a suitable structural concept

- Prestressing
- Limiting the reinforcement and concrete stresses
- Appropriate detailing and concrete property selection
- Proper curing of concrete

In this new version of Eurocode 2021, stress and crack limits are divided more specifically into two main criteria: appearance and durability, as shown in Table 3.1 and Table 3.2.

Table 3.1: Verifications, stress, and crack width limits for appearance (EN 1992-1-1:2021, Table 9.1 (NDP))

Verification	**Calculation of minimum reinforcement for crack control according to 9.2.2 under imposed deformation**	**Maximum bar diameter or maximum bar spacing according to 9.2.3 or alternatively Verification of crack width according to 9.2.4**	**Verification of reinforcement stresses to avoid yielding at SLS**
Combination of actions for calculating σ_s	Cracking forces according to 9.2.2	Quasi-permanent combination of actions	Characteristic combination of actions
Limiting value of crack width $w_{lim,cal}$ or stress σ_s	$\sigma_s \leq f_{yk}$ or $\sigma_s \leq \sigma_{s,lim}$ [a]	$w_{lim,cal} = 0{,}4$ mm $\sigma_s \leq f_{yk}$ or $\sigma_s \leq \sigma_{s,lim}$ [a]	$\sigma_s \leq 0{,}8 f_{yk}$ $\sigma_p \leq 0{,}8 f_{pk}$
NOTE $w_{lim,cal} = 0{,}4$ mm applies unless a National Annex gives different values.			
[a] A lower value $\sigma_s < f_{yk}$ may be needed to satisfy the crack width limits according to the maximum bar size (see Formula (9.5)).			

VGU Vietnamese-German University

Table 3.1 defines verification methods to control crack widths for aesthetic purposes, linking each method to specific load combinations and stress limits under various conditions:

- Minimum reinforcement for crack control under imposed deformations (section 3.2.2) aims to ensure sufficient steel is present to limit crack widths under restraint-induced cracking. Following cracking, the stress in the reinforcement must not exceed the yield strength or the lower stress limit, which may be specified in more detail in Equation (3.5).
- Maximum bar diameter or bar spacing for crack width verification (section 3.2.3 or 3.2.4) is based on quasi-permanent loads, and the default crack width value is 0,4 mm unless modified by the National Annex (NA).
- Avoid yielding in SLS for reinforcement stress verification is verified under characteristic loads, and stress must be kept below 80% of the yield strength to prevent excessive cracking.

Table 3.2 defines the maximum permissible crack widths $w_{\text{lim,cal}}$ based on exposure classes to prevent material degradation. This table considers exposure classes, types of structures, and the combinations of actions for crack width verification.

Table 3.2: Verifications, stress, and crack width limits for durability (EN 1992-1-1:2021, Table 9.2 (NDP))

Exposure Class	**Reinforced members; prestressed members with unbonded tendons and with bonded tendons with Protection Levels 2 or 3 according to 5.4.1(3)**		**Prestressed members with bonded tendons with Protection Level 1 according to 5.4.1(3) and pretensioned elements.**		
	combination of actions		**combination of actions**		
	quasi-permanent	**characteristic**	**quasi-permanent**	**frequent**	**characteristic**
X0, XC1	–	–	–	$w_{\text{lim,cal}} = 0{,}2\ \text{mm} \cdot k_{\text{surf}}$	–
XC2, XC3, XC4	$w_{\text{lim,cal}} = 0{,}3\ \text{mm} \cdot k_{\text{surf}}$		Decom-pression [b]	$w_{\text{lim,cal}} = 0{,}2\ \text{mm} \cdot k_{\text{surf}}$	
XD1, XD2, XD3 XS1, XS2, XS3		$\sigma_c \leq 0{,}6 f_{ck}$ [a,c]	–	Decompression[b]	$\sigma_c \leq 0{,}6 f_{ck}$ [a,c]
XF1, XF3 XF2, XF4	–				

NOTE 1 The specified values of $w_{\text{lim,cal}}$ apply unless a National Annex gives different values.

NOTE 2 The factor k_{surf} considers the difference between an increased crack width at the member surface and the required mean crack width i according to durability performance of the minimum cover: $1{,}0 \leq k_{\text{surf}} = c_{\text{act}}/(10\ \text{mm} + c_{\text{min,dur}}) \leq 1{,}5$.

c_{act} is a specified actual cover $\geq c_{\text{nom}}$ due to detailing or execution reasons.

[a] No limitation in serviceability conditions is necessary for stresses under bearings, partially loaded areas and plates of headed bars.

[b] The decompression limit requires that all parts of the bonded tendons or duct lie at least 25 mm within concrete in compression.

[c] The compressive stress σ_c may be increased to $0{,}66 f_{ck}$ if the cover is increased by 10 mm or confinement by transverse reinforcement is provided.

For instance, the maximum crack width for class XC2 is 0,3 mm with the factor k_{surf} under quasi-permanent loads for reinforced members. For prestressed members with bonded tendons with protection level 1, decompression must remain in compression with at least 25 mm bonded to prevent corrosion, and the maximum crack width for frequent loads is less than that of reinforced members, which is 0,2 mm with the factor k_{surf}. Additionally, the compression stress limits may be set at $0{,}6 f_{ck}$, which is the default limit to avoid microcracking, or $0{,}66 f_{ck}$ if the cover is increased by 10 mm or confinement is provided.

Regarding the factor k_{surf}, it considers the difference between an increased crack width at

the member surface and the required mean crack width:

$$k_{\text{surf}} = \frac{c_{\text{act}}}{10\,\text{mm} + c_{\text{min,dur}}} \qquad (1{,}0 \leq k_{\text{surf}} \leq 1{,}5) \tag{3.1}$$

where

c_{act} specified actual cover $\geq c_{\text{nom}}$

$c_{\text{min,dur}}$ minimum cover for durability given in Table 3.3 and Table 3.4

Table 3.3: Minimum concrete cover $c_{\text{min,dur}}$ for carbon steel - Carbonation (EN 1992-1-1:2021, Table 6.3 (NDP))

ERC	Exposure class (carbonation)							
	XC1		XC2		XC3		XC4	
	Design service life (years)							
	50	100	50	100	50	100	50	100
XRC 0,5	10	10	10	10	10	10	10	10
XRC 1	10	10	10	10	10	15	10	15
XRC 2	10	15	10	15	15	25	15	25
XRC 3	10	15	15	20	20	30	20	30
XRC 4	10	20	15	25	25	35	25	40
XRC 5	15	25	20	30	25	45	30	45
XRC 6	15	25	25	35	35	55	40	55
XRC 7	15	30	25	40	40	60	45	60

VGU Vietnamese-German University

From Table 3.3 and Table 3.4, the minimum concrete covers $c_{\text{min,dur}}$ depends on the lifespan design up to 100 years, exposure class and exposure resistance class (ERC). The ERC class is further classified into two categories, XRC, which specifies a resistance preventing corrosion induced by chloride ingress from penetration depth and XRDS, which specifies resistance against carbonation-induced corrosion.

3.1.2 Minimum reinforcement areas

Minimum reinforcement in reinforced concrete structures serves two critical purposes: controlling crack widths under service loads and preventing sudden brittle failure at ultimate loads. To achieve this, the reinforcement must be designed to resist the combined effects of bending moments and axial forces at a specified stress limit, ensuring the concrete section remains stable under actions. The required minimum reinforcement area can be calculated for three primary loading conditions, including pure bending, pure tension, and combined bending with axial force.

Table 3.4: Minimum concrete cover $c_{\text{min,dur}}$ for carbon steel - Chlorides (EN 1992-1-1:2021, Table 6.4 (NDP))

ERC	Exposure class (chlorides)											
	XS1		XS2		XS3		XD1		XD2		XD3	
	Design service life (years)						Design service life (years)					
	50	100	50	100	50	100	50	100	50	100	50	100
XRDS 0,5	20	20	20	30	30	40	20	20	20	30	30	40
XRDS 1	20	25	25	35	35	45	20	25	25	35	35	45
XRDS 1,5	25	30	30	40	40	50	25	30	30	40	40	50
XRDS 2	25	30	35	45	45	55	25	30	35	45	45	55
XRDS 3	30	35	40	50	55	65	30	35	40	50	55	65
XRDS 4	30	40	50	60	60	80	30	40	50	60	60	80
XRDS 5	35	45	60	70	70	—	35	45	60	70	70	—
XRDS 6	40	50	65	80	—	—	40	50	65	80	—	—
XRDS 8	45	55	75	—	—	—	45	55	75	—	—	—
XRDS 10	50	65	80	—	—	—	50	65	80	—	—	—

For pure bending:

$$A_{\text{s,min,w1}} = \frac{0{,}8\,\dfrac{h - h_{\text{c,eff}}}{h}\, f_{\text{ct,eff}} A_{\text{c,eff}}}{\sigma_{\text{s,lim}}} \geq \frac{0{,}2\, k_{\text{h}} f_{\text{ct,eff}} A_{\text{c}}}{f_{\text{yk}}}; \qquad A_{\text{s,min,w2}} = 0 \tag{3.2}$$

For pure tension:

$$A_{\text{s,min,w1}} = A_{\text{s,min,w2}} = \frac{f_{\text{ct,eff}} A_{\text{c,eff}}}{\sigma_{\text{s,lim}}} \geq \frac{0{,}5\, k_{\text{h}}\, f_{\text{ct,eff}} A_{\text{c}}}{f_{\text{yk}}} \tag{3.3}$$

For a combination of bending and axial force:

$$A_{\text{s,min,w1}} = \frac{0{,}3N_{\text{Ed}} + 0{,}8\,\dfrac{h - h_{\text{c,eff}}}{h}\, f_{\text{ct,eff}} A_{\text{c,eff}}}{\sigma_{\text{s,lim}}} \begin{cases} \geq \dfrac{0{,}3N_{\text{Ed}} + 0{,}2\, k_{\text{h}} f_{\text{ct,eff}} A_{\text{c}}}{f_{\text{yk}}} \\ \geq 0 \\ \leq \max\left\{ \dfrac{f_{\text{ct,eff}} A_{\text{c,eff}}}{\sigma_{\text{s,lim}}};\ \dfrac{0{,}5\, k_{\text{h}} f_{\text{ct,eff}} A_{\text{c}}}{f_{\text{yk}}} \right\} \end{cases} \tag{3.4}$$

$$A_{\text{s,min,w2}} = \frac{N_{\text{Ed}}}{\sigma_{\text{s,lim}}} - A_{\text{s,min,w1}} \qquad (0 \leq A_{\text{s,min,w2}} \leq A_{\text{s,min,w1}})$$

where

A_{c} the concrete area of the part of the section

$A_{s,min,w1}$ the minimum reinforcing steel area at the most tensioned face

$A_{s,min,w2}$ the minimum reinforcing steel area at the least tensioned face

The maximum stress permitted in the reinforcement can be figured out as the following, which ensures the resulting crack width remains below the allowable limit:

$$\sigma_{s,lim} \leq \frac{2{,}4 f_{ct,eff}}{h - h_{c,eff}} \cdot \frac{h}{\phi} \left(-c + \sqrt{c^2 + 1{,}5 \frac{\left(1 - \frac{h_{c,eff}}{h}\right) E_s \, w_{lim,cal} \phi}{k_w \, k_{1/r,simpl} \, f_{ct,eff}}} \right) \tag{3.5}$$

where

$k_{1/r,simpl} = 1{,}0$ for pure tension

$k_{1/r,simpl} = \left(1{,}2\frac{h}{d} - 0{,}1\right)$ for other cases

k_w a factor converting mean crack width into a calculated crack width in Section 3.2.4

$f_{ct,eff} = f_{ctm}$ the mean value of the tensile strength of the effective concrete

k_h a coefficient that allows for the effect of non-uniform self-equilibrating stresses, expressed as

$$k_h = 0{,}8 - 0{,}6\,(\min\{b; h\} - 0{,}3) \qquad (0{,}5 \leq k_h \leq 0{,}8)$$

VGU Vietnamese-German University

If a section has more than one layer of bar and one bar diameter, an equivalent bar diameter should be used in the expression Equation (3.6):

$$\phi_{eq} = \frac{n_1 \phi_1^2 + n_2 \phi_2^2}{n_1 \phi_1 + n_2 \phi_2} \tag{3.6}$$

For beams with a deep section exceeding 600 mm at the most highly stressed tension reinforcement, extra longitudinal reinforcement must be added to prevent excessive side-face cracking. This reinforcement should be spaced no more than 300 mm apart in the Equation (3.7) and placed between the neutral axis and the layer of main reinforcement nearest to it. This ensures proper crack control along the sides of the beam.

$$A_{s,web} = 0{,}2 \frac{f_{ct,eff}}{f_{yk}} \cdot b_w \cdot (d - x - a_1) \tag{3.7}$$

where

$A_{s,web}$ the additional longitudinal reinforcement on the two surfaces of the web

a_1 equal to 150 mm

3.1.3 Simplified control of cracking

The updated version of Eurocode simplifies crack control with clear guidelines for bar diameters and spacing.

Bar diameter

This expression provides a limiting condition for the bar diameter, ensuring that the resulting crack widths do not exceed the allowable crack width $w_{\text{lim,cal}}$. In the updated version of the standard, the allowable bar diameter and corresponding bar spacing depend on multiple parameters, including the reinforcement ratio, the ratio between the distance and effective depth, the allowable crack width, steel stress or strain, and a series of coefficients that account for flexural crack distribution, bond characteristics, and member geometry.

$$\phi \leq \frac{2{,}1\,\rho_{\text{p}}}{\frac{r}{d}\,k_{\text{fl,simpl}}\,k_{\text{b,simpl}}}\left(\frac{w_{\text{lim}}}{k_{\text{w}}\,k_{1/\text{r,simpl}}\,0{,}9\frac{\sigma_{\text{s}}}{E_{\text{s}}}}-1{,}5c\right) \tag{3.8}$$

where

$r = c_{\text{nom}} + \frac{\phi}{2}$ the edge distance of the first bar layer's centroid

$k_{\text{fl,simpl}} = \left(1 - 3{,}5\frac{a_{\text{y}}}{h}\right)$ if one face is in compression

$k_{\text{fl,simpl}} = 1{,}0$ if both faces are in tension

$k_{1/\text{r,simpl}} = 25\left(\frac{h}{d}-1\right)\rho_{\text{p}}+1{,}15\left(\frac{h}{d}\right)-0{,}1$

$k_{\text{b,simpl}} = 0{,}9$ for good bond conditions

$k_{\text{b,simpl}} = 1{,}2$ for poor bond conditions

The dependence of simplified factor $k_{1/\text{r,simpl}}$ on the reinforcement ratio reflects that an increase in reinforcement extends the compression zone, resulting in greater curvature at a constant steel strain.

Bar spacing

The maximum permissible bar spacing s_{l} is influenced by the same factors as the maximum allowable bar diameter. The formula ensures that the expected crack width remains within acceptable limits by limiting bar spacing, which plays a critical role in distributing and controlling cracks effectively.

$$s_1 \leq \frac{3{,}45\,\rho_p}{\frac{r^2}{d}\,k_{fl,simpl}^2\,k_{b,simpl}^2}\left(\frac{w_{lim,cal}}{k_w\,k_{1/r,simpl}\,0{,}9\frac{\sigma_s}{E_s}} - 1{,}5c\right)^2 \tag{3.9}$$

where

s_l bar spacing

σ_s stress permitted in the reinforcement closest to the most tensioned concrete surface after formation of all cracks and may be taken as the calculated stress from loads or the lower limit stress in Equation (3.5)

k_w a factor converting the mean crack width into a calculated crack width in Section 3.2.4

$\rho_p = \frac{A_s + \xi A_p}{b\,d}$ the reinforcement ratio

$k_{1/r,simpl} = 1{,}0$ for conservative

3.1.4 Refined control of cracking

In the direct method calculation, the crack width in reinforced concrete structures depends on three main factors. A coefficient k_w accounts for the bond properties between the steel reinforcement and the surrounding concrete. Second is the average crack spacing, showing how far apart cracks tend to form, being shown in detail in the following parts. Lastly, the difference in strains between the steel reinforcement and the concrete at the crack position indicates the amount of steel that has stretched due to loading, and the expression can be found Equation (3.15).

Calculated crack width

The updated crack width calculation is determined as the product of the new converting factor k_w, the mean crack spacing $s_{rm,cal}$ and the difference between the strain of the reinforcement ε_{sm} and the concrete ε_{cm}.

$$w_{k,cal} = k_w \cdot s_{rm,cal} \cdot (\varepsilon_{sm} - \varepsilon_{cm}) \tag{3.10}$$

where

$k_w = 1{,}7$ a factor converting the mean crack width into a calculated crack width

$s_{rm,cal}$ the calculated mean crack spacing

ε_{sm} the mean strain in the reinforcement closest to the most tensioned concrete surface

ε_{cm} the mean strain in the concrete between cracks at the same level of ε_{sm}

Different mean strains

The mean strains difference can be calculated using the following equation:

$$\varepsilon_{sm} - \varepsilon_{cm} = k_{1/r} \frac{\sigma_s - k_t \frac{f_{ct,eff}}{\rho_{p,eff}} \left(1 + \alpha_e \rho_{p,eff}\right)}{E_s} \geq 0{,}6 \frac{\sigma_s}{E_s} \tag{3.11}$$

where

σ_s the stress in tension reinforcement

$\alpha_e = \frac{E_s}{E_{cm}}$ the ratio between the modulus of elasticity of steel and concrete

$\rho_{p,eff}$ the effective reinforcement ratio

$$\rho_{p,eff} = \frac{A_s + \xi_1 A_p}{A_{c,eff}} \tag{3.12}$$

A_p the area of pre-tensioning or bonded post-tensioning tendons

$A_{c,eff}$ the effective area of concrete in tension surrounding the reinforcement, as shown in Figure 3.1 and Figure 3.2

VGU Vietnamese-German University

k_t a coefficient dependent on the duration and nature of the load as follows

$k_t = 0{,}6$ a) for short-term loading, or b) instantaneous loading, or c) long-term and crack formation stage, or d) repeated loading and crack formation stage

$k_t = 0{,}4$ e) long-term and stabilized cracking stage, or f) repeated loading and stabilized cracking stage

$k_{1/r}$ a curvature coefficient for the increase of the crack width

$k_{1/r} = \frac{h - x}{h - a_{y,i} - x}$ for general cases

$k_{1/r} = \frac{|x|}{a_{y,s} + |x|}$ when considering the least tensioned face of an element with both faces in tension

The effective area of concrete in tension is defined as the area surrounding the tensile reinforcement, with a depth of:
For a single layer of bars:

$$h_{c,eff} = \min\left\{ r_y + 5\phi;\ 10\phi;\ 3{,}5 r_y \right\} \leq |h - x| \tag{3.13}$$

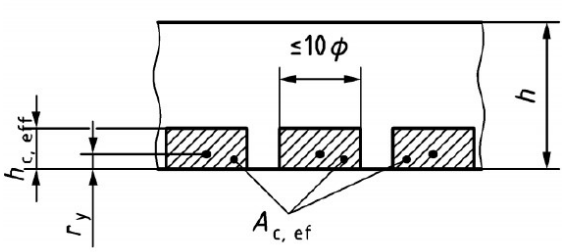


Figure 3.1: Isolated bars

For n layers of bars spaced s_y:

$$h_{c,eff} = \min\left\{r_y + 5\phi;\ 10\phi;\ 3{,}5r_y\right\} + s_y \leq |h - x| \tag{3.14}$$

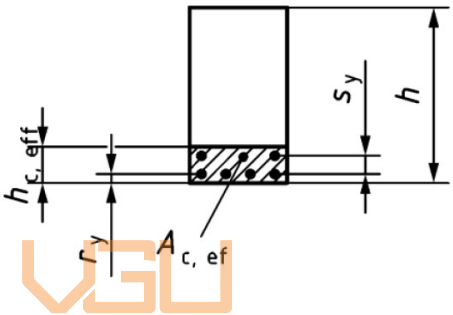


Figure 3.2: Group of bars

Another case of different mean strains is for elements subjected to restrained imposed strains and restrained at the edges may be calculated from the expression:

$$\varepsilon_{sm} - \varepsilon_{cm} = R_{ax}\varepsilon_{free} - k_t\frac{f_{ct,eff}}{E_{cm}} \geq 0 \tag{3.15}$$

where

$R_{ax} = 1 - \frac{\varepsilon_{restr}}{\varepsilon_{imp}}$	the restraint factor
$R_{ax} = 0{,}5$	for the very common case of the base of a wall
ε_{restr}	the strain which develops in the restrained element
ε_{imp}	the value of the imposed strain
ε_{free}	the imposed strain that develops after the construction stage

Mean crack spacing

Mean crack spacing refers to the average distance between cracks in reinforced concrete under tension. It depends on various factors, defined as

$$s_{r,m,cal} = 1{,}5c + \frac{k_{fl}k_b}{7{,}2} \cdot \frac{\phi}{\rho_{p,eff}} \leq 1{,}3(h - x) \tag{3.17}$$

where

k_{fl} factor accounts for the stress distribution within the effective concrete in tension area

$k_{fl} = \frac{h - h_{c,eff}}{h}$ for a rectangular cross-section subjected to pure bending

$k_{fl} = \frac{1}{2}\left(1 + \frac{h - x_g - h_{c,eff}}{h - x_g}\right)$ for general cases

x_g the depth of the neutral axis of the uncracked section

$k_b = 0{,}9 + 0{,}6\frac{\phi}{c_v}$ for elements cast in a poor casting position

$k_b = 0{,}9$ for elements cast in a good casting position

$k_{fl} = 1{,}0$ for pure tension

c_v the clear vertical cover of the bar to the top concrete surface

c the clear cover of the bar

VGU Vietnamese-German University

If the spacing of bonded reinforcement in the tension zone exceeds 10 times the bar diameter (10ϕ) or if no bonded reinforcement is present in the tension zone, the maximum crack spacing shall be calculated as follows:

$$s_{r,max} = 1{,}3(h - x) \tag{3.16}$$

3.2 Existing Eurocode 2

Crack control in reinforced concrete structures, as outlined in Eurocode 2 (EN 1992-1-1:2004), is governed by the principles of the SLS. The primary objective of crack control is to ensure that cracking remains within acceptable limits, preserving both the appearance and functionality of the structure while also safeguarding its durability over time.

3.2.1 General considerations

Cracking is an inherent behavior in reinforced concrete due to its composite nature, where the brittle concrete matrix is combined with ductile steel reinforcement. Structural mechanics provides the foundation for understanding this phenomenon. Cracks develop when the tensile strength of concrete is exceeded, which can occur under various forms of mechanical stress such as bending, shear, torsion, and direct tension. These stresses may result from external loads, restraints, or imposed deformations like thermal or shrinkage effects.

In addition to mechanical causes, material-related factors can also lead to cracking. These include plastic shrinkage during early-age concrete curing and expansive chemical reactions within the hardened concrete. These phenomena can compromise the integrity of concrete, even in the absence of external loading.

To manage cracking, Eurocode 2 provides recommended maximum crack width limits, which are essential for maintaining structural performance, especially in aggressive environments. These limits are summarized in Table 5 of the 2004 version, considering various parameters such as load types, bond conditions of the reinforcement, and exposure classes.

VGU Vietnamese-German University

Table 3.5: Recommended values of w_{max} (mm) (EN 1992-1-1:2004, Table 7.1N)

Exposure Class	**Reinforced members and prestressed members with unbonded tendons**	**Prestressed members with bonded tendons**
	Quasi-permanent load combination	**Frequent load combination**
X0, XC1	0,4[1]	0,2
XC2, XC3, XC4	0,3	0,2[2]
XD1, XD2, XS1, XS2, XS3		Decompression
Note 1: For X0, XC1 exposure classes, crack width has no influence on durability and this limit is set to give generally acceptable appearance. In the absence of appearance conditions this limit may be relaxed.		
Note 2: For these exposure classes, in addition, decompression should be checked under the quasi-permanent combination of loads.		

The exposure classes, defined based on environmental severity, range from non-aggressive

conditions (e.g. X0, XC1) to highly aggressive environments involving carbonation (XC2–XC4).

The permissible crack widths vary depending on both the environmental exposure and the structural system (reinforced vs prestressed concrete, bonded vs unbonded tendons). For example, in environments with minimal exposure risks like class XC1, where aesthetic concerns are minor, the limit may be relaxed up to 0,4 mm. In contrast, in highly aggressive environments such as XD3 or XS3, more stringent control is necessary, often requiring additional protective measures. These criteria are crucial for designing durable structures and preventing long-term deterioration due to environmental factors. Eurocode 2 offers two primary approaches for controlling cracks:

- Simplified method rules (section 3.3.3) – This approach uses prescriptive limits on bar spacing and bar diameters to ensure crack widths remain within acceptable limits. This method is often sufficient for standard design situations, especially when environmental conditions are less aggressive.
- Explicit crack width calculation (section 3.3.4) – This method involves calculating expected crack widths based on strain compatibility, reinforcement detailing, and material properties. It allows for precise control and is preferred in critical design scenarios.

As stated in section 3.3.4, crack widths can be calculated. Alternatively, a simplified method is to limit the size or spacing of the bars, as outlined in section 3.3.3.

VGU Vietnamese-German University

Both methods aim to balance structural efficiency with durability requirements. By adhering to the guidance in Eurocode 2, engineers can ensure that cracking does not lead to unacceptable performance or premature deterioration, particularly in structures exposed to challenging environmental conditions.

3.2.2 Minimum reinforcement areas

To prevent cracking in concrete elements that experience restraint or direct tension, Eurocode 2 mandates a minimum level of reinforcement. The main goal of this requirement is not to eliminate cracking entirely but to ensure that, if cracks occur, they are evenly distributed and limited in width. This approach helps maintain both structural integrity and long-term durability, especially under SLS conditions.

The minimum area of reinforcement is determined based on the tensile force that could cause deformation in the concrete section. This calculation is guided by Equation (4.1.2) in the standard, which links the required reinforcement area to the expected tensile force and the stress capacity of the reinforcing steel. This equation is used for the reinforcement position at which surface is more in tension of the determined cross-section (A_{ct}).

$$A_{s,min} = \frac{k_c \, k \, f_{ct,eff} \, A_{ct}}{\sigma_s} \tag{3.17}$$

where

$A_{s,min}$ the minimum reinforcing steel within the tensile zone

A_{ct} $= b \cdot h/2$

σ_s the permissible stress in the reinforcement immediately after cracking

$f_{ct,eff}$ the effective tensile strength of concrete at the time of cracking

k $= 1{,}0$ for webs with $h \leq 300$ mm or flanges with $b < 300$ mm

$= 0{,}65$ for webs with $h \geq 800$ mm or flanges with $b > 800$ mm

Other intermediate values are interpolated.

$k_c = 1{,}0$ for pure tension

for bending or bending combined with axial forces:

- for rectangular sections and webs of box sections and T-sections

$$k_c = 0{,}4\left[1 - \frac{\sigma_c}{k_1 \cdot (h/h^*) \cdot f_{ct,eff}}\right] \leq 1 \tag{3.18}$$

VGU Vietnamese-German University

- for rectangular sections and T- sections in the formula Equation (3.19)

$$k_c = 0{,}9\left[\frac{F_{cr}}{A_{ct} \cdot f_{ct,eff}}\right] \geq 0{,}5 \tag{3.19}$$

σ_c the mean stress of the concrete acting on the part of the section under consideration

$$\sigma_c = \frac{N_{Ed}}{bh} \tag{3.24}$$

N_{Ed} is the axial force

h^* adjusts based on section depth:

$h^* = h$ for $h < 1{,}0$ m

$h^* = 1{,}0$ m for $h \geq 1{,}0$ m

k_1 is a coefficient considering the effects of axial forces on the stress distribution

$k_1 = 1{,}5$ for compressive force

$k_1 = \frac{2h^*}{3h}$ for tensile forces

F_{cr} the absolute value of the tensile force within the flange immediately before cracking

The selection of stress σ_s in this calculation is critical and depends on factors such as bond conditions between steel and concrete and the bar diameter used. By incorporating these variables, the design ensures that the reinforcement is effective in controlling crack widths and avoiding localized failures, especially in zones vulnerable to tension. The coefficient k accounts for the influence of non-uniform self-equilibrating stresses, which reduce the effective restraint forces. On the other hand, coefficient k_c takes account of the stress distribution within the section immediately before cracking, values may be interpolated. For the details specific cases of k and k_c, which are referred to in the following.

A robust strategy is implemented to ensure that, even in the presence of axial forces or moments, the reinforcement provided is more than sufficient to effectively manage cracks and limit their width to acceptable levels, thus meeting essential serviceability and durability objectives.

In prestressed concrete members, when the combined effects of external loads and the prestressing force keep the section either fully in compression or subject to very low tensile stress (below a specified threshold), there is no need for minimum reinforcement for crack control. This is significant as the absence of cracks negates the requirement for reinforcement to address them.

VGU
Vietnamese-German University

3.2.3 Crack control without direct calculation

It is possible to identify a design limitation for bar diameter and spacing as an alternative to a direct crack width calculation. This approach ensures that the resulting crack widths under load and restraint loading remain constrained, as illustrated in the subsequent Table 3.6 and Table 3.7. These tables present the maximum permissible bar diameters for various steel stress levels and the critical restrictions on bar spacing. The tables are based on standardized assumptions regarding material properties, concrete cover, and stress distribution. They are intended to ensure that cracking remains within acceptable visual or functional limits.

Table 3.6 is used to find the maximum allowable bar diameter for the calculated service stress and the limited crack width value. Limiting crack width is based on the exposure class and loading types as defined in Table 3.5.

Table 3.7 then provides the maximum allowable bar spacing for the same stress and crack width values. For example, if the calculated steel stress based on the section analysis for the SLS combination loads is 280 MPa and the required crack width is 0,3 mm (for exposure class XC4), the simplified tables would specify that the maximum bar diameter is 12 mm and the maximum spacing is 150 mm. Therefore, reinforcement must be arranged using bars no larger than 12 mm and spaced no more than 150 mm apart to satisfy crack control requirements without direct calculation.

Table 3.6: Maximum bar diameter for crack control

Steel stress[2] [MPa]	Maximum bar size [mm]		
	$w_k = 0{,}4$ mm	$w_k = 0{,}3$ mm	$w_k = 0{,}2$ mm
160	40	32	25
200	32	25	16
240	20	16	12
280	16	12	8
320	12	10	6
360	10	8	5
400	8	6	4
450	6	5	–

Table 3.7: Maximum bar spacing for crack control

Steel stress[2] [MPa]	Maximum bar spacing [mm]		
	$w_k = 0{,}4$ mm	$w_k = 0{,}3$ mm	$w_k = 0{,}2$ mm
160	300	300	200
200	300	250	150
240	250	200	100
280	200	150	50
320	150	100	–
360	100	50	–

VGU Vietnamese-German University

Importantly, if the minimum reinforcement given by 3.3.2 is provided, crack widths typically remain acceptable when restraint-induced cracking, such as shrinkage, thermal effects, and bar diameters comply with Table 3.6, using steel stress from Equation (4.1.2). For the load-induced cracking, either Table 3.6 or Table 3.7 is followed, with stresses calculated for cracked sections under service loads.

Furthermore, adjustments are provided for special structural conditions. For instance, in bending sections where part of the section remains in compression, the maximum allowable bar diameter may be reduced using the expression Equation (3.20).

$$\phi_s = \phi_s^* \frac{f_{ct,eff}\, h_{cr}}{2{,}9\,(h-d)\cdot 2} \tag{3.20}$$

Similarly, in members subjected to uniform axial tension, a more stringent limit may be applied as expression Equation (3.21). These modifications account for changes in effective height and stress distribution, improving the reliability of crack control in more complex situations.

$$\phi_s = \phi_s^* \frac{f_{ct,eff}\, h_{cr}}{2{,}9\,(h-d)\cdot 8} \tag{3.21}$$

where

ϕ_s the adjusted maximum bar diameter

ϕ_s^* the maximum bar size given in Table 3.6

h the overall depth of the section

h_{cr} the tensile zone depth immediately prior to cracking

d the effective depth to the centroid of the outer layer of reinforcement

In deep beams (d $\geq$ 1000 mm), crack control may be compromised if reinforcement is concentrated in a narrow region. To address this, additional skin reinforcement should be provided along the side faces of the beam to distribute cracks more evenly and avoid excessive surface crack widths. The skin reinforcement should be placed between the level of tension steel and the neutral axis, and its area should not be less than that calculated from 3.3.2(2), using conservative assumptions, taking coefficient k as 0,5, and σ_s as f_{yk}. The steel stress used for skin reinforcement can also be taken as half the value of the main tension steel for simplification.

Finally, special care must be taken at locations where there are abrupt changes in stress, such as near changes in cross-section, concentrated loads, curtailed bars, or lap joints, since these zones are prone to wider cracks. While the simplified rules often provide adequate control, adherence to reinforcement detailing rules is outside the scope of this section.

VGU Vietnamese-German University

3.2.4 Crack control with direct calculation

As an introduction, crack width control may also be performed by direct calculation, which will be shown in more detail in this section. In order to calculate crack width, there are two key parameters, including the maximum crack spacing and the difference of mean strains, directly affect the calculation in the following expression Equation (3.22).

$$w_k = s_{r,max} \cdot (\varepsilon_{sm} - \varepsilon_{cm}) \tag{3.22}$$

where

$s_{r,max}$ the maximum crack spacing

ε_{sm} the mean strain in the reinforcement under the relevant combination of loads

ε_{cm} the mean strain in the concrete between cracks

The difference in mean strains between reinforcement and concrete can be further derived using:

$$\varepsilon_{sm} - \varepsilon_{cm} = \frac{\sigma_s - k_t \frac{f_{ct,eff}}{\rho_{p,eff}} \left(1 + \alpha_e \rho_{p,eff}\right)}{E_s} \geq 0{,}6 \frac{\sigma_s}{E_s} \tag{3.23}$$

where

σ_s the steel stress in tension

α_e the ratio E_s/E_{cm}, with E_{cm} being the modulus of elasticity of concrete

k_t a time-dependent factor

$k_t = 0.6$ for short-term loading

$k_t = 0.4$ for long-term loading

$\rho_{p,eff}$ the effective reinforcement ratio

$$\rho_{p,eff} = \frac{A_s}{A_{c,eff}} \tag{3.24}$$

$A_{c,eff}$ the effective area of concrete in tension surrounding the reinforcement

$h_{c,eff}$ the effective height in tensile area

$$h_{c,eff} = \min\left\{2{,}5(h-d); \frac{h-x}{3}; \frac{h}{2}\right\} \tag{3.25}$$

The effective area of concrete $A_{c,eff}$ can be estimated as the product of the member width and the effective tension depth $h_{c,eff}$. When only the overall section depth of the concrete structure is known, the $h_{c,eff}$ should be taken as the minimum of three possible values, clearly shown in the expression Equation (3.25). This conservative approach ensures proper crack width calculations by considering the most restrictive tension zone. Regarding crack spacing, it is influenced by several factors and may be calculated using the following expression

VGU Vietnamese-German University

$$s_{r,max} = k_3 c + k_1 k_2 k_4 \frac{\phi}{\rho_{p,eff}} \tag{3.26}$$

where

ϕ bar diameter

c the cover to the longitudinal reinforcement

k_1 a bond coefficient

$k_1 = 0{,}8$ for high bond bars

$k_1 = 1{,}6$ for plain surface bars

k_2 the strain distribution factor

$k_2 = 0{,}5$ for bending

$k_2 = 1{,}0$ for pure tension

k_3 typically 3,4

k_4 typically 0,425

In addition, maximum crack spacing can also be estimated according to the German DIN standard and in Schneider Bautabellen, using the following equation:

$$s_{r,max} = \frac{\phi_s}{3{,}6\,\rho_{p,eff}} \leq \frac{\sigma_s \phi_s}{3{,}6\,f_{ct,eff}} \tag{3.27}$$

In cases where reinforcement is not evenly distributed or exceeds the spacing limit with the spacing $s \leq 5\,(c + \phi/2)$, the following simplified expression may be used:

$$s_{r,max} = 1{,}3(h - x) \tag{3.28}$$

where h is the section depth and x is the neutral axis depth. In cases where crack spacing is significant, particularly when the angle between the axis of principal stress and the direction of reinforcement in two orthogonal directions exceeds 15°, it may be calculated as follows

$$s_{r,max} = \frac{1}{\dfrac{\cos\theta}{s_{r,max,y}} + \dfrac{\sin\theta}{s_{r,max,z}}} \tag{3.29}$$

where θ is the angle between the reinforcement and the principal tensile stress directions.

VGU
Vietnamese-German University

3.3 Summary

This chapter has provided a comprehensive overview of crack control provisions in Eurocode 2, showing the evolution from the established 2004 standard to the updated 2021 version. The new code provides a unified framework for calculating minimum reinforcement (Section 3.2.2) that separately handles pure tension, pure bending and combined actions. Furthermore, the refined method for direct crack width calculations (Section 3.2.4) introduces a new converting factor k_w, converting mean crack width to a calculated design value.

The 2021 edition successfully addresses several critical gaps than in the previous version. A highlight advancement is the clear separation of crack width limits into distinct criteria for appearance and durability, providing much clearer design guidance. This is complemented by the introduction of the k_{surf} factor, which accounts for influence of concrete cover depth to create a more realistic link between calculation and durability performance. Unlike the 2004 version, the minimum cover is just based on exposure class, while the updated code depends on design life (50 and 100 years) and exposure resistance class (XRC/XRDS), which helps to integrate durability design with life-cycle approach. The code also offers more refined rules for complex scenarios, such as the refined definition of the effective concrete area in tension $h_{c,eff}$ for members with multiple layers of reinforcement.

In conclusion, these refinements address previous gaps such as the unclear separation between durability and aesthetic limits and reliance on empirical tables by providing a unified analytical basis for crack width control. The new Eurocode 2 represents a substantial step forward in the design, ensuring improved prediction of serviceability and structural lifespan.

The following table synthesizes the key differences between the two code versions, highlighting this evolution:

Table 3.8: Comparison of crack-control provisions in EN 1992-1-1:2004 and EN 1992-1-1:2021

Point	**EN 1992-1-1:2004**	**EN 1992-1-1:2021**	**Note on improvement**
Crack width limits ($w_{k,max}$)	Table 7.1N	Table 9.1 NDP for appearance Table 9.2 NDP for durability, introducing k_{surf} factor	EC 2:2021, $c_{min,dur}$ (see section 3.3.1)
Minimum reinforcement ($A_{s,min}$)	$A_{s,min} = \dfrac{k_c \cdot k \cdot f_{ct,eff} \cdot A_{ct}}{\sigma_s}$	(i) $A_{s,min,w1} = \dfrac{0{,}8 \cdot \dfrac{h - h_{c,eff}}{h} f_{ct,eff} A_{c,eff}}{\sigma_{s,lim}} \geq \dfrac{0{,}2 k_h f_{ct,eff} A_c}{f_{yk}}$ $A_{s,min,w2} = 0$ (ii) $A_{s,min,w1} = A_{s,min,w2} = \dfrac{f_{ct,eff} A_{c,eff}}{\sigma_{s,lim}} \geq \dfrac{0{,}5 k_h f_{ct,eff} A_c}{f_{yk}}$ (iii) $A_{s,min,w1} = \dfrac{0{,}3 N_{Ed} + 0{,}8 \cdot \dfrac{h - h_{c,eff}}{h} f_{ct,eff} A_{c,eff}}{\sigma_{s,lim}} \begin{cases} \geq \dfrac{0{,}3 N_{Ed} + 0{,}2 k_h f_{ct,eff} A_c}{f_{yk}} \\ \geq 0 \\ \leq \max\left\{ \dfrac{f_{ct,eff} A_{c,eff}}{\sigma_{s,lim}}, \dfrac{0{,}5 k_h f_{ct,eff} A_c}{f_{yk}} \right\} \end{cases}$ $A_{s,min,w2} = \dfrac{N_{Ed}}{\sigma_{s,lim}} - A_{s,min,w1} \quad (0 \leq A_{s,min,w2} \leq A_{s,min,w1})$	EC 2:2021, $\sigma_{s,lim}$ (see section 3.3.2 in more detail). (i) for pure bending; (ii) for pure tension; (iii) for a combination and axial force.
Bar diameter limits (ϕ_s)	Table 7.2N for maximum bar diameter For bending: $\phi_s = \phi_s^* \dfrac{f_{ct,eff}}{2{,}9} \dfrac{k_c \cdot h_{cr}}{(h-d) \cdot 2}$ For tension: $\phi_s = \phi_s^* \dfrac{f_{ct,eff} \cdot h_{cr}}{2{,}9 \cdot (h-d) \cdot 8}$	$\phi \leq \dfrac{2{,}1 \rho_p}{\dfrac{r}{d} \cdot k_{fl,simpl} \cdot k_{b,simpl}} \left(\dfrac{w_{lim}}{k_w \cdot k_{1/r,simpl} \cdot 0{,}9 \dfrac{\sigma_s}{E_s}} - 1{,}5c \right)$	
Bar spacing (s_l)	Table 7.3N for maximum bar spacing	$s_l \leq \dfrac{3{,}45 \rho_p}{\dfrac{r^2}{d} \cdot k_{fl,simpl}^2 \cdot k_{b,simpl}^2} \left(\dfrac{w_{lim,cal}}{k_w \cdot k_{1/r,simpl} \cdot 0{,}9 \dfrac{\sigma_s}{E_s}} - 1{,}5c \right)^2$	
Crack spacing (s_r)	(i) $s_{r,max} = k_3 c + k_1 k_2 k_4 \dfrac{\phi}{\rho_{p,eff}}$ (ii) $s_{r,max} = 1{,}3(h-x)$ (iii) $s_{r,max} = \dfrac{1}{\dfrac{\cos\theta}{s_{r,max,y}} + \dfrac{\sin\theta}{s_{r,max,z}}}$	(i) $s_{r,m,cal} = 1{,}5c + \dfrac{k_{fl} k_b}{7{,}2} \cdot \dfrac{\phi}{\rho_{p,eff}} \leq 1{,}3(h-x)$ (ii) $s_{r,max} = 1{,}3(h-x)$	EC 2:2004: (i) for $s_r \leq 5(c + \phi/2)$; (ii) for $s_r > 5(c + \phi/2)$; (iii) for angle between directions $> 15^\circ$ EC 2:2021: (i) for $s \leq 10\phi$; (ii) $s > 10\phi$
Effective height ($h_{c,eff}$)	$h_{c,eff} = \min\left\{ 2{,}5(h-d);\ \dfrac{h-x}{3};\ \dfrac{h}{2} \right\}$	(i) $h_{c,eff} = \min\{r_y + 5\phi;\ 10\phi;\ 3{,}5 r_y\} \leq \lvert h - x \rvert$ (ii) $h_{c,eff} = \min\{r_y + 5\phi;\ 10\phi;\ 3{,}5 r_y\} + s_y \leq \lvert h - x \rvert$	EC 2:2021: (i) for a single layer of bars; (ii) for multiple layers of bars
Mean strains ($\varepsilon_{sm} - \varepsilon_{cm}$)	$\varepsilon_{sm} - \varepsilon_{cm} = \dfrac{\sigma_s - k_t \dfrac{f_{ct,eff}}{\rho_{p,eff}} \left(1 + \alpha_e \rho_{p,eff}\right)}{E_s} \geq 0{,}6 \dfrac{\sigma_s}{E_s}$	(i) $\varepsilon_{sm} - \varepsilon_{cm} = k_{1/r} \dfrac{\sigma_s - k_t \dfrac{f_{ct,eff}}{\rho_{p,eff}} \left(1 + \alpha_e \rho_{p,eff}\right)}{E_s} \geq 0{,}6 \dfrac{\sigma_s}{E_s}$ (ii) $\varepsilon_{sm} - \varepsilon_{cm} = R_{ax} \varepsilon_{free} - k_t \dfrac{f_{ct,eff}}{E_{cm}} \geq 0$	EC 2:2021: (i) for direct loads or imposed strains (ii) for restrained imposed strains and restrained at edges
Crack width (w_k)	$w_k = s_{r,max} \cdot (\varepsilon_{sm} - \varepsilon_{cm})$	$w_{k,cal} = k_w \cdot s_{rm,cal} \cdot (\varepsilon_{sm} - \varepsilon_{cm})$	EC 2:2021: $k_w = 1{,}7$

Vietnamese-German University

4. Application

4.1 Example for crack control calculation

4.1.1 Objective of the example

To illustrate the differences between the two versions of Eurocode 2, a comparative analysis is performed using hand calculations applied to a specific example. The example involves a typical, straightforward design of reinforced concrete structures where no special crack control measures are required. The calculations are presented step-by-step and implemented in an Excel spreadsheet to avoid repetitive manual work, reduce time consumption, and improve accuracy compared to handwritten methods. The objective is to identify and visualize key differences in intermediate parameters, providing numerical and graphical basis for comparing the two code versions before introducing experimental data. The reinforcement used in the example is uncoated, and the slab design does not incorporate any specialized crack control techniques. This analysis draws upon the direct provisions of the Eurocodes, supported by supplementary references such as the habilitation work of Tran, and the Schneider Bautabellen für Ingenieur mit Berechnungshinweisen und Beispielen by Albert.

VGU
Vietnamese-German University

4.1.2 Calculation procedure

To provide a broader basis for comparison between standards, a total of 15 specimens is considered, combining five section thicknesses (150 mm, 300 mm, 500 mm, 700 mm, 1000 mm) with three reinforcement diameters (12 mm, 14 mm, and 16 mm). The options of 10 mm and 20 mm bars were excluded, as the former is structurally insufficient for thicker beams and the latter is impractical for thin sections, which would hinder a meaningful comparison.

This variation enables the changes to be more effectively illustrated through graphical visualization, offering clearer insights than presenting only a single beam. Nevertheless, one specimen (E01.01) with a thickness of 150 mm and bar diameter 12 mm is selected as a representative case for detailed calculations, demonstrating both step-by-step procedures and conceptual methods.

To ensure consistency and avoid confounding effects, all beams are designed using the same concrete mix design, including identical steel grade, concrete cover, curing conditions, geometric dimensions, and loading conditions. Furthermore, the reinforcement ratio is kept as consistent as possible across all beams, ensuring a comparable steel contribution relative to the cross-section, with values maintained around 0,0029–0,0030. The only exception is found in the specimens with a thickness of 150 mm, where the reinforcement ratio shows a huge

difference due to the requirement; this variation will be explained in detail in the calculation section.

For the illustrated single-span slab with the thickness of 150 mm, shown in Figure 13, the imposed loads include the self-weight $g_{1,k}$, the weight of non-structural load $g_{2,k} = 1{,}5\ \text{kN/m}^2$ for assumption, and a live load $q_{1,k} = 3{,}0\ \text{kN/m}^2$, based on a typical office building assumption according to EN 1991-1-1:2021, Table 6.2. Regarding material properties, the design adopts exposure class XC1/XC2, concrete grade C25/30, and reinforcing steel grade B500.

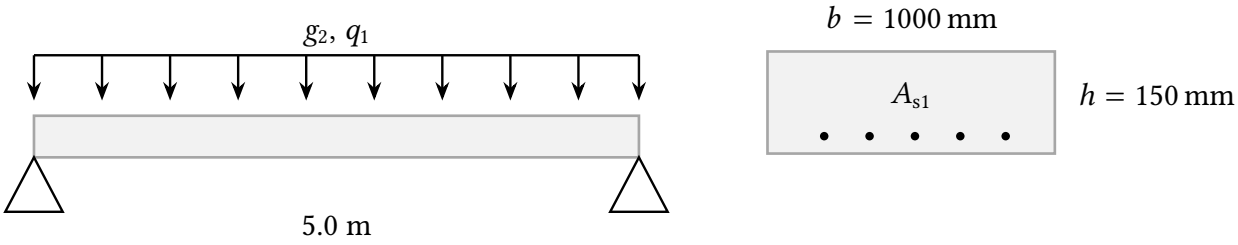


Figure 4.1: Simple reinforced slab and cross-section

Bending Design

Step 1: Concrete cover and effective depth

A longitudinal bar diameter of $\phi_{s,l} = 12$ mm is pre-selected. The nominal concrete cover is determined from

Vietnamese-German University

$$c_{nom} = c_{min} + \Delta c_{dev}$$

The minimum concrete cover is calculated as

$$c_{min} = \max\{c_{min,dur} - \Delta c_{dur,red} + \Delta c_{dur,abr};\ c_{min,b};\ 10\,\text{mm}\}$$

Substituting the selected values, including $c_{min,dur} = 15$ mm for XRC3 with design service life of 50 years, $\delta c_{dur,abr} = 0$ with no mechanical attack, $c_{min,b} = 12$ mm taken from Case 5, and $\delta c_{dev} = 5$ mm also taken from Case 5 (Kap. 6.5.3 for more detail).

$$c_{min} = \max\{15 - 10 + 0;\ 12;\ 10\} = 12\,\text{mm}$$

Thus,

$$c_{nom} = 12 + 5 = 17\,\text{mm}$$

A concrete cover of $c_v = 25$ mm is adopted, which satisfies

$$c_v \geq c_{nom}$$

The distance from the tension face to the centroid of the tensile reinforcement is therefore

$$d_1 = c_v + \frac{\phi_{s,l}}{2} = 25 + \frac{12}{2} = 31\,\text{mm}$$

Hence, the effective depth becomes

$$d = h - d_1 = 150 - 31 = 119\,\text{mm}$$

Step 2: Bending design in ULS

The design bending moment under ULS conditions is calculated using the design loads, applying safety factors of 1,35 for dead loads and 1,5 for live loads along the slab span. The design bending moment is

$$M_{Eds} = \frac{q_{1,d} + g_{1,d} + g_{2,d}}{8} \cdot l^2 = \frac{1{,}50 \cdot 3 + 1{,}35 \cdot (1{,}5 + 0{,}15 \cdot 1 \cdot 25)}{8} \cdot 5^2 = 36{,}21\,\text{kNm}$$

To determine the required reinforcement (A_{s1}), the ω-method is used, as referenced in the DIN standard and Schneider Tabellen, shown in Table 4.1. Based on the calculated coefficient μ_{Eds}, the corresponding value ω_1 is identified as 0,2007, from which the necessary reinforcement area is derived.

$$\mu_{Eds} = \frac{M_{Ed}}{b \cdot d^2 \cdot f_{cd}} = \frac{36{,}21}{1 \cdot 0{,}119^2 \cdot 14{,}17 \cdot 10^3} = 0{,}181$$

VGU Vietnamese-German University

The design material strengths are

$$f_{cd} = \frac{0{,}85\, f_{ck}}{1{,}5} = \frac{0{,}85 \cdot 25}{1{,}5} = 14{,}17\,\text{MPa} \tag{4.1}$$

$$f_{yd} = \frac{f_{yk}}{1{,}15} = \frac{500}{1{,}15} = 435\,\text{MPa} \tag{4.2}$$

Using the ω-method, the required reinforcement area is

$$A_{s1} = \omega_1 \cdot b \cdot d \cdot \frac{f_{cd}}{f_{yd}} + \frac{N_{Ed}}{f_{yd}} = 0{,}2007 \cdot 1 \cdot 0{,}119 \cdot \frac{14{,}17}{435} + \frac{0}{435} = 7{,}78\,\text{cm}^2$$

Thus, the required tensile reinforcement is $A_{s1} = 7{,}78\,\text{cm}^2$. Adopting $7\phi12$ provides

$$A_s = 7{,}92\,\text{cm}^2$$

The reinforcement ratio is

$$\rho_s = \frac{A_s}{b \cdot d} = \frac{7{,}92}{100 \cdot 11{,}9} = 0{,}0067$$

This results in a required A_{s1} of 7,78 cm^2, for which $7\phi12$ with A_s of 7,92 cm^2, would be selected, exceeding both the calculated requirement and the minimum reinforcement value presented

later. However, adopting $7\phi12$ would produce a reinforcement ratio of around 0,0066, significantly higher than the consistent target value of approximately 0,0029 and 0,0030, making incomparable comparison among specimen thicknesses. Alternatively, $3\phi12$ could be used, which meets the minimum reinforcement and results in a ratio closer to the target range. Nevertheless, this option would lead to higher steel stress and exceed the maximum allowable bar diameter for crack control, as discussed in later sections. Therefore, $7\phi12$ is ultimately selected to ensure both safety and compliance with design requirements.

VGU
Vietnamese-German University

μ_{Eds}	ω_1	$\xi = x/d$	$\zeta = z/d$	ε_{c2}	ε_{s1}	σ_{sd}
				‰	‰	N/mm^2
0,01	0,0101	0,030	0,990	-0,77	25,00	456,5
0,02	0,0203	0,044	0,985	-1,15	25,00	456,5
0,03	0,0306	0,055	0,980	-1,46	25,00	456,5
0,04	0,0410	0,066	0,976	-1,76	25,00	456,5
0,05	0,0515	0,076	0,971	-2,06	25,00	456,5
0,06	0,0621	0,086	0,967	-2,37	25,00	456,5
0,07	0,0728	0,097	0,962	-2,68	25,00	456,5
0,08	0,0836	0,107	0,956	-3,01	25,00	456,5
0,09	0,0946	0,118	0,951	-3,35	25,00	456,5
0,10	0,1058	0,131	0,946	-3,50	23,29	454,9
0,11	0,1170	0,145	0,940	-3,50	20,71	452,4
0,12	0,1285	0,159	0,934	-3,50	18,55	450,4
0,13	0,1401	0,173	0,928	-3,50	16,73	448,6
0,14	0,1519	0,188	0,922	-3,50	15,16	447,1
0,15	0,1638	0,202	0,916	-3,50	13,80	445,9
0,16	0,1759	0,217	0,910	-3,50	12,61	444,7
0,17	0,1882	0,232	0,903	-3,50	11,55	443,7
0,18	0,2007	0,248	0,897	-3,50	10,62	442,8
0,19	0,2134	0,264	0,890	-3,50	9,78	442,0
0,20	0,2263	0,280	0,884	-3,50	9,02	441,3
0,21	0,2395	0,296	0,877	-3,50	8,33	440,6
0,22	0,2529	0,312	0,870	-3,50	7,71	440,1
0,23	0,2665	0,329	0,863	-3,50	7,13	439,5
0,24	0,2804	0,346	0,856	-3,50	6,60	439,0
0,25	0,2946	0,364	0,849	-3,50	6,12	438,5
0,26	0,3091	0,382	0,841	-3,50	5,67	438,1
0,27	0,3239	0,400	0,834	-3,50	5,25	437,7
0,28	0,3391	0,419	0,826	-3,50	4,86	437,3
0,29	0,3546	0,438	0,818	-3,50	4,49	437,0
5.4 (NA.5): Linear-elastische Berechnung Biegebauteile $\xi > 0{,}45$ → Druckbewehrung empfehlenswert → A5						
0,30	0,3706	0,458	0,810	-3,50	4,15	436,7
0,31	0,3869	0,478	0,801	-3,50	3,82	436,4
0,32	0,4038	0,499	0,793	-3,50	3,52	436,1
0,33	0,4211	0,520	0,784	-3,50	3,23	435,8
0,34	0,4391	0,542	0,774	-3,50	2,95	435,5
0,35	0,4576	0,565	0,765	-3,50	2,69	435,3
0,36	0,4768	0,589	0,755	-3,50	2,44	435,0
0,37	0,4968	0,614	0,745	-3,50	2,20	434,8
Bemessungswert der Fließgrenze des Betonstahls wird unterschritten → Druckbewehrung empfehlenswert						

Table 4.1: Omega table without compression reinforcement.

Vietnamese-German University

Simplified crack width control according to EN 1992-1-1:2004

Step 1: Bending design in SLS

To assess crack width, a bending design under serviceability limit state conditions is necessary. This follows a similar process to the bending design in ultimate limit state conditions, but it applies different load combinations specific to service conditions. According to Schneider Bautabellen Table 5.31, the combination factors for office buildings are 0,7 for rare load case, 0,5 for frequent load case, and 0,3 for quasi-permanent load case. In practice, more realistic assumptions for the load case are recommended about 20% of the self-weight for non-structural surfaces and 50% of the live load. Such an approach gives more reasonable crack width predictions, as it better reflects the long-term deflection, creep, and crack development. However, for the purpose of simplification in this study, the quasi-permanent load case is taken as 20% of the ULS. This leads to smaller crack width values since the calculation is largely governed by the self-weight. Based on this simplification, the resulting quasi-permanent bending moment MSLS is 19,22 kNm. For the quasi-permanent load combination,

$$q_{\text{Ed,per}} = g_{1,\text{k}} + g_{2,\text{k}} + \psi_2 q_{1,\text{k}} = (1 \cdot 0{,}15 \cdot 25) + 1{,}5 + (3 \cdot 1 \cdot 0{,}3) = 6{,}15\,\text{kN/m}$$

The corresponding bending moment is

$$M_{\text{Ed,per}} = q_{\text{Ed,per}} \cdot \frac{l^2}{8} = 6{,}15 \cdot \frac{5{,}0^2}{8} = 19{,}22\,\text{kNm}$$

VGU Vietnamese-German University

The neutral axis depth can initially be estimated from the x/d ratio, using the effective depth and the reference values provided in the ω-method table. This ratio indicates the position of the neutral axis relative to the effective depth, which is crucial for defining stress distribution in the concrete section, verifying ductile behavior, and calculating the lever arm z for internal moment equilibrium. However, for the remaining section thicknesses, the bending moment is low relative to the section capacity, causing the calculated x/d to fall outside the range provided by the table. In such cases, an alternative formula from the habilitation work of Tran [27] (section 2.2.6), corresponds to Equation (4.3), is applied. Using this method, the final neutral axis depth x and lever arm z are 48 mm and 103 mm respectively. Using the adopted relation according to Tran,

$$k_{\text{x}} = \frac{x}{d} = \left(\sqrt{1 + \frac{2}{n_{\text{e}}\rho_{\text{s}}}} - 1\right) \cdot n_{\text{e}} \cdot \rho_{\text{s}} \tag{4.3}$$

$$k_{\text{x}} = \frac{x}{d} = \left(\sqrt{1 + \frac{2}{20 \cdot 0{,}0067}} - 1\right) \cdot 20 \cdot 0{,}0067 \approx 0{,}40$$

$$x = k_{\text{x}} \cdot d = 0{,}40 \cdot 119 = 47{,}6\,\text{mm}$$

Hence,

$$z = d - \frac{x}{3} = 119 - \frac{48}{3} = 103\,\text{mm}$$

Correctly determining the neutral axis depth x is vital for evaluating reinforcement strain and ensuring crack control. Since crack formation is linked to the tensile strain in the reinforcement and the tension zone depth, knowing the neutral axis position leads to a more accurate estimate of crack width and overall serviceability performance.

Step 2: Steel stress in the tensile reinforcement

Under bending, the tensile stress in the reinforcement σ_s can be estimated by dividing the design bending moment M_{Ed} by the product of the lever arm z and the area of tensile reinforcement A_s. The tensile steel stress is

$$\sigma_s = \frac{M_{Ed,per}}{z \cdot A_s} = \frac{19{,}22/1000}{0{,}103 \cdot 7{,}92 \cdot 10^{-4}} \approx 236\,\text{N/mm}^2 \tag{4.4}$$

It reflects the internal force equilibrium in a reinforced concrete section, where the bending moment is resisted by a couple formed by compressive forces in the concrete and tensile forces in the reinforcement. As a result, the calculated tensile stress in the reinforcement σ_s is roughly 236 N/mm².

VGU Vietnamese-German University

Step 3: Crack control without direct calculation

In the indirect method of crack width control, the allowable crack width is limited based on the exposure class. For exposure class XC2, the maximum allowable crack width is

$$w_{max} = 0{,}3\,\text{mm}$$

Using the calculated steel stress $\sigma_s = 236\,\text{N/mm}^2$ and this allowable crack width, the maximum permissible bar diameter ϕ_s^* and bar spacing s_{max} can be determined with the guidance of Table 3.6 and Table 3.7. In this example, a bar diameter of 12 mm and a spacing of 150 mm were selected, both of which comply with the prescribed limits.

To improve accuracy, an adjusted bar diameter ϕ_s is estimated using Equation (3.22) which accounts for the section's steel stress and geometric factors. The effective tension height is determined according to Eurocode 2 as follows

$$h_{c,eff} = \min\left\{2{,}5(h-d); \frac{h-x}{3}; \frac{h}{2}\right\} = \min\left\{2{,}5(150-119); \frac{150-47{,}6}{3}; \frac{150}{2}\right\} = 34{,}13\,\text{mm}$$

For $f_{ck} = 25\,\text{MPa}$, the design tensile strength of concrete is

$$f_{ctm} = 0{,}3 f_{ck}^{2/3} = 0{,}3 \cdot 25^{2/3} = 0{,}3 \cdot 8{,}55 = 2{,}56\,\text{MPa}$$

Substituting these values in Equation (3.20), the adjusted maximum bar diameter can be calculated as follows

$$\phi_s = \phi_s^* \frac{f_{ct,eff}\, h_{cr}}{2{,}9\,(h-d)\cdot 2} = 12 \cdot \frac{2{,}56 \cdot 34{,}13}{2{,}9 \cdot 31 \cdot 2} \approx 5{,}83\,\text{mm}$$

This value is significantly lower than the limiting maximum diameter based on the tensile steel stress,

$$\phi_{s,max} = \frac{f_{ct,eff}}{2{,}9} = 10{,}76\,\text{mm}$$

which indicates that the crack control requirement is satisfied. The resulting value of ϕ_s = 5,83 mm is significantly lower than the limiting maximum diameter based on tensile stress (10,76 mm), confirming that the selected reinforcement $\phi = 12\,\text{mm}$ is acceptable, which is larger than the requirement.

VGU
Vietnamese-German University

Refined crack width control according to EN 1992-1-1:2004 and DIN EN 1992-1-1/NA

Step 1: Effective reinforcement ratio

The effective height is

$$h_{c,eff} = \min\left\{2{,}5(h-d);\ \frac{h-x}{3};\ \frac{h}{2}\right\} = \min\left\{2{,}5\cdot 31;\ \frac{150-47.6}{3};\ \frac{150}{2}\right\} = 34{,}13\,\text{mm}$$

Thus, the effective concrete area becomes

$$A_{c,eff} = b\cdot h_{c,eff}\cdot 10^{-2} = 1000\cdot 34{,}13\cdot 10^{-2} = 341{,}3\ \text{cm}^2$$

The effective reinforcement ratio is

$$\rho_{p,eff} = \frac{A_s}{A_{c,eff}} = \frac{7{,}92}{341{,}3} = 0{,}0232$$

Step 2: Mean strain difference

For the long-term analysis, the effective concrete modulus is determined as follows

$$E_{c,eff} = \frac{E_{cm}}{1+\varphi(\infty,t_0)} \tag{4.5}$$

VGU Vietnamese-German University

The following parameters are adopted:

- $E_{cm} = 31\,000$ MPa, taken as the mean modulus of elasticity of concrete for the selected strength class
- $\varphi(\infty,t_0) = 2{,}1$, taken as the creep coefficient for a relative humidity of 80% and a loading age of $t_0 = 28$ days

Substituting these values into Equation (4.5) gives

$$E_{c,eff} = \frac{31\,000}{1+2{,}1} = 10\,000\,\text{MPa}$$

Based on the effective concrete modulus, the modular ratio is obtained as

$$\alpha_e = \frac{E_s}{E_{c,eff}} = \frac{200000}{10000} = 20$$

The mean strain difference is calculated as follows with $k_t = 0{,}4$ assuming long-term effect

$$\varepsilon_{sm} - \varepsilon_{cm} = \frac{\sigma_s - k_t\dfrac{f_{ct,eff}}{\rho_{p,eff}}\left(1+\alpha_e\rho_{p,eff}\right)}{E_s} \geq 0{,}6\frac{\sigma_s}{E_s}$$

$$\varepsilon_{sm} - \varepsilon_{cm} = 0{,}000857 > 0{,}000708$$

Hence, the conservative value is adopted.

$$\varepsilon_{sm} - \varepsilon_{cm} = 0{,}000857$$

Step 3: Maximum crack spacing

According to EN 1992-1-1:2004,

$$s_{r,max} = 3{,}4c + 0{,}8 \cdot 0{,}5 \cdot 0{,}425 \frac{\phi}{\rho_{p,eff}} = 3{,}4 \cdot 25 + 0{,}8 \cdot 0{,}5 \cdot 0{,}425 \frac{12}{0{,}0232} = 173\,\text{mm}$$

According to the DIN expression,

$$s_{r,max} = \frac{\phi}{3{,}6\rho_{p,eff}} = \frac{12}{3{,}6 \cdot 0{,}0232} = 143{,}7\,\text{mm}$$

The geometric limitation gives

$$s_{r,max} = 1{,}3(h - x) = 1{,}3(150 - 48) = 132{,}6\,\text{mm}$$

For a conservative design, the governing value is therefore

$$s_{r,max} = 132{,}6\,\text{mm}$$

VGU Vietnamese-German University

The mean crack spacing may be approximated as

$$s_{r,m} \approx 0{,}75\, s_{r,max} \approx 100\,\text{mm}$$

Step 4: Crack width

The crack width is

$$w_k = s_{r,m}\,(\varepsilon_{sm} - \varepsilon_{cm}) \approx 0{,}112\,\text{mm}$$

Thus, the calculated crack width is well below the allowable limit of 0,3 mm.

Minimum reinforcement according to EN 1992-1-1:2004

The minimum reinforcement is calculated using the following expression

$$A_{s,min} = \frac{k_c \, k \, f_{ct,eff} \, A_{ct}}{\sigma_s}$$

with $k_c = 0{,}4$ for the case of pure bending and $k = 1{,}0$ for the case of member depth below 300 mm, thus

$$A_{s,min} = \frac{0{,}4 \cdot 1{,}0 \cdot 2{,}56 \cdot 341{,}3}{236} = 1{,}48\,\text{cm}^2$$

Since

$$A_{s,min} = 1{,}48\,\text{cm}^2 < A_s = 7{,}92\,\text{cm}^2$$

the selected reinforcement is sufficient. Therefore, the final reinforcement according to EN 1992-1-1:2004 is $7\phi12$.

VGU
Vietnamese-German University

Simplified crack width control according to EN 1992-1-1:2021

The simplified method is based on explicit expressions for the maximum bar diameter and maximum spacing. The factor for one face in compression is

$$k_{\mathrm{fl,simpl}} = 1 - 3{,}5\frac{a_{\mathrm{y}}}{h} = 1 - 3{,}5\frac{31}{150} = 0{,}277$$

The curvature-related factor is

$$k_{1/\mathrm{r,simpl}} = 25\left(\frac{h}{d} - 1\right)\rho_{\mathrm{p}} + 1{,}15\frac{h}{d} - 0{,}1 = 25\left(\frac{150}{119} - 1\right)0{,}0067 + 1{,}15\frac{150}{119} - 0{,}1 = 1{,}39$$

For good bond condition, the simplified factor $k_{\mathrm{b,simpl}} = 0{,}9$.
The factor converting the mean crack width into the calculated crack width $k_{\mathrm{w}} = 1{,}7$.
The maximum allowable bar diameter is then

$$\phi \leq \frac{2{,}1\rho_{\mathrm{p}}}{\frac{r}{d}\cdot k_{\mathrm{fl,simpl}}k_{\mathrm{b,simpl}}}\left(\frac{w_{\mathrm{lim,cal}}}{k_{\mathrm{w}}k_{1/\mathrm{r,simpl}}\,0{,}9\frac{\sigma_{\mathrm{s}}}{E_{\mathrm{s}}}} - 1{,}5c\right)$$

$$\phi = \frac{2{,}1\cdot 0{,}0067}{0{,}277\cdot\frac{31}{119}\cdot 0{,}9}\left(\frac{0{,}3\cdot\frac{25}{10+15}}{1{,}7\cdot 1{,}39\cdot 0{,}9\cdot\frac{236}{200000}} - 1{,}5\cdot 25\right) \approx 17{,}78\ \mathrm{mm}$$

Vietnamese-German University

The maximum spacing is

$$s_{\mathrm{l}} \leq \frac{3{,}45\rho_{\mathrm{p}}}{\frac{r^2}{d}k_{\mathrm{fl,simpl}}^2k_{\mathrm{b,simpl}}^2}\left(\frac{w_{\mathrm{lim,cal}}}{k_{\mathrm{w}}k_{1/\mathrm{r,simpl}}\,0{,}9\frac{\sigma_{\mathrm{s}}}{E_{\mathrm{s}}}} - 1{,}5c\right)^2$$

$$s_{\mathrm{l}} = \frac{3{,}45\cdot 0{,}0067}{\frac{31^2}{119}0{,}277^2\cdot 0{,}9^2}\left(\frac{0{,}3\cdot\frac{25}{10+15}}{1{,}7\cdot 1{,}39\cdot 0{,}9\frac{236}{200000}} - 1{,}5\cdot 25\right)^2 \approx 310\ \mathrm{mm}$$

Hence, the selected reinforcement $7\phi 12$ satisfies the simplified crack control check.

Refined crack width control according to EN 1992-1-1:2021

Step 1: Effective reinforcement ratio

The effective height according to EN 1992-1-1:2021 is

$$h_{c,eff} = \min\{d_1 + 5\phi; 10\phi; 3{,}5d_1\} = \min\{31 + 5 \cdot 12; 10 \cdot 12; 3{,}5 \cdot 31\} = 91\,\text{mm}$$

This satisfies

$$h_{c,eff} = 91\,\text{mm} < |150 - 48| = 102\,\text{mm}$$

Thus, the effective concrete area becomes

$$A_{c,eff} = b \cdot h_{c,eff} \cdot 10^{-2} = 1000 \cdot 91 \cdot 10^{-2} = 910\,\text{cm}^2$$

The effective reinforcement ratio is

$$\rho_{p,eff} = \frac{A_s}{A_{c,eff}} = \frac{7{,}92}{910} = 0{,}0087$$

Step 2: Mean strain difference

The curvature coefficient is

$$k_{1/r} = \frac{h - x}{h - a_y - x} = \frac{150 - 48}{150 - 31 - 48} = 1{,}437$$

VGU Vietnamese-German University

The mean strain difference is calculated as follows with $k_t = 0{,}4$ assuming long-term effect

$$\varepsilon_{sm} - \varepsilon_{cm} = k_{1/r} \frac{\sigma_s - k_t \frac{f_{ct,eff}}{\rho_{p,eff}} \left(1 + \alpha_e \rho_{p,eff}\right)}{E_s} \geq 0{,}6 \frac{\sigma_s}{E_s}$$

$$\varepsilon_{sm} - \varepsilon_{cm} = 1{,}437 \frac{236 - 0{,}4 \frac{2{,}56}{0{,}0087} (1 + 20 \cdot 0{,}0087)}{200000} = 0{,}000703$$

Since

$$0{,}000703 < 0{,}000708,$$

the limiting value below is adopted for the crack-width check.

$$\varepsilon_{sm} - \varepsilon_{cm} = 0{,}000708$$

Step 3: Mean crack spacing

For pure bending,

$$k_{\mathrm{fl}} = \frac{h - h_{\mathrm{c,eff}}}{h} = \frac{150 - 91}{150} = 0{,}393$$

The mean crack spacing is then

$$s_{\mathrm{r,m,cal}} = 1{,}5c + \frac{k_{\mathrm{fl}} k_{\mathrm{b}} \phi}{7{,}2\rho_{\mathrm{p,eff}}} = 1{,}5 \cdot 25 + \frac{0{,}393 \cdot 0{,}9 \cdot 12}{7{,}2 \cdot 0{,}0087} = 105{,}26\,\mathrm{mm}$$

The upper limit is

$$1{,}3(h - x) = 1{,}3(150 - 48) = 132{,}6\,\mathrm{mm}$$

Hence,

$$s_{\mathrm{r,m,cal}} = 105{,}26\,\mathrm{mm} < 132{,}6\,\mathrm{mm}$$

Step 4: Crack width

The calculated crack width is

$$w_{\mathrm{k,cal}} = k_{\mathrm{w}}\, s_{\mathrm{r,m,cal}}\, (\varepsilon_{\mathrm{sm}} - \varepsilon_{\mathrm{cm}}) = 1{,}7 \cdot 105{,}26 \cdot 0{,}000703 = 0{,}126\,\mathrm{mm}$$

Thus, the crack width is below the allowable limit of 0,3 mm.

VGU
Vietnamese-German University

Minimum reinforcement according to EN 1992-1-1:2021

For pure bending, the limiting steel stress is determined from

$$\sigma_{s,lim} \leq \frac{2{,}4 \cdot f_{ct,eff}}{h - h_{c,eff}} \cdot \frac{h}{\phi} \left(-c + \sqrt{c^2 + 1{,}5 \frac{\left(1 - \frac{h_{c,eff}}{h}\right) E_s \, w_{lim,cal} \, \phi}{k_w \cdot k_{1/r,simpl} \cdot f_{ct,eff}}} \right)$$

$$\sigma_{s,lim} = \frac{2{,}4 \cdot 2{,}56}{150 - 91} \cdot \frac{150}{12} \left(-25 + \sqrt{25^2 + 1{,}5 \frac{\left(1 - \frac{91}{150}\right) 200000 \cdot 0{,}3 \cdot \frac{25}{10 + 15} \cdot 12}{1{,}7 \cdot 1{,}393 \cdot 2{,}56}} \right) = 313{,}6 \, \mathrm{N/mm^2}$$

The minimum reinforcement at the most tensioned face is then

$$A_{s,min,w1} = \frac{0{,}8 \frac{h - h_{c,eff}}{h} f_{ct,eff} \, A_{c,eff}}{\sigma_{s,lim}} \geq \frac{0{,}2 \, k_h \, f_{ct,eff} \, A_c}{f_{yk}}$$

$$A_{s,min,w1} = \frac{0{,}8 \cdot \frac{150 - 91}{150} \cdot 2{,}56 \cdot 0{,}091}{313{,}6} \geq \frac{0{,}2 \cdot 0{,}80 \cdot 2{,}56 \cdot 0{,}1365}{500}$$

$$A_{s,min,w1} = 2{,}34 \, \mathrm{cm^2} \geq 1{,}12 \, \mathrm{cm^2}$$

VSB Technical University

Hence, the code requirement is satisfied. The final reinforcement according to EN 1992-1-1:2021 is again $7\phi12$.

Table Results

Table 4.2 compares crack width control calculations between EN 1992-1-1:2004 and EN 1992-1-1:2021 for the reference specimen E01.01. The table includes intermediate parameters such as the effective reinforcement ratio, effective depth, crack spacing, strain difference, and the final crack width results.

Both codes predict crack widths well below the limiting value, confirming the adequate serviceability. Regarding the simplified method calculation, the 2021 version results in a much larger maximum bar spacing with roughly 308 mm, compared to 150 mm of the 2004 version. This outcome of the refined version may not be as safe as the current version. As the verification of refined method, the results of effective tension height $h_{c,eff}$ and effective concrete area $A_{c,eff}$ of the 2021 version are higher than about three times the values of the 2004 version, resulting in lower effective reinforcement ratio $\rho_{s,eff}$ value. Therefore, the revised version yields higher crack widths due to its refined formulation with some new conversion factor approaches. These numerical outcomes provide the remark for the extended beam series

analyzed in the following sections.

Table 4.2: Crack control results according to EN 1992-1-1:2004 and EN 1992-1-1:2021

PARAMETERS		EN 1992-1-1:2004	EN 1992-1-1:2021
Width of cross-section	b [mm]	1000	1000
Height of cross-section	h [mm]	150	150
Length	l [mm]	5000	5000
Concrete Grade	[-]	C25/30	C25/30
Concrete Cover	c_v [mm]	25	25
Effective Depth	d [mm]	119	119
Reinforcement Area	$A_{s,chosen}$	$7\phi12$	$7\phi12$
Reinforcement Ratio	ρ_s	0,0067	0,0067
Bending Moment in SLS	$M_{Eds,per}$	19,22	19,22
Neutral Axis Depth	x [m]	0,048	0,048
Lever Arm	z [m]	0,103	0,103
Working Steel Stress	σ_s [N/mm^2]	235,59	235,59
SIMPLIFIED METHOD CALCULATION			
Reinforcement chosen	A_s	$7\phi12$	$7\phi12$
Maximum Bar Spacing	s_{max} [mm] / s_1	150,00	308,36
Maximum Allowable Crack Width	$w_{k,max}$ [mm]	0,30	0,30
REFINED METHOD CALCULATION			
Effective Height	$h_{c,eff}$ [m]	0,034	0,091
Effective Concrete Area	$A_{c,eff}$ [m^2]	0,03	0,09
Effective Reinforcement Ratio	$\rho_{p,eff}$	0,02	0,01
Mean Strain Difference	$\varepsilon_{sm} - \varepsilon_{cm}$	0,00071	0,00071
Maximum Crack Spacing	$s_{r,max}$ [mm]	132,60	132,60
Mean Crack Spacing	$s_{rm,calc}$ [mm]	99,45	105,29
Calculated Crack Width	w_k [mm]	0,113	0,127
Reinforcement chosen	A_s	$7\phi12$	$7\phi12$
MINIMUM REINFORCEMENT			
Minimum Reinforcement Area	$A_{s,min}$ [cm^2]	3,25	2,34

Vietnamese-German University

4.1.3 Results of extended beam series

An extended parametric study of 15 beam sections was conducted to systematically evaluate the influence of section depth (150 mm to 1000 mm) and bar diameter (12, 14, 16 mm) on crack control parameters according to EN 1992-1-1:2004, EN 1992-1-1:2021, and the German DIN standard. All specimens shared consistent material properties (C25/30 concrete, B500 reinforcement, 25 mm cover) and a nearly constant reinforcement ratio of approximately 0,0029 – 0,0030, ensuring a direct comparison of code-specific formulations.

Table 4.3: Parameters of beams

Beams	h [mm]	ϕ [mm]	A_s [cm^2]	ρ_s	d [mm]	x [mm]	$h_{c,eff}$ (2004)	$\rho_{s,eff}$ (2004)	$h_{c,eff}$ (2021)	$\rho_{s,eff}$ (2021)
E01.01	150	12	7,92	0,0067	119	48	34	0,0232	91	0,0087
E01.02	150	14	7,70	0,0065	118	47	34	0,0224	102	0,0075
E01.03	150	16	8,04	0,0069	117	47	34	0,0235	113	0,0071
E02.01	300	12	7,92	0,0029	269	78	74	0,0107	91	0,0087
E02.02	300	14	7,70	0,0029	268	77	74	0,0103	102	0,0075
E02.03	300	16	8,04	0,0030	267	78	74	0,0109	113	0,0071
E03.01	500	12	13,56	0,0029	469	135	77,50	0,0175	116	0,0117
E03.02	500	14	13,90	0,0030	468	136	80,00	0,0174	102	0,0136
E03.03	500	16	14,10	0,0030	467	137	82,50	0,0171	113	0,0125
E04.01	700	12	20,35	0,0030	669	196	77,50	0,0263	116	0,0175
E04.02	700	14	20,02	0,0030	668	195	80,00	0,0250	127	0,0158
E04.03	700	16	20,10	0,0030	667	195	82,50	0,0244	113	0,0178
E05.01	1000	12	28,56	0,0029	969	280	77,50	0,0369	116	0,0246
E05.02	1000	14	27,80	0,0029	968	277	80,00	0,0348	127	0,0219
E05.03	1000	16	28,14	0,0029	967	278	82,50	0,0341	138	0,0204

VGU Vietnamese-German University

Table 4.3 summarizes some key intermediate parameters for all beam specimens and highlights the influence of section depth, bar diameter, and standards on the effective reinforcement ratio. A key difference was observed in the calculation of the ratio $\rho_{s,eff}$. The 2004 standard is consistently higher $\rho_{s,eff}$ than the 2021 standard. This is a direct consequence of the older code's definition of the $h_{c,eff}$, which results in a smaller $A_{c,eff}$. Specifically, from the thickness 150 to 300 mm, the revised $h_{c,eff}$ of 2021 version has 1,5 to 3 times higher than that of the 2004 standard and the gaps reduce when increasing section depths since the new definition of the refined formula. Furthermore, the 2021 version also considers the layers of reinforcement, which may reflect the reinforcement ratio better of the cross-section concrete area and those beams of E03.01, E04.01, E04.02, E05.01, E05.02 and E05.03 are specimens with two layers reinforcement, which can be found in more detail in the Excel file calculations.

Table 4.4: Calculated crack spacing results

Beams	Maximum Calculated Crack Spacing			Mean Calculated Crack Spacing		
	DIN 1992	EC2:2004	EC2:2021	DIN 1992	EC2:2004	EC2:2021
E01.01	133	133	133	100	99	105
E01.02	134	134	134	100	100	112
E01.03	134	134	134	100	100	107
E02.01	206	276	210	155	207	158
E02.02	248	290	254	186	217	191
E02.03	273	289	284	205	217	213
E03.01	104	202	160	78	151	136
E03.02	119	222	186	89	167	140
E03.03	134	244	181	100	183	162
E04.01	65	163	145	49	122	109
E04.02	77	180	171	58	135	128
E04.03	88	197	176	66	148	132
E05.01	44	140	122	33	105	91
E05.02	53	154	143	40	115	107
E05.03	60	165	163	45	124	122

VGU Vietnamese-German University

Table 4.4 shows the calculated crack spacing values for all specimens. EN 1992-1-1:2004 consistently predicts the largest spacings while the DIN standard predicts the smallest. The updated EN 1992-1:2021 generally provides intermediate values, moderating the prediction of its predecessor. The version of 2004 generally produces larger predicted crack spacings, and especially, the calculated crack spacings of diameter 12 result in the largest gap between standards and this trend reduces either crack spacing or gaps when increasing bar sizes. Noticeably, the value of maximum and mean calculated crack spacings between standards of beam thickness of 150 mm shows lower than that of 300 mm beam thickness due to the restraint, which will be discussed in more detail in the following section.

From both table results above, since there are some refined formulations between Eurocode standards, these values provide clearly fundamental parameters and point out the differences between the two versions. Hence, this significantly contributes to the aim of the comparative analysis between these two Eurocode design approaches, which will be further illustrated in Section 4.1.4 and discussed in Section 4.1.5.

4.1.4 Comparative analysis

The calculated crack spacings and crack widths for all specimens are visualized in Figure 4.2, Figure 4.3, and Figure 4.4, based on the results of Table 4.4. The results reveal clear and consistent trends among the design standards.

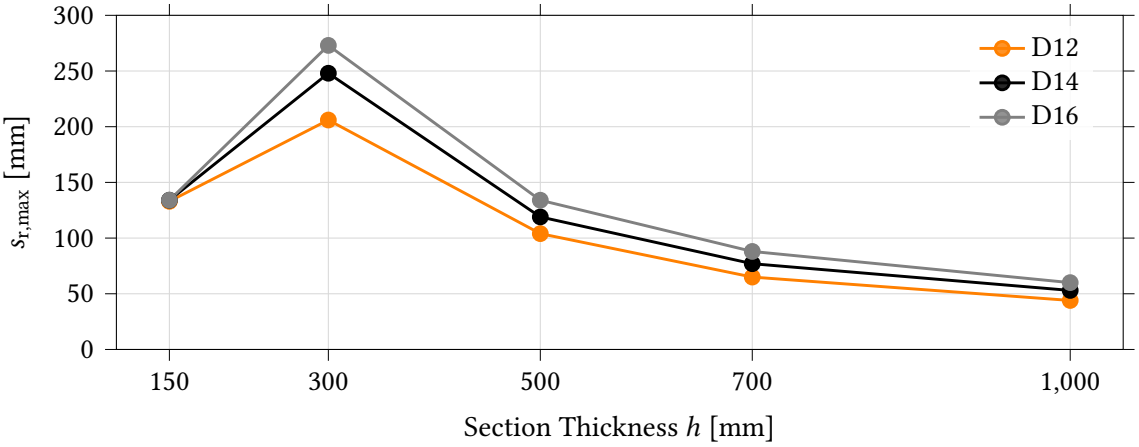
Crack Spacing

Figure 4.2 and Figure 4.3 present the calculated maximum and mean crack spacings for the 15 specimens, revealing clear and consistent trend among standards.

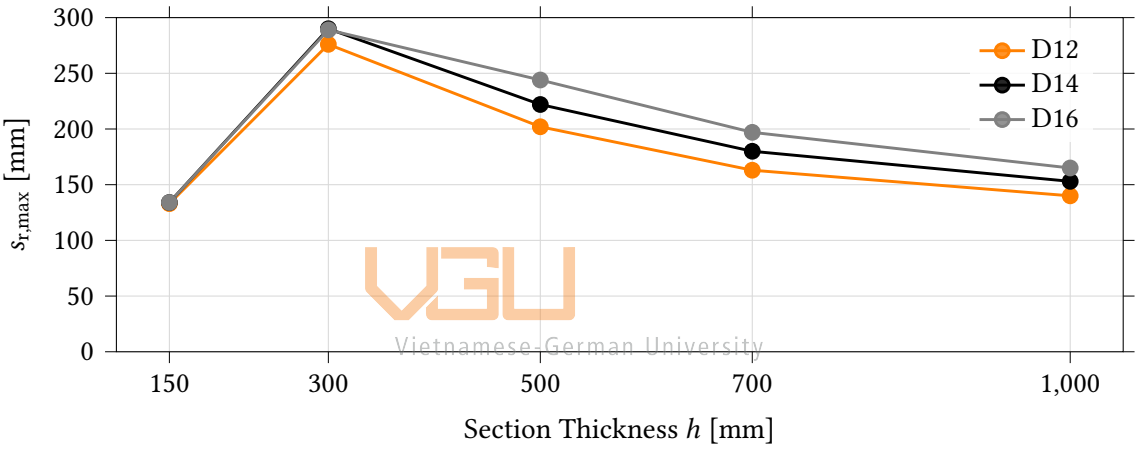
As shown in Figure 4.2, EN 1992-1-1:2004 consistently yields the highest maximum crack spacing, with values exceeding those of the DIN standard and EN 1992-1-1:2021 by up to 40% in shallow sections. EN 1992-1-1:2021 remains in between, reflecting its revised definition of effective tension zone. Noticeably, the governing condition of thin to medium members (150 – 300 mm) shifts. The maximum crack spacing limit for cases where bar spacing exceeds a threshold of 5(c+ $\phi/2$) in 2004 and 10ϕ in 2021 controls the calculation. This causes the predicted spacings from all standards to coverage, as seen in specimens E01.01 – E01.03 and E02.01 – E02.03. For thicker sections (> 400 mm), the spacing decreases gradually, reaching approximately 140 – 165 mm at 1000 mm in the version 2004 and 122 – 163 mm in the version of 2021.

Figure 4.3 demonstrates a similar trend for mean crack spacing. Both standards show decreasing crack spacing with increasing section depth, but the slope is slightly steeper in the version of 2021, indicating a higher sensitivity to thickness assumptions in the updated standard. For thickness sections are medium to high (300 – 1000 mm), the 2021 version predicts 15 – 25% smaller spacings than the 2004 standard, while for the thin section of 150 mm the results a slightly higher of the 2021 version.

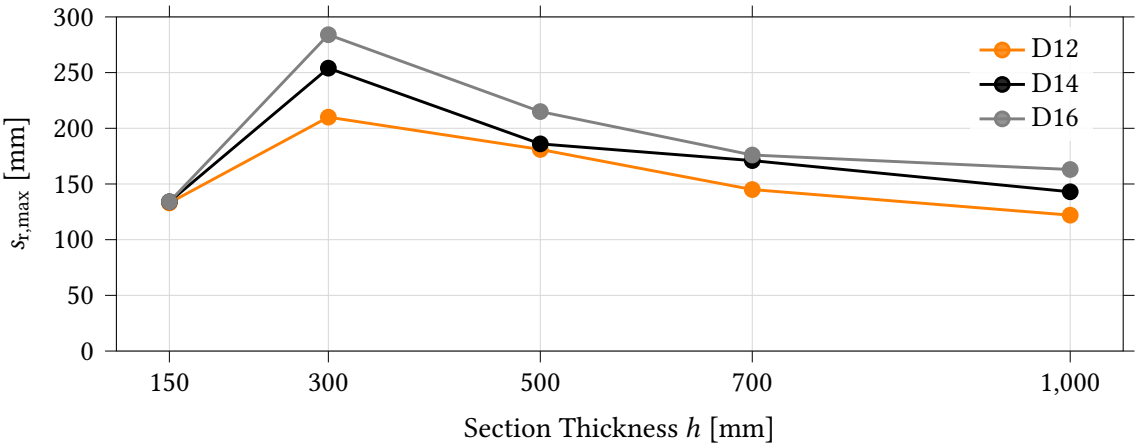
Across all results, crack spacing demonstrates a strong influenced by the effective reinforcement ratio ρ_{eff} and bar diameter. The thickness section also indirectly affects its impact on the effective area of concrete. A larger bar diameter directly enlarges the crack spacing and reduces the ρ_{eff} within the same section. Especially, the refined model introduces the $h_{\text{c,eff}}$ which is directly considered by bar diameter, contributing to increasing the $A_{\text{c,eff}}$ and reducing the ρ_{eff}. Conversely, smaller bars (ϕ12 mm) create denser reinforcement distribution and slightly smaller crack spacings. The variation in spacing among three bar diameters remains below 10%, confirming that bar size and effective reinforcement ratio are the main influence when cover is assumed to be constant.



(a) DIN EN 1992-1-1/NA

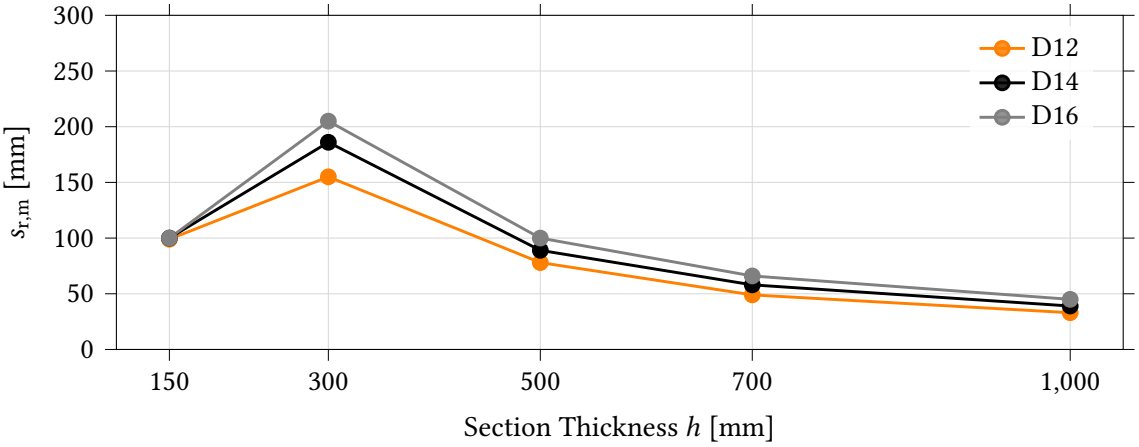


(b) EN 1992-1-1:2004

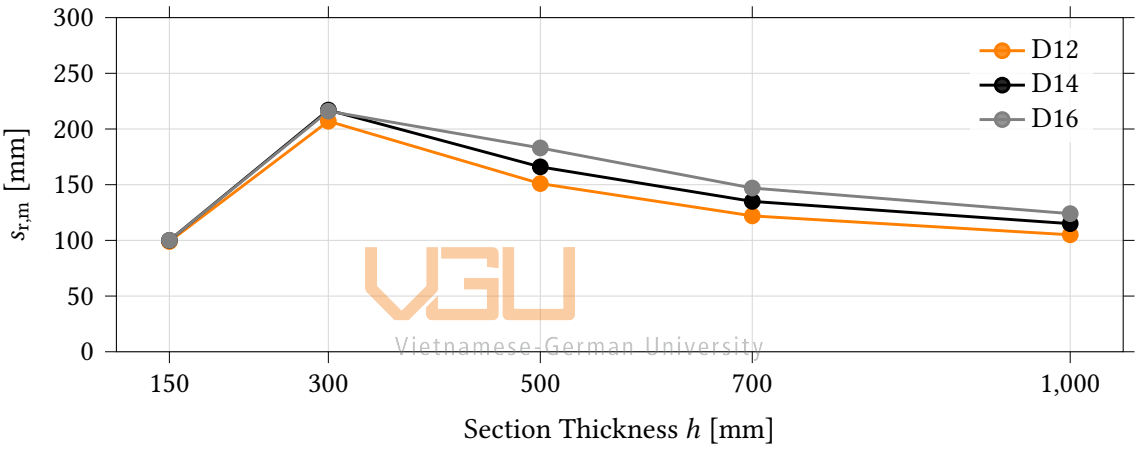


(c) EN 1992-1-1:2021

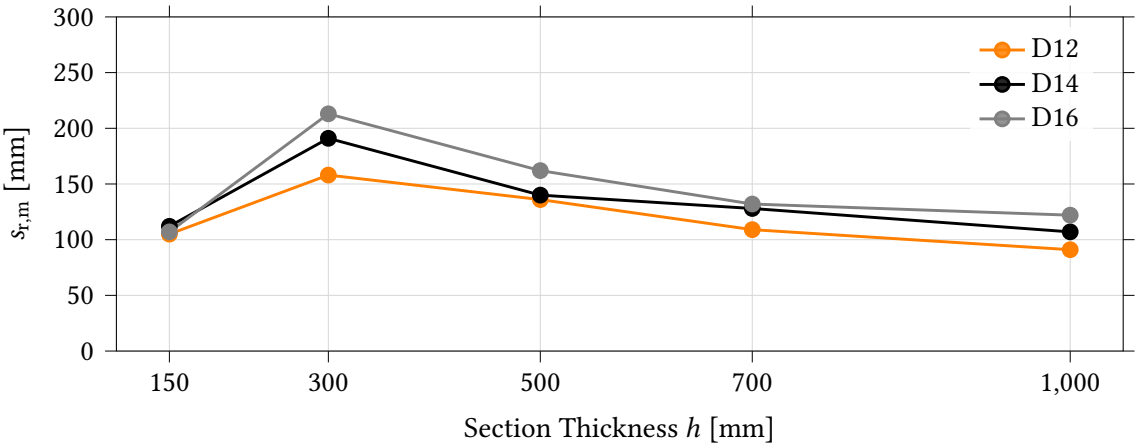
Figure 4.2: Maximum crack spacing for bar diameters D12, D14, and D16 according to (a) DIN EN 1992-1-1/NA, (b) EN 1992-1-1:2004, and (c) EN 1992-1-1:2021



(a) DIN EN 1992-1-1/NA



(b) EN 1992-1-1:2004



(c) EN 1992-1-1:2021

Figure 4.3: Mean crack spacing for bar diameters D12, D14, and D16 according to (a) DIN EN 1992-1-1/NA, (b) EN 1992-1-1:2004, and (c) EN 1992-1-1:2021

Crack Width

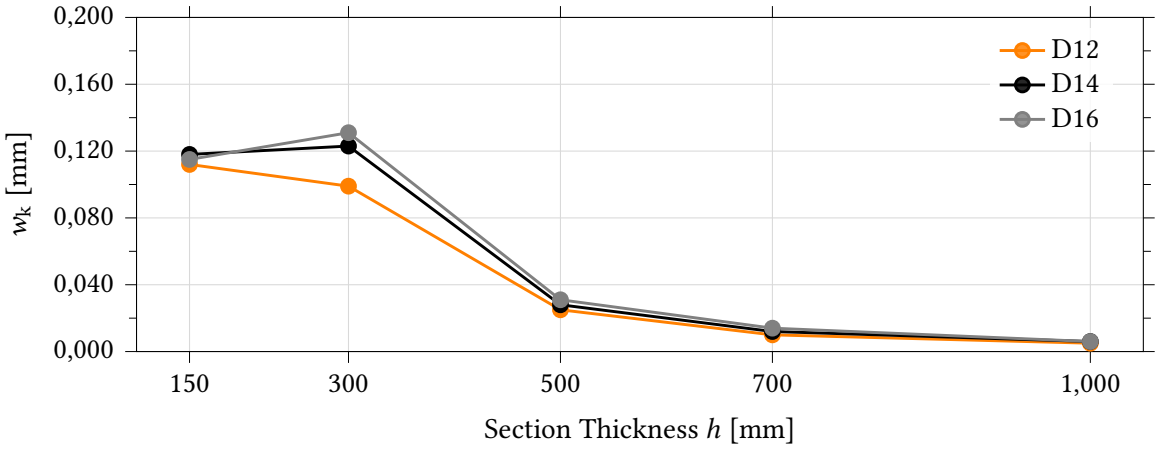
Figure 4.4 presents the final calculated crack widths w_k. All predicted values are well below the typical serviceability limit of 0,3 – 0,4 mm, confirming that all standards provide safe designs for the considered loading. The value of EN 1992-1-1:2004 is slightly lower than EN 1992-1-1:2021, ranging from 0,112 at 150 mm to 0,0014 mm at 1000 mm. The refined model is generally higher at larger bar sizes and lower for large sections. At 300 mm thickness, w_k is about 0,129 mm and the value drop sharply as the thickness increases, reaching 0,0056 mm at 500 mm and 0,016 mm at 1000 mm. Furthermore, the same trend is observed for all diameters, but the magnitude varies slightly. The diameter of 12 has recorded the smallest width while the diameter of 16 yields the largest and the variation between diameters is roughly 15 – 20% at thin sections but becomes negligible in thick members.

At smaller depths (150 – 300 mm), the value of w_k rises rapidly, indicating higher steel stress in slender members. The reason for this increase is to meet the requirements of minimum reinforcement, avoiding inadequate reinforcement and being prone to cracking. Beyond the thickness of 500 mm, the results of every code converge and remain almost constant below 0,02 mm, confirming that larger beam sections provide beam sections with greater stiffness and lower surface strain.

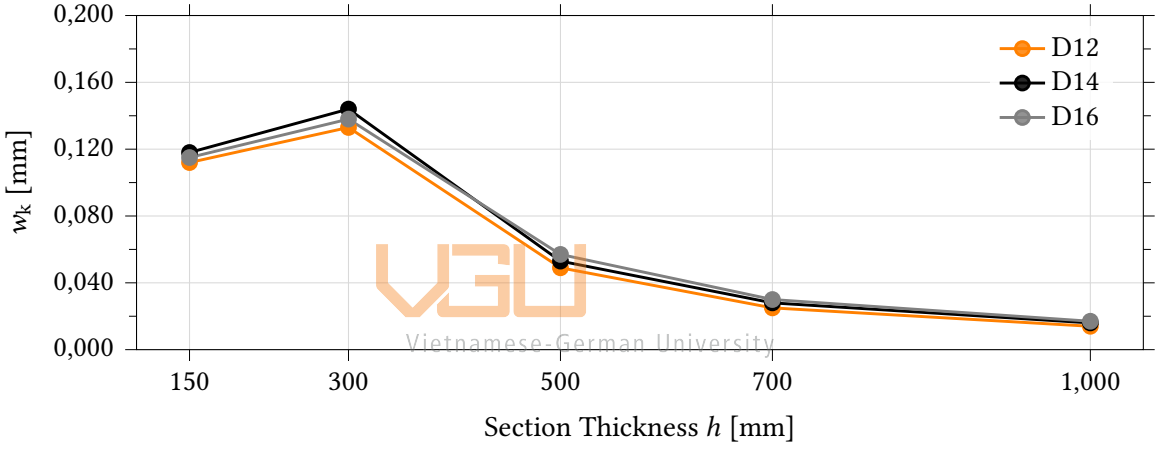
When comparing standards, EN 1992-1-1:2004 relies on the empirical coefficients k_1 and k_2 in the crack spacing expression. But the higher value of w_k in EN 1992-1-1:2021 considers the refined k_{fl} and $k_{1/r}$ factors together with the conversion coefficient k_w. This coefficient transforms the mean crack width into a design value, considering bond and stress distribution near the surface.

Vietnamese-German University

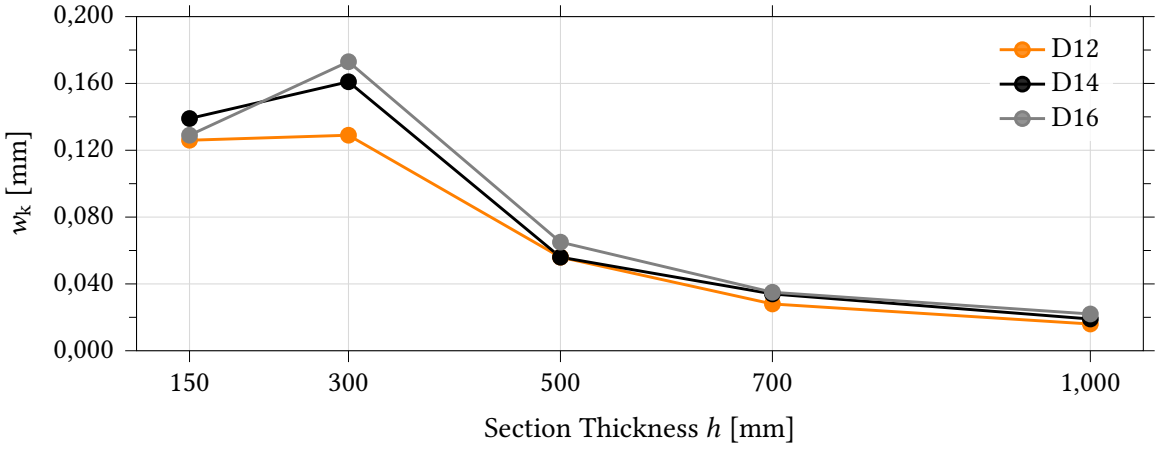
Regarding the trend of bar diameter from 12 to 16, the trend is also consistent with the theoretical expression that smaller bars yield narrower cracks. This effect also clearly shows the decrease in crack width from thin sections with small diameters to thick sections with large diameters. Hence, it is quite obvious that the changes in crack width are purely affected by the thickness geometry and bar size.



(a) DIN EN 1992-1-1/NA



(b) EN 1992-1-1:2004



(c) EN 1992-1-1:2021

Figure 4.4: Crack width for bar diameters D12, D14, and D16 according to (a) DIN EN 1992-1-1/NA, (b) EN 1992-1-1:2004, and (c) EN 1992-1-1:2021

4.2 Experiment setup

All test reinforced concrete beam specimens were prepared and poured by lecturers of VGU in collaboration with Mr. Ven, the laboratory engineer who mainly carried out the tests and recorded at the VGU's laboratory. Due to the scope and time restraints, the results of three tested beams were selected for analysis. The beams differ in overall dimensions, loading conditions, and concrete strength class. All were reinforced with grade B350 steel, but the reinforcement layout (bar size and quantity) varies between specimens. Detailed properties are summarized in Table 12, and photographs with reinforcement details are provided in Appendix.

Regarding the weather conditions, the beams were placed outdoors under a shielded roof, exposed to ambient air. Relative humidity was typically roughly 50-80% with natural daily fluctuations, ambient temperature and airflow were not actively controlled (typical temperatures in Binh Duong province of Vietnam are between 25 and 35 Celsius degrees according to the climate data). These conditions can influence moisture and shrinkage and to limit variability, all three beams were kept in the same location under identical storage conditions prior to testing.

Cracking was mapped on both faces at every load step, including primary and secondary cracks. Very fine surface microcracks that remained confined to the cover were not considered in the record, as they normally do not develop further and just mainly affect the aesthetic of the surface elements.

VGU
Vietnamese-German University

Table 4.5: Specimen specifications

Specifications	**Beam B01**	**Beam B02**	**Beam B03**
Length [mm]	3600	2500	3000
Effective Length [mm]	3200	2050	2200
Width [mm]	150	200	200
Height [mm]	440	400	400
Longitudinal Reinforcement	$3\phi12$	$4\phi22$	$4\phi22$
Concrete Grade	C35/45	C25/30	C30/37
Reinforcement Grade	B350	B350	B350
Loading Type	1 unsymmetric point	2-point load	2-point load
Loading P [kN]	60	236	268

Table 4.5 shows three reinforced beams, denoted as B01, B02 and B03 were prepared with various geometrical dimensions, reinforcement configuration and loading conditions. Beam B01 was subjected to unsymmetrical point load of 60 kN, while beams B02 and B03 were tested under two-point load of 236 kN and 286 kN respectively. The concrete grade ranges from C25/30 to C35/45.

4.3 Experimental results

After illustrating a detailed concept comparison between EN 1992-1-1:2004 and EN 1992-1-1:2021 via the example calculations in Section 4.1. In this section, crack recorded of experimental beams in laboratory can be more practical to compare between standards. To validate and compare the crack control methods of two versions using experimental data from three tested beams. This section aims to apply both standards to real beam specimens with recorded crack patterns and evaluate the practical application and reliability of the updated Eurocode 2.

4.3.1 Experiment calculation

To ensure a consistent basis for comparison, the crack control calculations for these experimental beams were performed using the same step-by-step procedures outlined for the theoretical example in Section 4.1.2, applying both EN 1992-1-1:2004 and EN 1992-1-1:2021.

For additional reference comparison and to provide further insight into the general cracking trends, the crack control method from the habilitation work of Tran was also applied, which helps to support for the perspective in the comparison. This model of crack control shares a similar mechanical basis with Eurocode and DIN standards, as it fundamentally attributes crack spacing to the bond between concrete and reinforcement. However, it improves the expressions to be adjusted to reflect the specific experimental observations as follows:

VGU Vietnamese-German University

$$s_{cr,m} = 0{,}75\, s_{cr,max} = \frac{1{,}5\, \phi_s}{4\, k_b\, \rho_{s,ef}} = 0{,}75\, d\, (1 - k_x) \tag{4.6}$$

with k_b is the ratio between the average bond stress and the concrete tensile strength: with k_b being the ratio between the average bond stress and the concrete tensile strength:

$$k_b = 0{,}97 \left(\frac{1 + n_e \rho_{s,ef}}{\rho_{s,ef}^2} \cdot \frac{\phi_s}{E_s} \right)^{\frac{1}{4}} \cdot \sqrt{\frac{f_c^{3/4}}{f_{ctm}}} \tag{4.7}$$

and the effective reinforcement ratio can be estimated as usual, where $h_{c,eff} = 2{,}5 \cdot d_1$.

4.3.2 Experiment results

Figure 4.5 and Figure 4.6 clearly show all three beams' properties, material specifications, loading, crack measurement and crack control methods among standards (DIN standard, EN 1992-1-1:2004, EN 1992-1-1:2021 and Tran method). Among these, the two Eurocode versions are mainly used for comparative analysis and discussion.

Overview of beam properties and material specifications

Three beams of B01, B02 and B03 were analyzed with different dimensions, reinforcement arrangement and material strengths. The specimen B01 measured 150 x 440 mm, while B02 and B03 were 200 x 400 mm. The effective lengths were 3200 mm, 2050 mm and 2200 mm for B01, B02 and B03 respectively. The cover thickness was 25 mm for B01 and 34 mm for both B02 and B03. The concrete grades varied between specimens: C35/45 for B01, C25/30 for B02 and B30/37 for B03, resulting in different compressive strengths f_{cm}, designed compressive strengths f_{cd}, tensile strengths f_{ct} and elastic moduli of concrete E_{cm}. In addition, all beams are reinforced with B350 steel with f_{yk} = 350 MPa and E_s = 200 GPa. The layout reinforcement of B01 is $3\phi12$ with reinforcement ratio ρ = 0,0055. B02 and B03 each have $4\phi22$ with ρ = 0,0218. The effective depths d is recorded as 409 mm for B01 and 349 mm for both B02 and B03. Due to the loading conditions, types and load values are different from three beams, resulting in the varied in working steel stress σ_s under service load: 447 MPa for B01, 194,7 MPa for B02 and 239,1 MPa for B03.

Crack record

The experimental crack observations showed that all beams developed multiple cracks along the tension face. The crack spacing of all beams were measured manually, as shown in Appendix for reference. The maximum recorded crack spacings were 230 mm for B01, 275 mm for B02 and 215 mm for B03. The mean crack spacings were roughly 162 mm, 159 mm and 149 mm respectively. Further comparisons of crack spacings results will be illustrated in the following.

Crack width calculation according to standards

In the simplified method of EN 1992-1-1:2004, the maximum allowable crack width w_k,max was taken as 0,4 mm for all beams, which XC1 was assumed for the exposure class (interior environment, dry condition). The adjusted bar diameters were 23 mm, 56 mm and 39 mm for three beams respectively. The corresponding maximum allowable spacings $s_{l,max}$ were 100 mm, 300 mm and 250 mm, which is based on table-based value as shown in Table 3.6 and Table 3.7. However, maximum bar diameter and bar spacing in the EN 1992-1-1:2021 had the refined specific formulations, leading to unrealistically large calculated values. The excel file will be attached to this paper to show fully these results. Therefore, the chosen of maximum bar spacing and bar diameter listed in the table result were individually selected based on limit calculations. Hence, the selection of bar diameters of all three beams is well satisfied with the compliance.

For the refined method, the effective heights $h_{c,eff}$ of the version 2004 were 77,5 mm, 86 mm and 87 mm whereas the $h_{c,eff}$ values of the 2021 edition are nearly double of beams B02 and B03 with 161 mm and the $h_{c,eff}$ of B01 was 91 mm. The main reason for this huge variation is

due to the definition of $h_{c,eff}$. As a result, the effective concrete areas $A_{c,eff}$ are also much higher than the 2004 version as well as the effective reinforcement ratio ρ_{eff}. Overall, the resulting crack width of the 2021 version were 0,9 mm, 0,14 mm and 0,17 mm respectively, which were moderately higher than those of the 2004 standard with 0,29 mm, 0,13 mm and 0,17 mm.

According to the Habilitation of Tran approach, the $h_{c,eff}$ of B01 was as the same as that in the 2004 standard with 77,5 mm. However, the $h_{c,eff}$ of B02 and B03 were different, recorded at 127,5 mm. Since the refined experimental formulation, the mean crack spacing $s_{r,m}$ and the maximum spacings $s_{r,max}$ with the introduction of bond strengths factor k_b were different from the two Eurocode standards. Further comparisons of crack spacing among standards will be illustrated in later figures.

VGU
Vietnamese-German University

INPUT DATA			**Beam B01**	**Beam B02**	**Beam B03**
Beam dimensions					
Length	l	[mm]	3600	2500	3000
Effective length	l_{eff}	[mm]	3200	2050	2200
Width	b	[mm]	150	200	200
Height	h	[mm]	440	400	400
Cover thickness	c_v	[mm]	25	34	34
Longitudinal reinforcement diameter	Φ_{sl}	[mm]	16	22	22
Number of long. rebars	[-]		3	4	4
Stirrup reinforcement diameter	Φ_{st}	[mm]	0	6	6
SPECIFICATION OF MATERIALS					
Concrete					
Density of reinforced concrete	γ_c	[kN/m^3]	25	25	25
Concrete grade	[-]		C35/45	C25/30	C30/37
Characteristic compressive strength	f_{ck}	[MPa]	35	25	30
Mean value compressive strength	f_{cm}	[MPa]	43	32	46
Designed compressive strength	f_{cd}	[MPa]	19,83	14,17	17,00
Tensile concrete strength	f_{ct}	[MPa]	3,2	2,6	2,9
Modulus elasticity of concrete	E_{cm}	[MPa]	34000	31000	33000
Effective depth	d	[mm]	407	349	349
Depth	d_1	[mm]	33	51	51
Effective concrete area	A_c	[cm^2]	611	698	698
Reinforcement B350					
Characteristic yield strength	f_{yk}	[MPa]	350	350	350
Design yield strength	f_{yd}	[MPa]	304,35	304,35	304,35
Modulus elasticity of steel	E_s	[MPa]	200000	200000	200000
Reinforcement area	A_s	[cm^2]	6,03	15,20	15,20
Reinforcement ratio	ρ	[-]	0,0099	0,0218	0,0218
Modular ratio	n_e	[-]	5,88	6,45	6,06
Relative depth compression zone	k_x	[-]	0,29	0,41	0,40
Neutral axis depth	x	[mm]	117	142	139
LOADING PARAMETERS					
Type of loading	[-]		1 unsymmetric point	2-point load	2-point load
Support conditions	[-]		Pinned-Pinned	Pinned-Roller	Pinned-Roller
Load values	P	[kN]	80	236	268
Self-weight load	g_k	[kN/m]	1,65	2	2
Total bending moment	M_{Eds}	[kNm]	62,112	104,301	128,510
Working steel stress	σ_s	[N/mm^2]	256,9	194,7	239,1

VGU Vietnamese-German University

Figure 4.5: Excel Based Results

CRACK RECORD					
Maximum crack spacing	$s_{r,max}$	[mm]	230	275	215
Minimum crack spacing	$s_{r,min}$	[mm]	90	75	95
Mean crack spacing	$s_{r,m}$	[mm]	162	158,9	148,9
CRACK WIDTH CALCULATION EN 1992-2004 (SIMPLIFIED METHOD)					
Maximum allowable crack width	$w_{k,max}$	[mm]	0,4	0,4	0,4
Adjusted bar diameters	Φ_s	[mm]	22	56	39
Maximum bar spacing	$s_{l,max}$	[mm]	100	300	250
CRACK WIDTH CALCULATION EN 1992-2021 (SIMPLIFIED METHOD)					
Chosen bar diameter	Φ_s	[mm]	12	22	22
Chosen bar spacing	s_l	[mm]	150	150	150
CRACK WIDTH CALCULATION EN 1992-2004 (REFINED METHOD)					
Effective height	$h_{c,eff}$	[mm]	82,5	86	87
Effective concrete area	$A_{c,eff}$	[cm^2]	123,8	171,8	174,0
Effective reinforcement ratio	ρ_{eff}	[-]	0,049	0,088	0,087
Mean strain difference	$\varepsilon_{sm} - \varepsilon_{cm}$	[-]	0,0010	0,0008	0,0010
Maximum bar spacing - DIN	$s_{r,max}$	[mm]	91,2	69,1	70,0
Maximum bar spacing - EC2004	$s_{r,max}$	[mm]	141	158	158
Mean bar spacing - DIN	$s_{r,m}$	[mm]	68,4	51,8	52,5
Mean bar spacing - EC2004	$s_{r,m}$	[mm]	105,6	118,4	118,8
Crack width - EC2004	w_k	[mm]	0,15	0,13	0,17
High bonding coefficient	k_1	[-]	0,8	0,8	0,8
Strain distribution coefficient - bending	k_2	[-]	0,5	0,5	0,5
Correction factor	k_3	[-]	3,4	3,4	3,4
Correction factor	k_4	[-]	0,425	0,425	0,425
Short-term loading	k_t	[-]	0,6	0,6	0,6
CRACK WIDTH CALCULATION EN 1992-2021 (REFINED METHOD)					
Effective height	$h_{c,eff}$	[mm]	113	161	161
Effective concrete area	$A_{c,eff}$	[cm^2]	169,5	322,0	322,0
Effective reinforcement ratio	ρ_{eff}	[-]	0,036	0,047	0,047
Mean strain difference	$\varepsilon_{sm} - \varepsilon_{cm}$	[-]	0,0011	0,0009	0,0012
Mean bar spacing	$s_{r,m,cal}$	[mm]	79,3	85,8	85,8
Maximumbar spacing	$s_{r,max}$	[mm]	105,7	114,4	114,4
Crack width	w_k	[mm]	0,1	0,1	0,2
CRACK WIDTH CALCULATION BY HABILITATION_TRAN					
Effective height	$h_{c,eff}$	[mm]	82,5	127,5	127,5
Effective concrete area	$A_{c,eff}$	[cm^2]	124	255	255
Effective reinforcement ratio	ρ_{eff}	[-]	0,049	0,060	0,060
Bond strength	k_b	[-]	0,94	0,92	0,92
Maximum bar spacing	$s_{r,max}$	[mm]	289,9	206,7	209,9
Mean bar spacing	$s_{r,m}$	[mm]	217,4	155,0	157,5

Vietnamese-German University

Figure 4.6: Excel Based Results

Comparative analysis

Table 4.6, Figure 4.7 and Figure 4.8 present the values of measured, calculated maximum and mean crack spacings of beams B01, B02 and B03 according to different standards, including DIN, EN 1992-1-1:2004, EN 1992-1-1:2021 and the Habilitation Tran approach. The table below shows the measured mean crack spacing for beams ranged from 148,9 mm for B03 to 178 mm for B01 and the maximum crack spacing was 275 mm for beam B02.

Table 4.6: Measured and calculated crack spacings

Beams	Measured Crack Spacing			Maximum Calculated Crack Spacing				Mean Calculated Crack Spacing			
	Min	Mean	Max	DIN	EC2:2004	EC2:2021	Tran	DIN	EC2:2004	EC2:2021	Tran
B01	90	178,0	243	91	141	106	290	68	106	79	217
B02	75	159,7	275	69	158	114	207	52	118	86	155
B03	95	148,9	215	70	158	114	210	52	119	86	157

Overall, the DIN standard produced the smallest maximum and mean calculated crack spacings, ranging from 69 mm to 91 mm and from 52 mm to 68 mm across beams. The EN 1992-1-1:2004 values were higher with 141 mm to 158 mm for maximum crack spacing $s_{r,max}$ and 106 mm to 119 mm for mean crack spacing $s_{r,m,calc}$. However, the EN 1992-1-1:2021 yields result a slight lower at 114 mm of $s_{r,max}$ and around 86 mm of $s_{r,m,calc}$, which was consistent for all specimens. In contrast, the Habilitation Tran method predicted substantially the largest crack spacing values across all beams.

VGU Vietnamese-German University

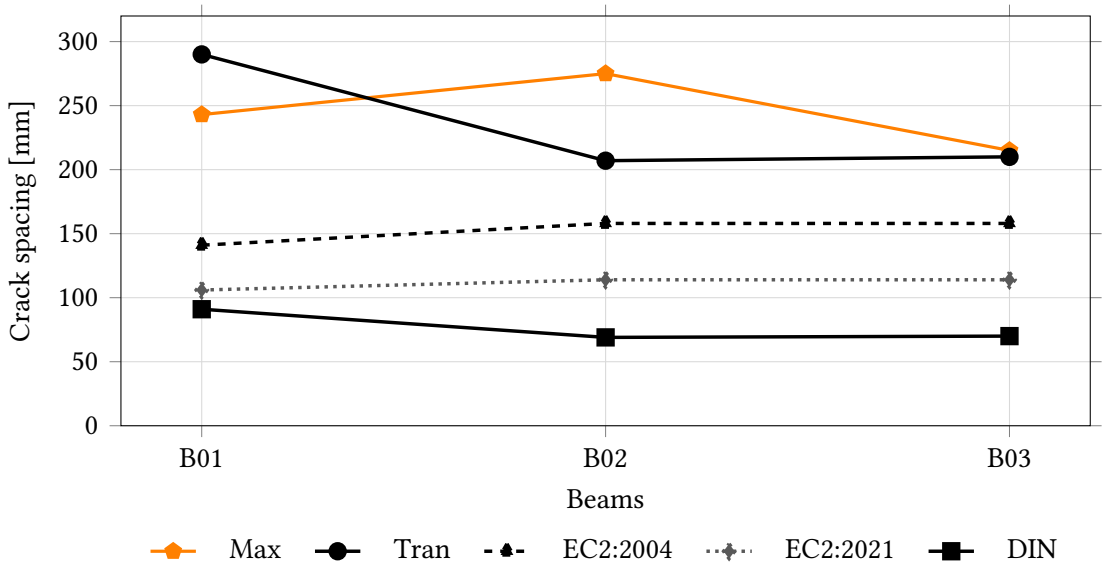


Figure 4.7: Comparison of measured maximum crack spacing and calculated maximum crack spacing according to different methods

As observed in Figure 4.7 and Figure 4.8, almost standards stay consistent below the experimental trend across three beams and the magnitude of each differs following their formulation.

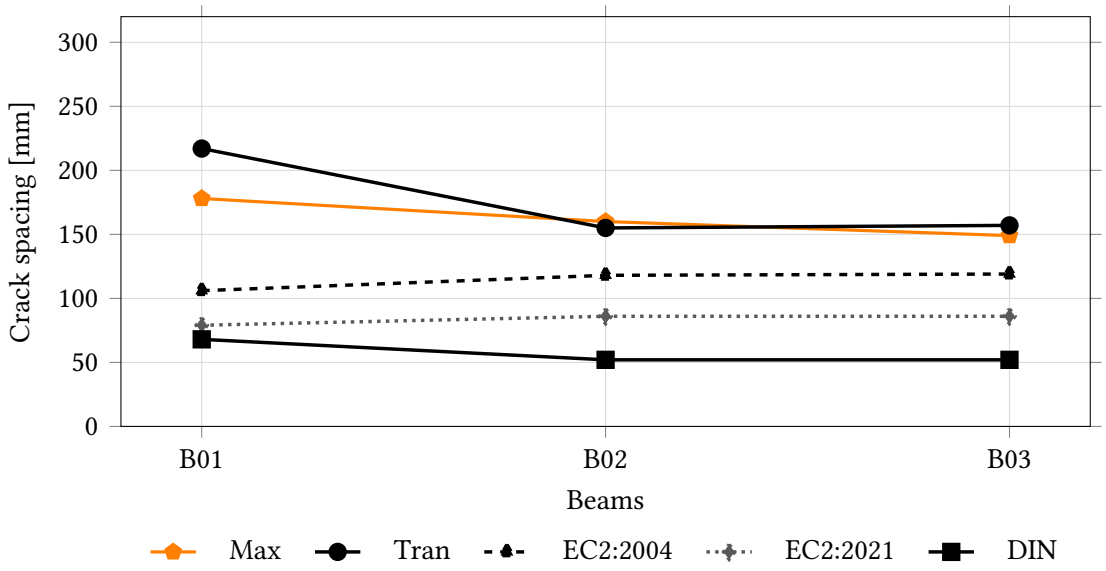


Figure 4.8: Comparison of measured mean crack spacing and calculated mean crack spacing according to different methods

The DIN standard provides the most conservative results among standards, which is underestimated by roughly 50 – 75% of the measured crack spacing, due to simplified expression. In contrast, the Habilitation Tran method integrating a bond strength coefficient k_b exhibits the closest value of $s_{r,max}$ with the measurement but the mean crack spacing $s_{r,m}$ yields the largest, especially for B01 (238 mm). Since the coefficient k_b linking concrete and reinforcement interaction, a higher k_b in B01 indicates weaker bond conditions and produces larger crack spacing.

EN 1992-1-1:2004 and EN 1992-1-1:2021 results in a significant reduction in the predicted crack spacing. The $s_{r,max}$ and $s_{r,m,calc}$ are about 28% lower in the 2021 version, compared to those values of the 2004 version. Noticeably, the refined model predictions are mostly constant for all three beams, for B01 is 79 mm and 86 mm is for both B02 and B03.

Table 4.7: Measured and calculated crack spacing ratios

Beams	**Measured Crack Spacing**			$s_{r,max,cal}/s_{r,m,measured}$				$s_{r,m,cal}/s_{r,m,measured}$			
	Min	**Mean**	**Max**	**DIN**	**EC2:2004**	**EC2:2021**	**Tran**	**DIN**	**EC2:2004**	**EC2:2021**	**Tran**
B01	90	178,0	243	0,513	0,791	0,594	1,629	0,384	0,593	0,445	1,222
B02	75	159,7	275	0,433	0,989	0,716	1,294	0,324	0,741	0,537	0,971
B03	95	148,9	215	0,470	1,064	0,768	1,410	0,352	0,798	0,576	1,057
Minimum				0,433	0,791	0,594	1,294	0,324	0,593	0,445	0,971
Average				0,472	0,948	0,693	1,444	0,354	0,711	0,520	1,083
Maximum				0,513	1,064	0,768	1,629	0,384	0,798	0,576	1,222
Coefficient of variation (%)				6,9	12,1	10,6	9,6	6,9	12,1	10,6	9,6

Table 4.7 demonstrates the ratios of calculated to measured crack spacing, serving as a direct measure of predictive accuracy, as a ratio of 1,0 indicates an exact prediction. If the

ratio is below 1,0, it indicates a conservative underestimation; otherwise, the ratio above 1,0 indicates an overestimation.

EN 1992-1-1:2004 illustrates the highest accuracy, which is 0,948 of average ratio for maximum crack spacing. This means 94,8 % of the measured mean value used for comparison and very close to a perfect prediction. Only the beam B03 slightly overestimates with the ratio of 1,064.

In contrast, the DIN and EN 1992-1-1:2021 standards are the most conservative. Their average ratios for maximum spacing are 0,693 and 0,520 respectively, which indicates the underestimation of the spacing by approximately 49% and 29% on average. For the method of Tran, the results are the least conservative with an average ratio of 1,444 for maximum crack spacing and 1,083 for mean value, which are overestimated the spacing by nearly 50% on average.

In general, the refined model is the most reliable method between two Eurocode versions, showing the lowest CoV at 10,6%. It predicts consistently conservative with a little scatter across all three different beams. However, the version of 2004 shows the highest accuracy in this study, nearly reaching the ratio 1,0.

VGU
Vietnamese-German University

5. Discussion

5.1 Comparison between EN 1992-1-1:2004 and EN 1992-1-1:2021

The comprehensive analysis conducted in this study, including both a theoretical parametric calculation and experimental validation and this enables a direct comparison of crack control provisions between EN 1992-1-1:2004 and EN 1992-1-1:2021. The results consistently demonstrate a change in the approach, where the updated 2021 standard generally yields more conservative and uniform crack width predictions compared to the older provision.

A critical change lies in the fundamental crack width expression itself. The version of 2004 accounts for the worst-case crack in design by directly using the maximum crack spacing, which is over conservative method. This is reflected in the experimental results (Table 4.6), where $s_{r,max}$ values of the 2004 version (141 – 158 mm) are significantly higher than measured mean spacings. In contrast, the revised standard uses the mean crack spacing with the conversion factor to the design crack spacing. This method is generally based on the mean behavior, resulting in less sensitive to extreme values, as observed in Table 4.7.

Vietnamese-German University

Another comparative analysis is quite clearly shown the difference in the effective tension zone between two standards. For thin to medium sections, the EN 1992-1-1:2004 approach, which defines the effective height $h_{c,eff} = (h-x)/3$ proves more suitable, where slender members are not deep enough to have a low stress region far from the bar. Conversely, for medium to thick sections, the EN 1992-1-1:2021 approach with $h_{c,eff} = d_1 + 5\phi$ becomes superior. In massive members, crack is a localized phenomenon governed by bond stress around the bars, not the full depth of the tensile zone. Therefore, the version of 2021 reflects better this local mechanics than the 2004 standard.

In addition, this shift collectively illustrates the relation between accuracy and conservatism. From the experimental comparison (Table 4.7), EN 1992-1-1:2004 provides the most accurate predictions with an average ratio of spacing close to 1,0. In contrast, EN 1992-1-1:2021 predicts underestimation spacing, exhibiting a very low Coefficient of Variation (CoV = 10,6%). Therefore, while the older code offers better alignment and predictions, the new version seems to shift toward safer and more uniform outcomes.

In summary, the evolution of crack width formulation reflects the improvement in mechanical theory. The new provision enhances the coefficients with specific cases of the members, prioritizing consistent and conservative outcomes.

5.2 Influence of key mechanical factors

One of the critical influences on differences between the two Eurocode standards is rooted in the changes of fundamental mechanism, mainly redefining the effective concrete area $A_{c,eff}$ in tension. EN 1992-1-1:2004 defines this area based on overall section geometry. For this, the effective height $h_{c,eff}$ is a function of the section height h, the neutral axis depth x and the effective depth to the reinforcement d, which leads to a variable definition as observed in the parametric study. In the numerical and experimental examples, geometrical and material properties are tried to set as equal as possible for 15 specimens. It clearly showed that the $h_{c,eff}$ of thin to medium beam thicknesses define by $(h-x)/3$, whereas larger thicknesses (500–1000 mm) is typically governed by $2{,}5(h-d)$. This distinction is also evident in the experimental beams that the $h_{c,eff}$ of beam thickness of 400 mm (B02 and B03) follows the condition $(h-x)/3$, while for the thickness of 440 mm (B01), the governing condition corresponds to $2{,}5(h-d)$. In contrast, the revised definition is to deal with inconsistencies in its current definition and contributes to reducing scatter. Instead, it directly links the effective area to the reinforcement itself. For a beam with one layer of reinforcement, $h_{c,eff}$ is defined as $d_1 + 5\phi$ and a beam with two layers incorporates the additional spacing between bars (s_y). By making the effective area a function of diameter, the newer formula directly scales the tension zone of concrete to the physical capacity for stress transfer in the bar reinforcement. A larger bar diameter has a stronger bond and influences a greater volume of surrounding concrete.

Furthermore, the updated code introduces refined coefficients that address known physical phenomena previously skipped, specifically the factors k_{fl} and $k_{1/r}$. In EN 1992-1-1:2004, the factor $k2$ is used for accounting the strain distribution between pure tension and bending. The value $k2 = 1$ for the entire cross-section in tension, creating new large cracks that form further apart. For $k_2 = 0{,}5$ is for bending when a stress gradient is, with only part of the section in tension. Therefore, the tensile force is lower, which is easier to form cracks and close together. However, the problem is that this concept is based on the stress gradient of the whole cross-section instead of the local stress around the reinforcing bar. Consequently, using $k_2 = 0{,}5$ for all bending members is less effective when the effective area around the bar in large beam in bending is small. This can lead unrealistically small crack spacings being calculated for bending elements. In the revised EN 1992-1-1:2021, the new coefficient k_{fl} replaces k_2 to better reflect the stress distribution effect. The k_{fl} explicitly relates the non-uniform tensile stress to the geometry of the member through the neutral axis depth and the effective tension height. It depends on the actual local stress state around the reinforcement. This improvement can enhance the physical consistent transition between tension and bending conditions.

Simultaneously, the new $k_{1/r}$ coefficient accounts for the increase in crack width from the level of reinforcement to concrete surface due to curvature. The version of 2004 generally assumes this visible at the concrete surface and neglects the physical of crack geometry. In flexural members, cracks are not uniform, increase wider at the tensile face due to the strain

gradient in the section. Therefore, the refined approach takes the coefficient $k_{1/r}$ into account, which incorporates the geometry of the section, the neutral axis depth. This factor helps to ensure a more realistic and reliable serviceability design.

From the discussion above, it can be concluded that the updates introduced in EN 1992-1-1:2021 represent a major refinement of the crack control mechanism. By redefining effective concrete are to be directly linked to the reinforcement layout and introducing new coefficients that better capture local stress distribution and surface crack geometry. This new model ensures a more reliable and realistic assessment of crack behavior in flexural members.

5.3 Practical implications for designers

From the result of the comparative analysis suggested that EN 1992-1-1:2021 is a more conservative design approach, it reflects the better stress distribution in the refined calculation and better assurance of durability, but leads to over-designed problems, especially for crack spacing consideration. Furthermore, this could potentially increase material costs and affect the heavily stressed members where serviceability limits are governing. While the 2004 standard might have offered more economical designs, the 2021 edition prioritizes robustness and safety, minimizing unexpected risk of cracking, particularly in complex geometries. Ultimately, the choice between applying either method depends on various design scenarios, structure types and the function of structures, but the goal of engineers is to ensure a balance between cost efficiency and long-term structural performance.

VGU Vietnamese-German University

5.4 Limitation and future research

Although this study offers insights into the comparison of EN 1992-1-1:2004 and EN 1992-1-1:2021 for crack control in reinforced concrete structures, there are some limitations within the scope of this thesis. First, the initial analysis was performed on a specific group of beam specimens characterized by a consistent reinforcement ratio and concrete cover. Although this approach facilitated a controlled comparison, its findings may not fully represent the interaction of these parameters in broader practical scenarios. For instance, the concrete cover thickness directly influences the effective tension area, and its variation could yield different results.

A significant limitation identified in both code methodologies is the simplified treatment of bond stress. Notably, the crack width models in both Eurocode versions do not incorporate the effects of anchorage length in their calculations. In practice, insufficient anchorage can lead to a breakdown in bond, subsequently resulting in the development of wider cracks. Experimentally, a primary constraint was the absence of highly precise crack width measurement equipment, which would have enabled a more direct and accurate comparison with theoretical models. Furthermore, minor inconsistencies during specimen preparation, such as variations

in reinforcement placement or concrete cover, may have contributed to slight inaccuracies in the measured crack spacing.

To address these limitations, several directions for future investigation are recommended. The scope of research should be expanded to include a wider range of structural elements, such as slabs and columns, with varied reinforcement layouts and concrete cover depths. This would provide a more robust validation of the refined standard. Additionally, future models should integrate the influence of anchorage length to better reflect the effects of localized bond stress variations on crack spacing and width. Finally, a comprehensive comparative design of a typical structure using both standards would be invaluable to quantify the economic impact of the conservatism inherent in the 2021 standard.

VGU
Vietnamese-German University

6. Conclusion and Recommendations

In conclusion, this study has provided a comprehensive comparison of the crack control provisions in EN 1992-1-1:2004 and the updated EN 1992-1-1:2021 through a detailed parametric study with experimental measurement. The case study illustrates the shift between the two standards. The 2004 version demonstrates high accuracy, supported by the close alignment between its crack spacing and the experimental values. In contrast, the 2021 version is designed to enhance the safety margins, which consistently yields more uniform and conservative predictions.

The core of this evolution is the improvement of mechanisms. The refined definition of the effective concrete area from $(h - x)/3$ and $2{,}5(h - d)$ to $(d_1 + 5\phi)$ provides a more physically realistic approach, particularly for thick sections where cracking is a localized phenomenon. Furthermore, the introduction of new coefficients k_{fl}, $k_{1/\mathrm{r}}$ and k_{w} capture better local stress states and crack geometry.

A critical key finding is the suitability of each standard depending on the geometry of members. EN 1992-1-1:2004 may perform better for thin to medium sections where its global model aligns well with flexural behavior. In contrast, EN 1992-1-1:2021 applies better for medium to thick sections, where its localized model is being improved.

VGU
Vietnamese-German University

In real-world applications, the new standard tends to more conservative approaches to managing crack widths, which may increase the reinforcement requirements for serviceability. Meanwhile, the 2004 version might be more cost-effective for standard components, the 2021 edition sets a more robust framework for critical structures.

Future research should focus on validating the new code for a wide range of elements like slabs, integrating the effect of bonding detailing and conducting a full-scale analysis to quantify the conservatism.

Appendix

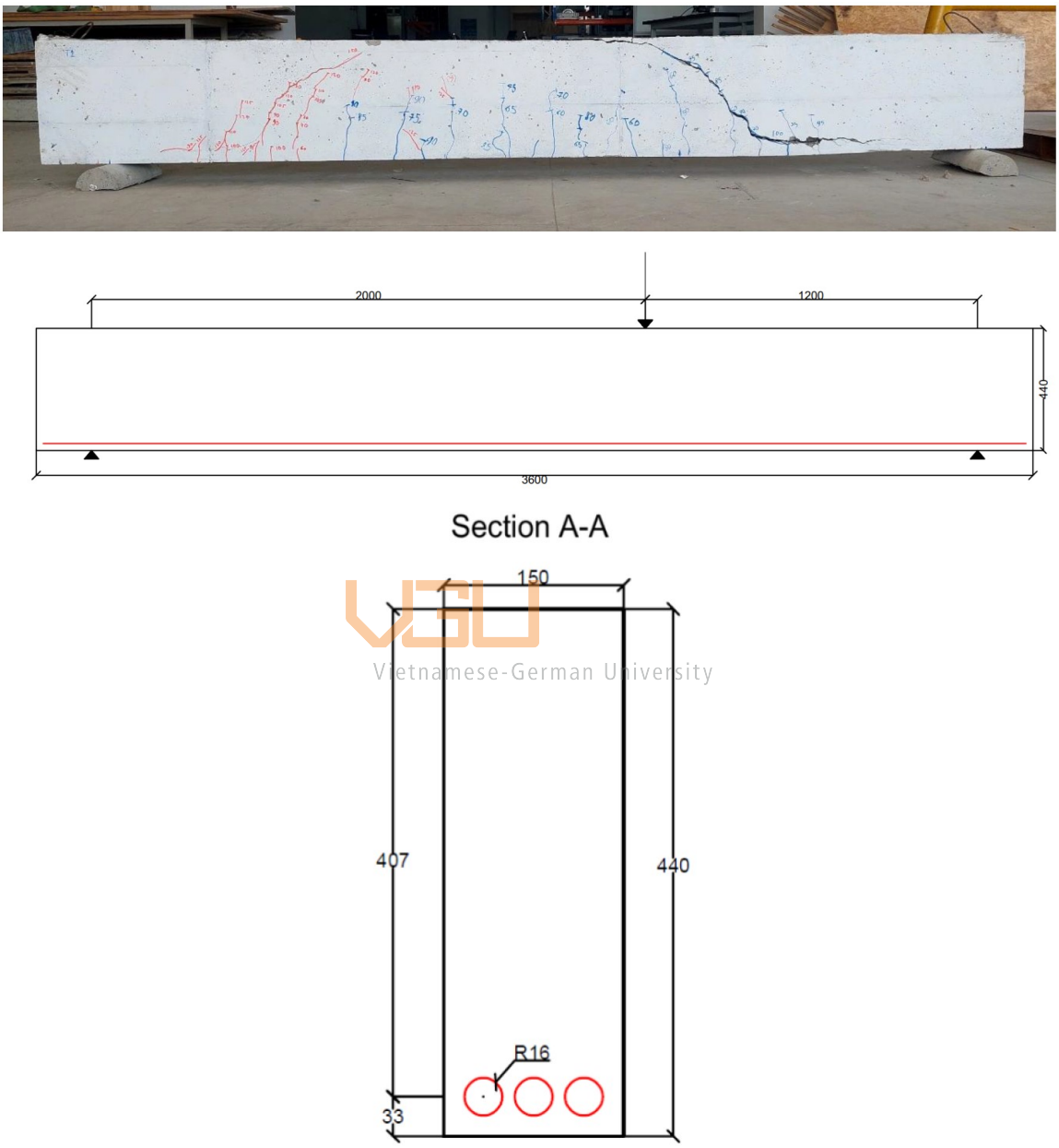


Figure A.1: Beam B01

VGU
Vietnamese-German University

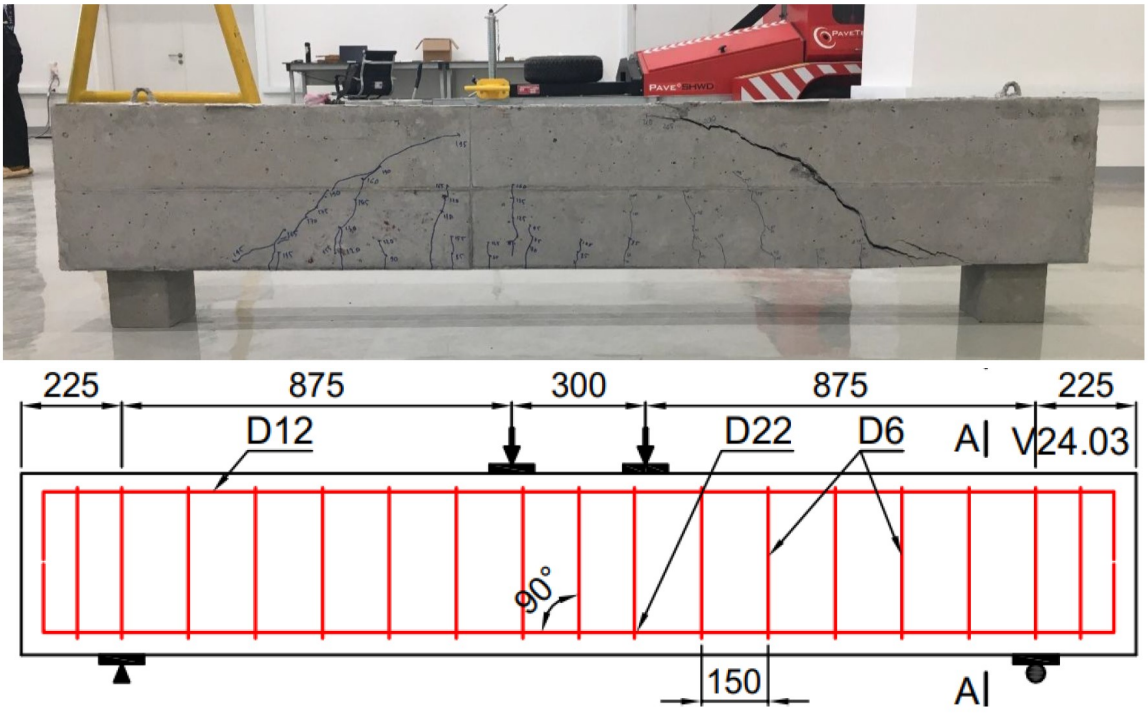


Figure A.2: Beam B02

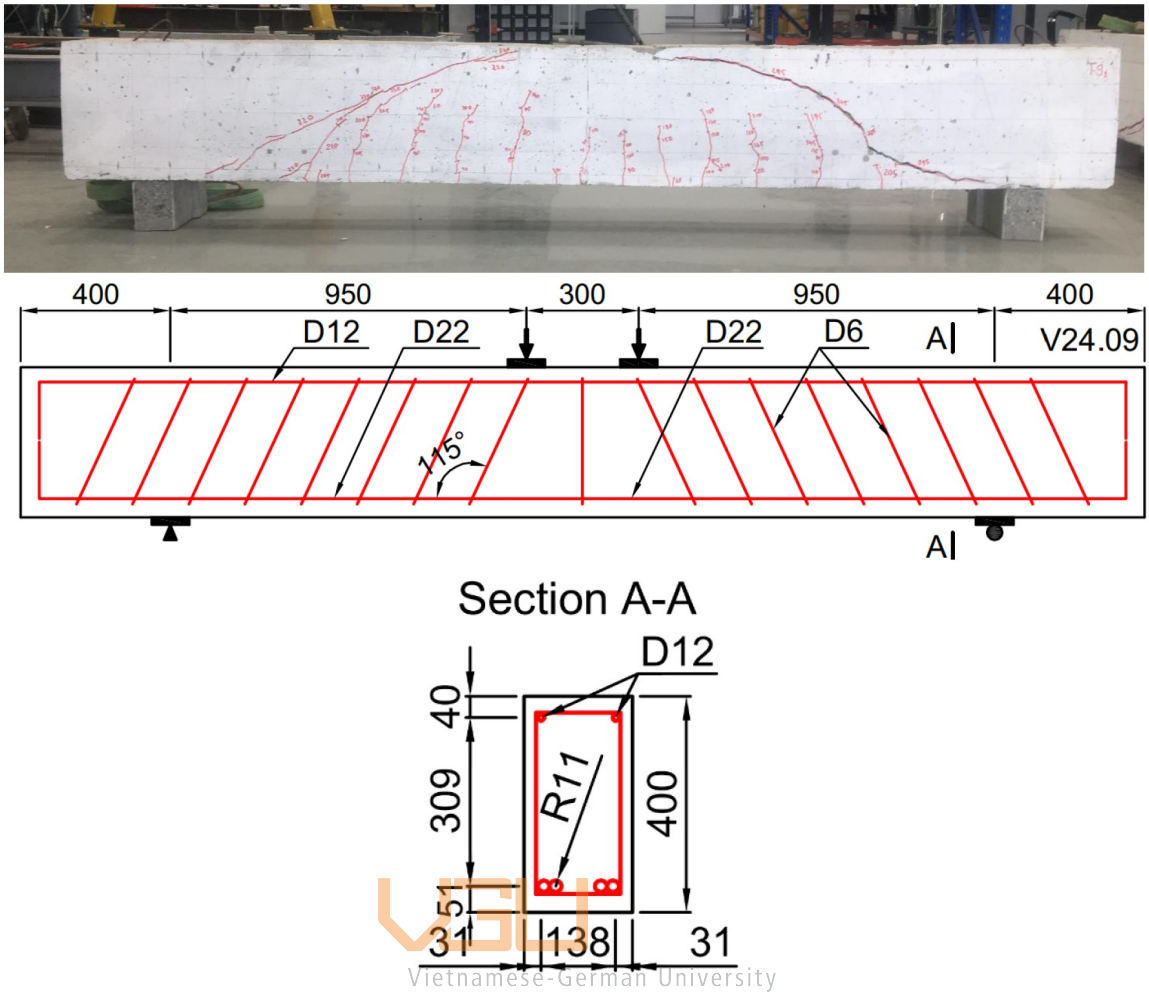


Figure A.3: Beam B03

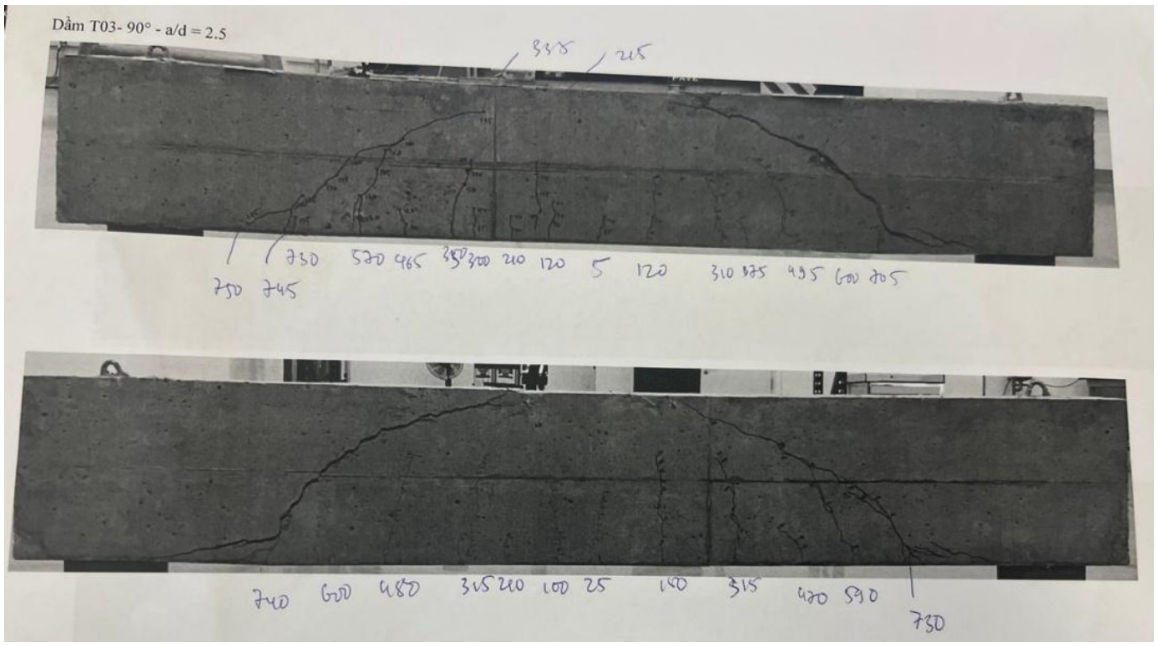


Figure A.4: Crack Spacing Record of Beam B02

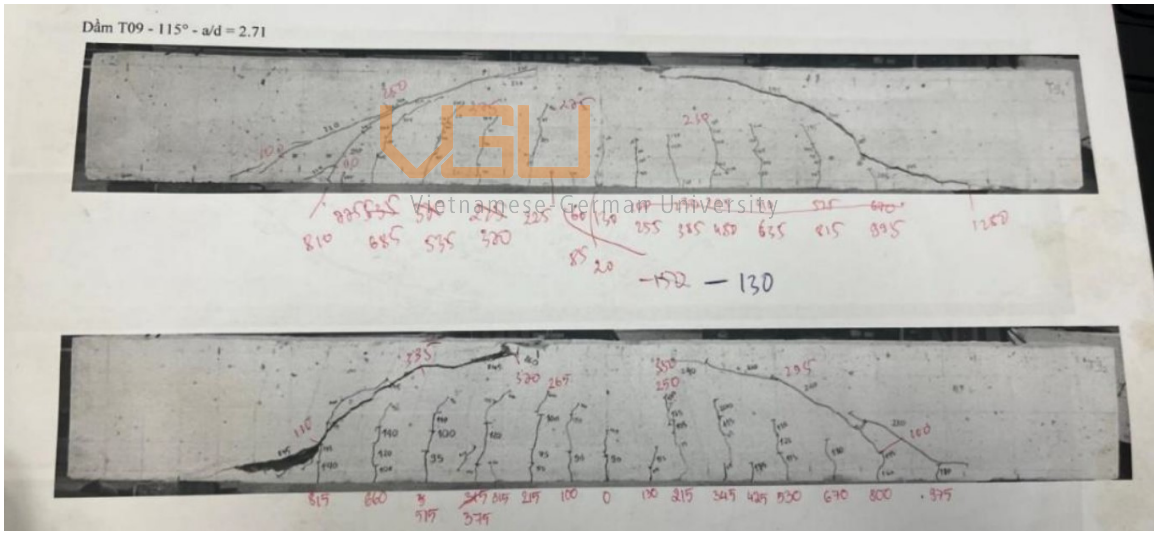


Figure A.5: Crack Spacing Record of Beam B03

VGU Vietnamese-German University



Figure A.6: Sample Testing Beam at VGU Lab

VGU
Vietnamese-German University

References

[1] Arifullah, H. and Zabihullah Dalil, S. "The Control of Flexural Cracks in the Design of Reinforced Concrete Beams for Kabul City s Exposure Condition". *Kardan Journal of Engineering and Technology* (Dec. 25, 2022), p. 1. ISSN: 2706-7815. DOI: 10.31841/KJET.2022.23.

[2] Askar, M., Al-Kamaki, Y., Ferhadi, R., & Majeed, H. *Cracks in Concrete Structures Causes And Treatments: A Review*. The Journal of Duhok University, 26, 148–165. 2023.

[3] Bisschop. *Drying shrinkage microcracking in cement-based materials*. 2012. URL: https://www.researchgate.net/publication/266851187_Drying_shrinkage_microcracking_in_cement-based_materials (visited on 10/13/2025).

[4] Chahar, A. S. and Pal, P. "Study on various properties of reinforced concrete – A review". *Materials Today: Proceedings*. International Conference on Advances in Construction Materials and Structures 65 (Jan. 1, 2022), pp. 597–602. ISSN: 2214-7853. DOI: 10.1016/j.matpr.2022.03.193.

[5] Committee, A. "ACI 224.3R-95: Joints in Concrete Construction" (1995).

[6] Committee, A. *ACI 224.1R-07: Causes, Evaluation, and Repair of Cracks in Concrete Structures*. American Concrete Institute, 2007. ISBN: 978-0-87031-234-2. DOI: 10.14359/18555.

[7] Committee, A. *ACI 231R-10: Report on Early-Age Cracking Causes, Measurement, and*. Studocu. 2010. URL: https://www.studocu.com/row/document/%E5%A4%A9%E6%B4%A5%E5%A4%A7%E5%AD%B8/computer-programming-and-application/aci-committee-231-aci-231r-10-report-on-early-age-cracking-causes-measurement-and-mitigation-american-concrete-institute-aci-2010/10325724 (visited on 10/13/2025).

[8] Committee, A. *ACI 308R-16: Guide to External Curing of Concrete*. studylib.net. 2016. URL: https://studylib.net/doc/27198972/aci-308r-16-guide-to-external-curing-of-concrete (visited on 10/20/2025).

[9] Fonseca et al., J. "Alkali-Aggregate Reaction: Definition, Influence and Control". *Engineering and Applied Sciences* 3.1 (2018), p. 12. ISSN: 2575-2022. DOI: 10.11648/j.eas.20180301.13.

[10] Fookes, P. and Lee, E. "The Engineering Geology of Concrete in Hot Drylands". *Quarterly Journal of Engineering Geology and Hydrogeology* 52 (Mar. 28, 2019), qjegh2018–185. DOI: 10.1144/qjegh2018-185.

[11] Fuhaid & Niaz. *Carbonation and Corrosion Problems in Reinforced Concrete Structures*. 2022.

Vietnamese-German University

[12] Garnica, G. Z. “Analysis of shear transfer mechanisms in concrete members without shear reinforcement based on kinematic measurements” (2018).

[13] Gilbert and Nejadi. *R435: An Experimental Study of Flexural Cracking in Reinforced Concrete Members Under Sustained Loads*. 2004.

[14] Golewski, G. L. “The Phenomenon of Cracking in Cement Concretes and Reinforced Concrete Structures: The Mechanism of Cracks Formation, Causes of Their Initiation, Types and Places of Occurrence, and Methods of Detection—A Review”. *Buildings* 13.3 (Mar. 2023). Number: 3, p. 765. ISSN: 2075-5309. DOI: 10.3390/buildings13030765.

[15] Ha, J.-H., Jung, Y. su, & Cho, Y. *Thermal crack control in mass concrete structure using an automated curing system*. Automation in Construction, 45, 16–24. 2014.

[16] Klausen, A. E. and Kanstad, T. “The effect of shrinkage reducing admixtures on drying shrinkage, autogenous deformation, and early age stress development of concrete”. *Structural Concrete* 22 (S1 2021), E596–E606. ISSN: 1751-7648. DOI: 10.1002/suco.201900583.

[17] Layang, S. “CRACKS IN REINFORCED CONCRETE BEAM”. *BALANGA: Jurnal Pendidikan Teknologi dan Kejuruan* 10.1 (June 30, 2022). Number: 1, pp. 6–12. ISSN: 2723-1216. DOI: 10.37304/balanga.v10i1.3277.

[18] Lopes, A. V. and Lopes, S. M. R. “Revisiting Cracking in Reinforced Concrete Beams: An Updated Analysis”. *Applied Sciences* 13.6 (Jan. 2023), p. 3926. ISSN: 2076-3417. DOI: 10.3390/app13063926.

[19] Mindess, S., Young, J. F., and Darwin, D. *Concrete*. Accessed online. 2003. (Visited on 10/20/2025).

[20] Mujalli, M. A. et al. “Evaluation of the Tensile Characteristics and Bond Behaviour of Steel Fibre-Reinforced Concrete: An Overview”. *Fibers* 10.12 (Dec. 2022), p. 104. ISSN: 2079-6439. DOI: 10.3390/fib10120104.

[21] Neville, A. *Properties of Concrete by A M Neville — PDF — Concrete — Mortar (Masonry)*. 2011. URL: https://www.scribd.com/document/350943966/Properties-of-Concrete-by-a-m-Neville (visited on 06/10/2025).

[22] NRMCA. *CIP 42: Thermal Cracking of Concrete*. ConcreteState. 2009. URL: https://www.concretestate.org/nrmca-concrete-in-practice.html (visited on 10/20/2025).

[23] Pérez, A. et al. “Serviceability Limit States according to the new Eurocode 2 proposal: Description and justifications of the proposed changes”. *Hormigón y Acero* (Jan. 26, 2023). ISSN: 0439-5689, 0439-5689. DOI: 10.33586/hya.2023.3104.

[24] Poursaee, A. and Ross, B. “The Role of Cracks in Chloride-Induced Corrosion of Carbon Steel in Concrete—Review”. *Corrosion and Materials Degradation* 3.2 (June 2022), pp. 258–269. ISSN: 2624-5558. DOI: 10.3390/cmd3020015.

VGU Vietnamese-German University

[25] Röhling, S. and Meichsner, H. *Rissbildungen im Stahlbetonbau: Ursachen - Auswirkungen - Maßnahmen*. German. Stuttgart: Fraunhofer IRB Verlag, 2018. ISBN: 978-3-8167-9645-9.

[26] Tenório Filho, J. R., De Belie, N., and Snoeck, D. "The Effects of Internal Curing and Shrinkage Cracking Avoidance on the Corrosion of Reinforced Concrete Walls with Superabsorbent Polymers". *Applied Sciences* 14.16 (Jan. 2024), p. 6901. ISSN: 2076-3417. DOI: 10.3390/app14166901.

[27] Tran, N. L. "Shear strength of slender reinforced concrete members without shear reinforcement". Habilitation. 2018.

VGU
Vietnamese-German University

Structural Concrete Research Group

Bachelor Thesis Series

A. Shear, Punching, Torsion

[2026] **Dang My Kao Kim, Nguyen**

Shear and Punching Shear Design of Reinforced Concrete Structures according to the New Generation of Eurocode 2. Vietnamese-German University, **BCE-2026-01**.

Supervisors: Dr.-Ing. habil. Ngoc Linh Tran, Prof.-Ing. Christian Kulas

[2026] **Viet Hung, Nguyen**

Effect of longitudinal reinforcement distribution on the shear strength of slender concrete members without shear reinforcement. Vietnamese-German University, **BCE-2026-03**.

Supervisors: Dr.-Ing. habil. Ngoc Linh Tran, Prof.-Ing. Christian Kulas

B. Cracking

[2026] **Ngoc Anh Thu, Nguyen**

Cracking in Reinforced Concrete Structures. Vietnamese-German University, **BCE-2026-02**.

Supervisors: Dr.-Ing. habil. Ngoc Linh Tran, Prof.-Ing. Christian Kulas

VGU
Vietnamese-German University